

DYNAMICS OF SINGULAR COMPLEX ANALYTIC VECTOR FIELDS WITH ESSENTIAL SINGULARITIES II

ALVARO ALVAREZ-PARRILLA*

Grupo Alximia SA de CV
Ensenada, Baja California, CP 22800, México

JESÚS MUCIÑO-RAYMUNDO

Centro de Ciencias Matemáticas
Universidad Nacional Autónoma de México, Morelia, México

ABSTRACT. The singular complex analytic vector fields X on the Riemann sphere $\widehat{\mathbb{C}}_z$ belonging to the family

$$\mathcal{E}(r, d) = \left\{ X(z) = \frac{1}{P(z)} e^{E(z)} \frac{\partial}{\partial z} \mid P, E \in \mathbb{C}[z] \right\},$$

where P is monic, $\deg P = r$, $\deg E = d$, $r + d \geq 1$, have a finite number of poles on the complex plane and an isolated essential singularity at infinity (for $d \geq 1$). Our aim is to describe geometrically X , particularly the singularity at infinity. In order to do so, we use the natural one to one *correspondence* between X , a global singular analytic distinguished parameter $\Psi_X(z) = \int^z P(\zeta) e^{-E(\zeta)} d\zeta$, and the Riemann surface \mathcal{R}_X of this distinguished parameter. We introduce (r, d) -*configuration trees* which are weighted directed rooted trees. An (r, d) -configuration tree completely encodes the Riemann surface \mathcal{R}_X and the singular flat metric associated on \mathcal{R}_X . The (r, d) -configuration trees provide “parameters” for the complex manifold $\mathcal{E}(r, d)$, which give explicit geometrical and dynamical information; a valuable tool for the analytic description of $X \in \mathcal{E}(r, d)$. Furthermore, given X , the phase portrait of the associated real vector field $\Re(X)$ on the Riemann sphere is decomposed into $\Re(X)$ -invariant components: half planes and finite height strips. The germ of X at infinity is described as a combinatorial word (consisting of hyperbolic, elliptic, parabolic and entire angular sectors having the point at infinity of $\widehat{\mathbb{C}}_z$ as center). The structural stability, under perturbation in $\mathcal{E}(r, d)$, of the phase portrait of $\Re(X)$ is characterized by using the (r, d) -configuration trees. We provide explicit conditions, in terms of r and d , as to when the number of topologically equivalent phase portraits of $\Re(X)$ is unbounded.

2020 *Mathematics Subject Classification*. Primary: 32S65; Secondary: 37F75, 30F10, 30D20, 32M25.

Key words and phrases. Complex analytic vector fields and Riemann surfaces and Essential singularities.

* Corresponding author.

CONTENTS

1. Introduction	3
2. Different facets for singular analytic vector fields $X \in \mathcal{E}(r, d)$	7
2.1. Vector fields, differential forms, orientable quadratic differentials, flat metrics, distinguished parameters, Riemann surfaces	7
2.2. The singular complex analytic dictionary	8
3. Analytic characteristics of $X \in \mathcal{E}(r, d)$	9
3.1. Order of growth at a singular point of X	9
3.2. Asymptotic values of Ψ_X	9
3.3. Poles and zeros of X	10
4. Branch points of \mathcal{R}_X	12
4.1. Local ramification data for \mathcal{R}_X	12
4.2. Branch point enumeration	13
4.3. Approximation of $X \in \mathcal{E}(r, d)$, $d \geq 1$, via rational vector fields X_n	16
5. The geometry of the Riemann surface \mathcal{R}_X ; setup for the proof of Main Theorem	20
5.1. Branch points of \mathcal{R}_X as vertices	20
5.2. The families of surfaces \mathcal{R}_X having only one vertex	21
5.3. Diagonals of \mathcal{R}_X as edges	22
5.4. Geometrical building blocks and the weights of edges	23
6. Why is the geometrical description of $\mathcal{E}(r, d)$ difficult?	27
7. Combinatorial objects: (r, d) -configuration trees	28
8. Low degree significative examples, from X to Λ_X	33
8.1. $X \in \mathcal{E}(r, 0)$ has $r \geq 1$ poles on \mathbb{C}_z and Ψ_X is a polynomial map	33
8.2. Vector fields in $\mathcal{E}(3, 0)$ with three simple poles	35
8.3. $X \in \mathcal{E}(0, d)$ has an isolated essential singularity at $\infty \in \widehat{\mathbb{C}}_z$, no zeros or poles	41
8.4. $X \in \mathcal{E}(r, d)$ has $r \geq 1$ poles on \mathbb{C}_z and an isolated essential singularity at $\infty \in \widehat{\mathbb{C}}_z$	44
9. Proof of Main Theorem: description of the family $\mathcal{E}(r, d)$ via combinatorial scheme	54
9.1. From $X \in \mathcal{E}(r, d)$ to an (r, d) -configuration tree Λ_X	55
9.2. From an (r, d) -configuration tree Λ_X to the (r, d) -skeleton of Λ_X	58
9.3. From the (r, d) -skeleton of Λ_X to the Riemann surface \mathcal{R}_X	59
9.4. The equivalence relation on (r, d) -configuration trees	63
10. Decomposition of the phase portraits into invariant components	64
11. On the topology of $\Re(X)$	66
12. The essential singularity at ∞	67
13. Relations with other works	73
13.1. The case that all critical and asymptotic values are real	73
13.2. Relations with Belyi's functions	74
13.3. Relation with complex correspondence principle in mechanics	75
13.4. Future work	76
14. Epilogue	78
References	80

1. INTRODUCTION

Motivated by the nature of meromorphic and essential singularities of complex analytic vector fields on Riemann surfaces [37], [38], [26], [2], [3], we study the larger families

$$(1) \quad \mathcal{E}(r, d) = \left\{ X(z) = \frac{1}{P(z)} e^{E(z)} \frac{\partial}{\partial z} \mid \begin{array}{l} P, E \in \mathbb{C}[z], P \text{ monic,} \\ \deg P = r, \deg E = d, r + d \geq 1 \end{array} \right\},$$

of vector fields on the Riemann sphere $\widehat{\mathbb{C}}$, having r poles on \mathbb{C} and an isolated essential singularity at ∞ (for $d \geq 1$). The appearance of poles is one of the main new features, respect to the previous work in [2].

Each $X \in \mathcal{E}(r, d)$ is provided with a global singular analytic distinguished parameter

$$(2) \quad \Psi_X(z) = \int^z P(\zeta) e^{-E(\zeta)} d\zeta : \mathbb{C}_z \longrightarrow \widehat{\mathbb{C}}_t,$$

which in turn has an associated Riemann surface

$$(3) \quad \mathcal{R}_X = \{(z, \Psi_X(z))\},$$

whose origin can be traced back to the seminal work of R. Nevanlinna [40], [41].

Thus there is a bijective correspondence, induced by Ψ_X , between

$$(4) \quad X \in \mathcal{E}(r, d) \longleftrightarrow \left\{ \begin{array}{l} \text{branched coverings } \pi : \mathcal{R}_X \longrightarrow (\widehat{\mathbb{C}}_t, \frac{\partial}{\partial t}) \text{ having} \\ d \text{ logarithmic branch points over } \infty, \\ d \text{ logarithmic branch points over } \{a_\sigma\} \subset \mathbb{C}_t, \\ r \text{ finitely ramified branch points over } \{\tilde{p}_\iota\} \subset \mathbb{C}_t \end{array} \right\},$$

where $\pi(z, t) = t$. Along this work, $(\widehat{\mathbb{C}}_z, X)$ denotes a pair, Riemann sphere and a singular complex analytic vector field, $((\mathbb{C}_z, z_0), X)$ denotes a germ of a singular analytic vector field X on (\mathbb{C}_z, z_0) . The work of M. Taniguchi [45], [46] is a key-stone for understanding the right side of (4). Analogous correspondences have been previously used in [2], [3], [4]. The function Ψ_X is single valued, as a consequence there exists a biholomorphism $\mathbb{C}_z \cong \mathcal{R}_X$ and $(\Psi_X)_* X = \frac{\partial}{\partial t}$ providing a *global flow box* for X , see Lemma 2.4.

The Riemann surface \mathcal{R}_X can be naturally described by gluing half planes \mathbb{H}^2 and finite height strips $\{0 < \Im(t) < h\}$, see Lemma 5.9.

Three natural cases arise from the values (r, d) :

- $X \in \mathcal{E}(r, 0)$ has r poles on \mathbb{C}_z and Ψ_X is a polynomial map. See W. M. Boothby [16], [17] for pioneering work and S. K. Lando *et al.* [31] chapters 1 and 5 for advances in the combinatorial direction.
- $X \in \mathcal{E}(0, d)$ has an isolated essential singularity at $\infty \in \widehat{\mathbb{C}}_z$, no zeros or poles. Ψ_X is an infinitely ramified covering map as in (4); see R. Nevanlinna [40] chapter XI, M. Taniguchi [45], [46]; and [2].
- $X \in \mathcal{E}(r, d)$, $r, d \geq 1$, has r poles on \mathbb{C}_z and an isolated essential singularity at $\infty \in \widehat{\mathbb{C}}_z$. Ψ_X is an infinitely ramified covering map as in (4).

Obviously, $\mathcal{E}(r, d)$ is an open complex submanifold of \mathbb{C}^{r+d+1} , see [3]. However for the study of analytical, geometrical and topological aspects of X and Ψ_X , “geometrical parameters” that shed light on the description of the vector fields are desirable. Recall for instance the role of the critical value map $\{f(z)_c = z^2 + c\} \mapsto c$, as dynamical parameters for the Mandelbrot set of the quadratic family; our search is for parameters with analogous properties. In our case, even though the map

$$\{\text{coefficients of } P(z), E(z) \text{ from } X\} \mapsto \left\{ \begin{array}{l} \text{critical and asymptotic values} \\ \{\tilde{p}_i\} \cup \{a_\sigma\} \subset \mathbb{C}_t \text{ of } \Psi_X \end{array} \right\}$$

is holomorphic, *the critical and asymptotic values of Ψ_X are insufficient to completely describe the family $\mathcal{E}(r, d)$* ; see Example 8.5, Figure 13 for an instance in $\mathcal{E}(0, 3)$ and Corollary 14.1.

The classical notion of divisor for $X \in \mathcal{E}(r, 0)$, as a meromorphic section of the tangent line bundle $T\widehat{\mathbb{C}}_z$, provides a finite collection of pairs; poles and zeros with their orders. The divisor characterizes the vector field up to multiplicative factor, see Lemma 4.2. However, for $d \geq 1$ the essential singularity of X at ∞ encodes the information related to the exponential. Following the idea of divisor, for the transcendental case $d \geq 1$, we introduce a non-Hausdorff compactification of \mathbb{C}_z with $2d$ copies of ∞ . This allows us to obtain a finite collection of triplets; branch points in (4) with their ramification index. The triplets play the role of the divisor for $X \in \mathcal{E}(r, d)$, see §4.2 and Definition 5.1. An advantage is that the information contained in the triplets includes the poles of X , the critical and asymptotic values of Ψ_X .

However, the information contained in the triplets is not enough for a complete description of X . With this in mind, in Definition 7.7, we introduce (r, d) -*configuration trees* Λ_X which are weighted directed rooted trees that completely encode the branched Riemann surfaces \mathcal{R}_X , for $X \in \mathcal{E}(r, d)$. They provided explicit “geometrical parameters”, which allows us to obtain a *complete global analytical and geometrical description* for X .

The *vertices* of Λ_X are the triplets associated to the branch points in \mathcal{R}_X , over \mathbb{C}_t as in (4), including their ramification index.

The *weighted edges* of Λ_X provide us with the relative position of the branch points on \mathcal{R}_X , *i.e.* two pieces of information:

- 1) each *edge* specifies which pair of branch points share the same sheet of \mathcal{R}_X ,
- 2) the *weight* of the edge tells us the relative number of sheets of \mathcal{R}_X , we must go “up or down” on the surface in order to find another sheet containing other branch points.

Letting

$$\mathcal{E}(r, d)^* \doteq \left\{ X \in \mathcal{E}(r, d) \mid \begin{array}{l} \mathcal{R}_X \text{ has at least two branch points over different} \\ \text{critical and asymptotic values of } \Psi_X \end{array} \right\},$$

we have:

Main Theorem $((r, d)$ -configuration trees as parameters for $\mathcal{E}(r, d)$).

For each pair (r, d) , $r + d \geq 2$, there is an isomorphism, as complex manifolds of dimension $r + d + 1$, between $\mathcal{E}(r, d)^$ and equivalence classes of (r, d) -configuration trees with at least two vertices, *i.e.**

$$\mathcal{E}(r, d)^* \cong \{ [\Lambda_X] \mid \Lambda_X \text{ is a } (r, d)\text{-configuration tree with at least two vertices} \}.$$

The vector fields avoided in $\mathcal{E}(r, d)^*$ are of two kinds; those in $\mathcal{E}(0, 1)$ and those in $\mathcal{E}(r, 0)$ with a unique pole. In §8 explicit examples of Λ_X can be found, while in §6 a digression on some of the difficulties encountered in the proof of the Main Theorem, are presented. Moreover, these difficulties require the consideration of classes $[\Lambda_X]$ of (r, d) -configuration trees; the description of the classes, roughly speaking, originates from a re-labelling of the vertices of Λ_X , see Definition 9.5. The proof is presented in §9, with the description of the equivalence relation and their classes $[\cdot]$ in §9.4. Our Main Theorem extends results of [2] §8.5 in the families $\mathcal{E}(0, d)$, to the families $\mathcal{E}(r, d)$ with $r + d \geq 1$.

We decode the information at ∞ , that is we shall answer the following question:

How can we describe the essential singularity of X at $\infty \in \widehat{\mathbb{C}}_z$, for $X \in \mathcal{E}(r, d)$?

The classical idea, which has its roots in the work of I. Bendixon, A. A. Andronov and F. Dumortier *et al.* (see [5] p. 304, [6] p. 84 and theorem 5.1 in [2]), is to look at the germ at infinity $((\widehat{\mathbb{C}}_z, \infty), X)$ and try to split into a finite union of hyperbolic H , elliptic E , parabolic P and entire \mathcal{E} angular sectors, this last based upon $e^z \frac{\partial}{\partial z}$ at infinity; see Equation (104) and Figure 21. Thus obtaining a cyclic word \mathcal{W}_X associated to $((\widehat{\mathbb{C}}_z, \infty), X)$.

For the essential singularity of X at ∞ the analytic/topological nature of the invariants of X is certainly a novel aspect, see §14, recalling that:

- The germ at infinity $((\widehat{\mathbb{C}}_z, \infty), X)$, which is a local analytic invariant of X under biholomorphism germs of $(\widehat{\mathbb{C}}_z, \infty)$, and also under complex affine transformations $Aut(\mathbb{C}) \subset PSL(2, \mathbb{C})$ of \mathbb{C}_z .
 - The cyclic word $\mathcal{W}_X = W_1 W_2 \cdots W_k$, which is a local topological invariant of $\Re(X)$ under local homeomorphism of $(\widehat{\mathbb{C}}_z, \infty)$ preserving the orientation.
- The following theorem answers the above posed question, as well as the dynamical description of X and equivalently for the phase portrait of its associated real vector field $\Re(X)$.

Theorem (Dynamical applications). *Let be $X \in \mathcal{E}(r, d)$.*

1) *The cyclic word \mathcal{W}_X associated to X at ∞ is recognized as*

$$(5) \quad ((\widehat{\mathbb{C}}_z, \infty), \Re(X)) \mapsto \mathcal{W}_X = W_1 W_2 \cdots W_k, \quad W_i \in \{H, E, P, \mathcal{E}\},$$

with exactly $2d$ letters $W_i = \mathcal{E}$.

- 2) *The cyclic word \mathcal{W}_X is a topological invariant of the germ $((\widehat{\mathbb{C}}_z, \infty), \Re(X))$.*
- 3) *Let $((\mathbb{C}_z, \infty), Y)$ be a singular complex analytic vector field germ, the following are equivalent:*
 - *The germ $((\mathbb{C}_z, \infty), Y)$ is analytically equivalent to the restriction of a vector field $X \in \mathcal{E}(r, d)$ for $d \geq 1$.*
 - *The cyclic word \mathcal{W}_Y of the germ $((\mathbb{C}_z, \infty), \Re(Y))$ satisfies that*
 - i) *the residue of the 1-form of time ω_Y of Y is $Res(\omega_Y, \infty) = 0$,*
 - ii) *the Poincaré–Hopf index of Y is $PH(Y, 0) = 2 + r$,*
 - iii) *the word \mathcal{W}_Y has exactly $2d \geq 2$ entire sectors \mathcal{E} .*
- 4) *The phase portrait of $\Re(X)$ is structurally stable (under perturbations in $\mathcal{E}(r, d)$) if and only if*
 - i) *X has only simple poles,*
 - ii) *all edges of Λ_X have non-zero imaginary component.*
- 5) *The number of non topologically equivalent phase portraits*

$$\{\Re(X) \mid X \in \mathcal{E}(r, d)\} \quad \text{on } \widehat{\mathbb{C}}_z$$
is infinite if and only if

$$(r, d) \in \{(r \geq 2, 1), (r \geq 1, 2), (r \geq 0, d \geq 3)\}.$$

For the accurate assertions and proofs, see Theorem 12.3, Theorem 11.2 and Theorem 11.3 respectively. A stronger version of the decomposition of the phase portrait into $\Re(X)$ -invariant components, can be found as Theorem 10.1.

Throughout this work, the objects previously described are related via the diagram

$$\begin{array}{c}
X \in \mathcal{E}(r, d) \\
\swarrow \quad \searrow \\
[\Lambda_X] \quad \longleftrightarrow \quad (r, d)\text{-soul} \quad \longrightarrow \quad \underbrace{((\widehat{\mathbb{C}}_z, \infty), X)}_{\substack{\text{local analytic} \\ \text{invariant of } X \text{ at } \infty}} \quad \longrightarrow \quad \underbrace{\mathcal{W}_X = W_1 W_2 \cdots W_k}_{\substack{\text{local topological} \\ \text{invariant of } \Re(X) \text{ at } \infty}}.
\end{array}$$

The *soul* of X , Definition 9.7, is the smallest flat Riemann surface inside \mathcal{R}_X that encodes all the combinatorial information of X (the analogous idea appears in riemannian geometry [19] as the soul, and vector fields [38] §5.2 as dynamical locus). Summing up, the Main Theorem provides the global, on $\widehat{\mathbb{C}}$, analytic bijection between

- a vector field $X \in \mathcal{E}(r, d)$,
- a class $[\Lambda_X]$ of (r, d) -configuration trees, and
- an (r, d) -soul.

Clearly, the germ $((\widehat{\mathbb{C}}_z, \infty), X)$, does not determine the class of X in $\mathcal{E}(r, d)/\text{Aut}(\mathbb{C})$, see Remark 12.2.

Moreover, the topological classification of functions Ψ_X is coarser than the topological classification of phase portraits of vector fields $\Re(X)$, for $\mathcal{E}(r, d)$, see Remark 11.4. In particular, for $X \in \mathcal{E}(r, d)$ the Riemann surface \mathcal{R}_X admits an infinite number of half planes \mathbb{H}^2 if and only if $d \geq 1$. However, following R. Nevanlinna, Example 13.2 provides a Riemann surface admitting a decomposition in an infinite number of half planes, where the corresponding vector field does not belong to any $\mathcal{E}(r, d)$.

The study of complex functions and vector fields under geometric tools (in our context: combinatorial with complex weights) is possible due to the richness of their geometric structure, the roots of which goes back to H. Schwarz [42] and F. Klein [29]. Our Main Theorem provides a geometrical characterization of the vector fields X , functions Ψ_X and Riemann surfaces \mathcal{R}_X originated from the families $\mathcal{E}(r, d)$. It enhances the work of A. Speiser [43], R. Nevanlinna [40], [41] p. 291 and G. Elfving [21] on the classification, via line complexes, of (simply connected) Riemann surfaces \mathcal{R}_X related to meromorphic functions Ψ_X . M. Taniguchi [45] & [46] and K. Biswas *et al.* [13], [14] & [15] develop analytic aspects of the functions Ψ_X , for $d \geq 1$. More recently, the study of parameter spaces for complex analytic vector fields is a current subject of interest; *e.g.* J. Muciño-Raymundo *et al.* [38], [37] in the rational case; B. Branner *et al.* [18], M.-E. Frías-Armenta *et al.* [24], K. Dias *et al.* [20], M. Kilmeš *et al.* [28] in the polynomial case.

Some of the proofs presented are based upon technical results of [2], however the minimal previous results, evidence and examples provided in this work allow for a self contained reading and understanding.

As future work, see §13.4: in the combinatorial framework recall the fruitful ideas of Belyı functions and dessin's d'enfants, promoted by A. Grothendieck; (r, d) -configuration trees follow this, see §13.4.1. The extension of these ideas to $\mathcal{E}(r, d)$ will be appear elsewhere. A clear topological description of \mathcal{R}_X as a ramified covering, see (4), is missing for the more general vector field $Y(z) = (Q(z)/P(z))e^{E(z)}\frac{\partial}{\partial z}$ having zeros: it remains for future projects. The possible construction of effective local parameters for $\mathcal{E}(r, d)$, avoiding the equivalence classes in $\{[\Lambda_X]\}$ are discussed in the Epilogue §14.

2. DIFFERENT FACETS FOR SINGULAR ANALYTIC VECTOR FIELDS $X \in \mathcal{E}(r, d)$

2.1. Vector fields, differential forms, orientable quadratic differentials, flat metrics, distinguished parameters, Riemann surfaces. Let

$$(6) \quad X(z) = \frac{1}{P(z)} e^{E(z)} \frac{\partial}{\partial z} \in \mathcal{E}(r, d), \quad \deg P = r, \deg E = d, \quad r + d \geq 1,$$

be a singular complex analytic vector field in the family (1). The polynomials describing it can be expressed as

$$(7) \quad \begin{aligned} P(z) &= (z - p_1) \cdots (z - p_r) \doteq z^r + b_1 z^{r-1} + \cdots + b_r, \\ E(z) &= \mu (z - e_1) \cdots (z - e_d) \doteq \mu (z^d + c_1 z^{d-1} + \cdots + c_d), \quad \mu \in \mathbb{C}^*. \end{aligned}$$

Note that if $d = 0$ then $P(z)$ is non necessarily monic, so in this case, let

$$(8) \quad \lambda \doteq e^{E(z)} = e^{\mu c_0} \in \mathbb{C}^*.$$

We denote by

$$(9) \quad \mathcal{P} \doteq \{p_1, \dots, p_\iota, \dots, p_r\}$$

the set of *poles of X* , allowing repetitions.

The *associated singular analytic differential form*,

$$(10) \quad \omega_X = P(z) e^{-E(z)} dz,$$

is such that $\omega_X(X) \equiv 1$, also called the 1-form of time of X .

A *singular analytic quadratic differential \mathcal{Q}* on $\widehat{\mathbb{C}}_z$ is *orientable* if it is globally given as $\mathcal{Q} = \omega \otimes \omega$, for some singular analytic differential form ω on $\widehat{\mathbb{C}}_z$. In our case we have the quadratic differential,

$$(11) \quad \mathcal{Q}_X = \omega_X \otimes \omega_X = P^2(z) e^{-2E(z)} dz^2.$$

The singular *horizontal trajectories* of \mathcal{Q}_X on $\mathbb{C}_z \setminus \mathcal{P}$ are equivalent to the trajectories of the real vector field $\Re(X)$, see for instance equation (2.2) of [2].

Since ω_X is holomorphic on \mathbb{C}_z , the local notion of *distinguished parameter* can be extended as below (see [30], [44] for the local case).

Definition 2.1. Let $X \in \mathcal{E}(r, d)$, the map

$$\Psi_X(z) = \int_{z_0}^z P(\zeta) e^{-E(\zeta)} d\zeta : \mathbb{C}_z \longrightarrow \widehat{\mathbb{C}}_t$$

is a *global distinguished parameter for X* (note the dependence on $z_0 \in \mathbb{C}_z$).

The *singular flat Riemannian metric g_X with singular set $\mathcal{P} \subset \mathbb{C}_z$* on $\mathbb{C}_z \setminus \mathcal{P}$ is defined as the pullback under $\Psi_X : (\mathbb{C}_z \setminus \mathcal{P}, g_X) \rightarrow (\mathbb{C}_t, \delta)$, where δ is the usual flat Riemannian metric on \mathbb{C}_t . The singularities of g_X at $p_\iota \in \mathcal{P}$ are cone points with angle $(2\nu_\iota + 2)\pi$, where $-\nu_\iota \leq -1$ is the order of the pole p_ι of X . The trajectories of $\Re(X)$ and $\Im(X)$ are unitary geodesics in $(\mathbb{C}_z \setminus \mathcal{P}, g_X)$.

The graph of Ψ_X

$$\mathcal{R}_X = \{(z, t) \mid t = \Psi_X(z)\} \subset \mathbb{C}_z \times \widehat{\mathbb{C}}_t$$

is a Riemann surface. Let $\pi_{X,1}$ and $\pi_{X,2}$ be the projections from \mathcal{R}_X to \mathbb{C}_z and $\widehat{\mathbb{C}}_t$, respectively. The flat metric on $(\mathcal{R}_X, \pi_{X,2}^*(\frac{\partial}{\partial t}))$ is induced by the usual metric on $(\widehat{\mathbb{C}}, \delta)$, equivalently $(\widehat{\mathbb{C}}_t, \frac{\partial}{\partial t})$, via the projection of $\pi_{X,2}$. Since $\pi_{X,1}$, as in Diagram 12, is an isometry.

Lemma 2.2. *The following diagram commutes*

$$(12) \quad \begin{array}{ccc} (\widehat{\mathbb{C}}_z, X) & \xleftarrow{\pi_{X,1}} & (\mathcal{R}_X, \pi_{X,2}^*(\frac{\partial}{\partial t})) \\ & \searrow \Psi_X & \downarrow \pi_{X,2} \\ & & (\widehat{\mathbb{C}}_t, \frac{\partial}{\partial t}). \end{array}$$

Moreover, Ψ_X is single valued, by removing $\infty \in \widehat{\mathbb{C}}_z$. The projection $\pi_{X,1}$ is a biholomorphism between

$$(\mathcal{R}_X, \pi_{X,2}^*(\frac{\partial}{\partial t})) \quad \text{and} \quad (\mathbb{C}_z, X).$$

□

In what follows, unless explicitly stated, we shall use the abbreviated form \mathcal{R}_X instead of the more cumbersome $(\mathcal{R}_X, \pi_{X,2}^*(\frac{\partial}{\partial t}))$, see Figures 7, 8, 11 and 14.

In Diagram 12 we abuse notation slightly by saying that the domain of Ψ_X is $\widehat{\mathbb{C}}_z$. This is a delicate issue.

Remark 2.3. By integrating along asymptotic paths associated to asymptotic values of Ψ_X at the essential singularity $\infty \in \widehat{\mathbb{C}}_z$, the choice of initial z_0 and end points z for the integral defining Ψ_X can be relaxed to include $\infty \in \widehat{\mathbb{C}}_z$ as end point, see Definition 3.4 and Figure 2.

Lemma 2.4. 1. The map Ψ_X is a global flow box of X , i.e.

$$(\Psi_X)_* X = \frac{\partial}{\partial t} \quad \text{on the whole } \mathbb{C}_z.$$

2. For fixed initial condition $z_0 \in \mathbb{C}_z \setminus \mathcal{P}$, the maximal (under analytic continuation) time domain of the complex flow φ of X is provided by \mathcal{R}_X , that is

$$\varphi(z_0, \cdot) : \mathcal{R}_X \setminus \bigcup_{p_i \in \mathcal{P}} \{(p_i, \tilde{p}_i)\} \longrightarrow \mathbb{C}_z \setminus \mathcal{P},$$

is a maximal complex trajectory solution.

Proof. For assertion 2, note that the punctured $\mathcal{R}_X \setminus \bigcup_{p_i \in \mathcal{P}} \{(p_i, \tilde{p}_i)\}$ is a translation Riemann surface, following [48] §3.3 and [36]. Moreover, \mathcal{R}_X is provided with singular horizontal and vertical foliations $\Re(\pi_{X,2}^*(\frac{\partial}{\partial t}))$, $\Im(\pi_{X,2}^*(\frac{\partial}{\partial t}))$, of real and imaginary time. In the spirit of Riemann surface theory, the complex trajectory $\varphi(z_0, \cdot) \doteq \pi_{X,1}(\cdot)$ is holomorphic and single valued function of the variable in this punctured Riemann surface. □

2.2. The singular complex analytic dictionary.

Proposition 2.5 (Dictionary between the singular analytic objects originating from $X \in \mathcal{E}(r, d)$, [2] p. 137). The following diagram describes a canonical one-to-one correspondence between its objects

$$(13) \quad \begin{array}{ccc} & X(z) = \frac{1}{P(z)} e^{E(z)} \frac{\partial}{\partial z} & \\ \swarrow & & \searrow \\ \omega_X(z) = P(z) e^{-E(z)} dz & & \Psi_X(z) = \int^z P(\zeta) e^{-E(\zeta)} d\zeta \\ \updownarrow & & \updownarrow \\ \mathcal{Q}_X = P^2(z) e^{-2E(z)} dz^2 & & (\mathcal{R}_X, \pi_{X,2}^*(\frac{\partial}{\partial t})) \\ \swarrow & & \searrow \\ & ((\mathbb{C}, g_X), \Re(X)) & \end{array}$$

□

Remark 2.6. The correspondence must be understood up to choice of initial point z_0 for the integral defining the global distinguished parameter. Thus, Ψ_X and $\Psi_X + \mathfrak{t}_0$ are considered the same object.

3. ANALYTIC CHARACTERISTICS OF $X \in \mathcal{E}(r, d)$

3.1. Order of growth at a singular point of X . In the classic literature, the *order of growth* or *growth order* at ∞ is defined for entire functions, these invariants extend for vector fields, see [2] §4.1 and references therein. In the present work, we only require the use of the *1-order*.

Let $\psi : (\mathbb{C} \setminus \{0\}, 0) \rightarrow \mathbb{C}$ be a germ of a complex analytic function with an isolated singularity at $z = 0$; i.e. ψ has a pole or an isolated essential singularity at the origin. We can define for $\varepsilon > 0$

$$M_\varepsilon(\psi) = \max_{|z|=\varepsilon} \{\log |\psi(z)|\}.$$

When the number $\rho \in \mathbb{R}$ determined by

$$\rho(\psi) = \limsup_{\varepsilon \rightarrow 0} \frac{\log(M_\varepsilon(\psi))}{-\log(\varepsilon)}$$

exists, it is called the *1-order of growth* of ψ at 0.

Definition 3.1. Let $((\mathbb{C}, 0), X(z) = f(z) \frac{\partial}{\partial z})$ be a germ of a singular analytic vector field, with 0 an isolated singularity of X . The *1-order of X at 0* is the corresponding 1-order of f , i.e. $\rho(X) := \rho(f)$. Analogously, if $\omega(z) = dz/f(z)$ is a germ of a differential form with 0 an isolated singularity of ω , then ω inherits the *1-order* from that of the function $1/f$.

Lemma 3.2 ([2] p. 144). *If $X = \frac{1}{P(z)} e^{E(z)} \frac{\partial}{\partial z} \in \mathcal{E}(r, d)$, then at $z = \infty$,*

$$X \text{ has 1-order } \rho(X) = \deg(E(z)) = d.$$

In this case the 1-order of ω and Ψ_X agree and is the negative of the 1-order of X .

□

3.2. Asymptotic values of Ψ_X . Asymptotic values for meromorphic functions in the classical setting appear in many instances, see [27] p. 66, [40] pp. 298–303, we follow W. Bergweiler *et al.* [11], essentially verbatim from Definition 3.3 to Definition 3.6, below.

Let $\Psi : \mathbb{C}_z \rightarrow \widehat{\mathbb{C}}_t$ be a meromorphic function, a priori not related to some vector field. The inverse function Ψ^{-1} can be defined on a Riemann surface which is conformally equivalent to \mathbb{C} via Ψ^{-1} . We want to study the singularities of Ψ^{-1} . This can be done by adding to \mathbb{C}_z some ideal points and defining neighborhoods of these points.

Definition 3.3. Take $a \in \widehat{\mathbb{C}}_t$ and denote by $D(a, \rho)$ the disk of radius $\rho > 0$ (in the spherical metric) centred at a . For every $\rho > 0$, choose a component $U(\rho)$ of $\Psi^{-1}(D(a, \rho))$ in such a way that $\rho_1 < \rho_2$ implies $U(\rho_1) \subset U(\rho_2)$. Note that the function $U : \rho \rightarrow U(\rho)$ is completely determined by its germ at 0.

Two possibilities can occur for the germ of U :

1) $\cap_{\rho>0} U(\rho) = \{z_0\}$, $z_0 \in \mathbb{C}_z$. In this case $a = \Psi(z_0)$.

Moreover, if $a \in \mathbb{C}_t$ and $\Psi'(z_0) \neq 0$, or $a = \infty$ and z_0 is a simple pole of Ψ , then z_0 is called an *ordinary point*.

On the other hand, if $a \in \mathbb{C}_t$ and $\Psi'(z_0) = 0$, or if $a = \infty$ and z_0 is a multiple pole of Ψ , then z_0 is called a *critical point* and a is called a *critical value*. We also say that the critical point z_0 *lies over* a .

2) $\cap_{\rho>0} U(\rho) = \emptyset$. Then we say that our choice $\rho \rightarrow U(\rho)$ defines a *transcendental singularity* of Ψ^{-1} , and that the transcendental singularity U *lies over* a .

For every $\rho > 0$, the open set $U(\rho) \subset \mathbb{C}_z$ is called a *neighborhood of the transcendental singularity* U . So if $z_k \in \mathbb{C}_z$, we say that $z_k \rightarrow U$ if for every $\rho > 0$ there exists k_0 such that $z_k \in U(\rho)$ for $k \geq k_0$.

Definition 3.4. If U is a transcendental singularity of Ψ^{-1} then a is an *asymptotic value* of Ψ , which means that there exists an *asymptotic path* $\alpha(\tau) : (0, \infty) \rightarrow \mathbb{C}_z$ tending to ∞ such that $\lim_{\tau \rightarrow \infty} \Psi(\alpha(\tau)) = a$.

In particular, it follows that every neighborhood $U(\rho)$ of a transcendental singularity U is unbounded.

If a is an asymptotic value of Ψ , then there is at least one transcendental singularity over a . Certainly there can be many different transcendental singularities as well as critical and ordinary points over the same point a .

Definition 3.5. A transcendental singularity U over a is called *direct* if there exists $\rho > 0$ such that $\Psi(z) \neq a$ for $z \in U(\rho)$, this is also true for all smaller values of ρ . Moreover, U is called *indirect* if it is not direct, *i.e.* for every $\rho > 0$ the function Ψ takes the value a in $U(\rho)$, in which case the function Ψ takes the value a infinitely often in $U(\rho)$.

Definition 3.6. The transcendental singularity U is a *logarithmic branch point* over a if $\Psi : U(\rho) \rightarrow D(a, \rho) \setminus \{a\}$ is a universal covering for some $\rho > 0$. The (unbounded) neighborhoods $U(\rho)$ are called *exponential tracts*.

The simplest case of a direct singularity is a logarithmic branch point, see Example 4.1.

A simple example of an indirect singularity is given by the inverse function of $\sin(z)/z$, where the asymptotic value 0 is a limit point of critical values. In fact W. Bergweiler and A. Eremenko prove that “If f is a meromorphic function of finite order, then every indirect singularity of f^{-1} is a limit of critical points”. However more complicated examples show that this is not always the case. See theorem 1 of [11] for further discussion and details.

3.3. Poles and zeros of X . When we apply the above definitions to germs of the distinguished parameter Ψ_X , centered at the isolated singularities $\{p_1, \dots, p_r, \infty\}$ of $X \in \mathcal{E}(r, d)$, three cases appear; poles, zeros and essential singularities. The local analytic normal forms of poles and zeros of X are well known, due to several authors. Figure 1 shows their real phase portraits, for further details see [37], [2] p. 133 and examples 4, 5 and 6 in [4].

Remark 3.7. *Analytic normal form for poles.* The point $p_i \in \mathcal{P}$ is a pole of X , having order¹ $-\nu_i \leq -1$. This corresponds to a critical point of Ψ_X , thus a *finite covering* $\Psi_X : U(\rho) \rightarrow D(\tilde{p}_i, \rho) \setminus \{\tilde{p}_i\}$ where

$$\tilde{p}_i = \Psi(p_i) \text{ is the critical value.}$$

Furthermore, because of the local analytic normal forms, up to local biholomorphism

$$(14) \quad X(z) = \frac{1}{(z - p_i)^{\nu_i}} \frac{\partial}{\partial z} \quad \text{and} \quad \Psi_X(z) = \frac{(z - p_i)^{\nu_i + 1}}{\nu_i + 1} \quad \text{on } (\mathbb{C}, p_i).$$

The local phase portrait of $\Re(X)$ at p_i has $2(\nu_i + 1)$ hyperbolic sectors.

¹We convene that the order $-\nu_i$ of a pole p_i is to be negative.

Remark 3.8. *Analytic normal form for zeros.* The point $\infty \in \widehat{\mathbb{C}}_z$ is a zero for $X \in \mathcal{E}(r, d)$ if and only if $r \geq 1$ and $d = 0$. In which case ∞ is the unique zero of X and has order $s \doteq r + 2 \geq 3$. Ψ_X is a polynomial and ∞ is a pole of it. Using $\{w\}$ as a local chart at ∞ , the local analytic normal forms of X and Ψ_X on $(\mathbb{C}_w, 0)$ are

$$(15) \quad X(z) = w^s \frac{\partial}{\partial w} \quad \text{and} \quad \Psi_X(z) = \frac{w^{1-s}}{(1-s)}, \quad s \geq 3.$$

The local phase portrait of $\Re(X)$ at ∞ has $2(s-1)$ elliptic sectors.

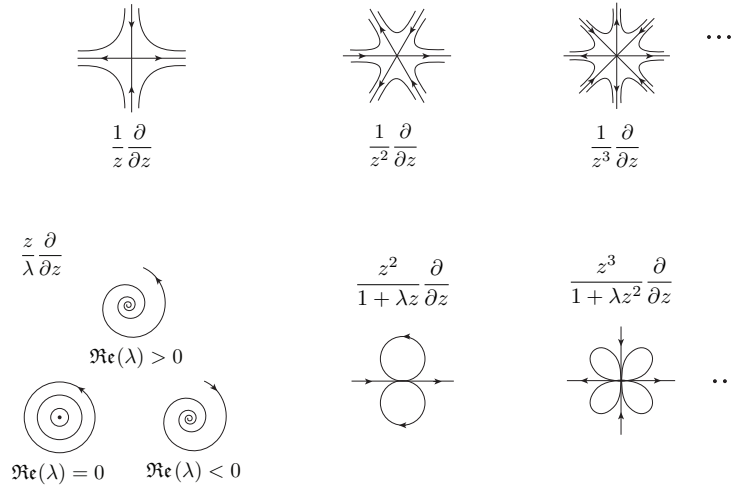


FIGURE 1. Normal forms of X and phase portraits of $\Re(X)$ at poles or zeros in $z = 0$. Top row: for a pole of order $-\nu_i \leq -1$, the phase portrait has $2(\nu_i + 1)$ separatrices arriving or leaving the pole and $2(\nu_i + 1)$ hyperbolic sectors. Bottom row: simple zeros and zeros of order $s \geq 2$, here $\lambda = \text{Res}(\omega_X, 0)$. For simple zeros, the phase portrait is the pullback via $\Psi_X(z) = \lambda \log z$ of the constant vector field $Y(t) = \frac{\partial}{\partial t}$. For $s \geq 2$ the trajectories of $\Re(X)$ form a flower with $2(s-1)$ elliptic sectors. In our case $X \in \mathcal{E}(r, 0)$, note that $\lambda = 0$ and $s \geq 3$.

Summing up, and recalling (8).

Proposition 3.9 (Topological properties of $X \in \mathcal{E}(r, 0)$). *Let*

$$X(z) = \frac{\lambda}{P(z)} \frac{\partial}{\partial z} \in \mathcal{E}(r, 0), \quad \deg P = r \geq 1, \quad \lambda \in \mathbb{C}^*,$$

be a rational vector field, the following properties hold.

- 1) X has a zero of order $r + 2 \geq 3$ at $\infty \in \widehat{\mathbb{C}}_z$.
- 2) The local phase portrait of $\Re(X)$ at ∞ has $2(r+1)$ elliptic sectors.
- 3) X has a pole of order $-\nu_i$ at p_i (a zero of $P(z)$ of order ν_i).
- 4) The local phase portrait of $\Re(X)$ at p_i has $2(\nu_i + 1)$ hyperbolic sectors.
- 5) The global phase portrait of X has a decomposition into
 - $2r$ half planes $(\overline{\mathbb{H}}_{\pm}^2, \frac{\partial}{\partial t})$ and
 - M finite height horizontal strips of the form $(\{0 \leq \Im(t) \leq h\}, \frac{\partial}{\partial t})$, where $0 \leq M \leq r-1$ and each $h > 0$.

Proof. Assertion (5) follows by a topological description of the separatrices of $\Re(X)$ from the saddle points p_i ; see Figure 10 for examples of the assertions (4)–(5), in the case of three simple poles. More detail about the decomposition in (5), will be provided in Lemma 5.9. \square

A simple example that will be used throughout follows.

Example 3.1. Consider the vector field

$$(16) \quad X(z) = \frac{\lambda}{(z - p_1)^r} \frac{\partial}{\partial z} \in \mathcal{E}(r, 0), \quad r \geq 1,$$

and its distinguished parameter

$$(17) \quad \Psi_X(z) = \frac{1}{\lambda} \int_{z_0}^z (\zeta - p_1)^r d\zeta = \frac{1}{\lambda(r+1)} ((z - p_1)^{r+1} - (z_0 - p_1)^{r+1}).$$

the pole p_1 of X is the critical point of Ψ_X and its critical value is

$$(18) \quad \tilde{p}_1 = \Psi_X(p_1) = -\frac{1}{\lambda(r+1)} (z_0 - p_1)^{r+1}.$$

See also Example 8.2. The vector field in Equation (16) is such that, \mathcal{R}_X has only one branch point. Whence these vector fields define vector fields in $\mathcal{E}(r, d) \setminus \mathcal{E}^*(r, d)$ which are forbidden in the Main Theorem.

4. BRANCH POINTS OF \mathcal{R}_X

4.1. Local ramification data for \mathcal{R}_X . For $d \geq 1$, the point $\infty \in \widehat{\mathbb{C}}_z$ is an isolated essential singularity of

$$X(z) = \frac{1}{P(z)} e^{E(z)} \frac{\partial}{\partial z},$$

and the distinguished parameter Ψ_X , belongs to the family

$$(19) \quad SF_{r,d} = \left\{ \Psi_X(z) = \int_{z_0}^z P(\zeta) e^{-E(\zeta)} d\zeta \mid P, E \in \mathbb{C}[z], \deg P = r, \deg E = d \right\},$$

of *structurally finite entire functions of type (r, d)* , see [45]. We recall the simplest object.

Example 4.1. Consider the vector field

$$(20) \quad X(z) = e^{\mu(z+c_1)} \frac{\partial}{\partial z} \in \mathcal{E}(0, 1)$$

and its corresponding distinguished parameter

$$(21) \quad \Psi_X(z) = \frac{1}{\mu} \int_{z_0}^z e^{-\mu(\zeta+c_1)} d\zeta = \frac{1}{\mu} (e^{-\mu(z_0+c_1)} - e^{-\mu(z+c_1)}),$$

with $\mu \in \mathbb{C}^*$, $c_1 \in \mathbb{C}$ as in (7). Of course $\infty \in \widehat{\mathbb{C}}_z$ is an isolated essential singularity of both. Moreover, Ψ_X has two asymptotic values

$$(22) \quad a_1 = \frac{1}{\mu} e^{-\mu(z_0+c_1)} \in \mathbb{C}_t \quad \text{and} \quad a_2 = \infty \in \widehat{\mathbb{C}}_t$$

with exponential tracts the half planes

$U_1(\rho) = \{z \in \mathbb{C}_z \mid \Re(\mu z) > \rho\}$ and $U_2(\rho) = \{z \in \mathbb{C}_z \mid \Re(\mu z) < -\rho\}$ respectively. The multivalued function

$$\Psi_X^{-1}(t) = \frac{1}{\mu} \log \left(-\frac{e^{\mu(z_0+c_1)}}{t \mu e^{\mu(z_0+c_1)} - 1} \right) - c_1$$

has two logarithmic branch points: one over the finite asymptotic value a_1 and the other over the asymptotic value $a_2 = \infty$. Note that Equation (20) defines a forbidden stratum in the whole family $\mathcal{E}(r, d)$ of the Main Theorem.

In order to determine the Riemann surface \mathcal{R}_X precisely, one needs the knowledge of the branch points under $\pi_{X,2}$

$$(23) \quad \{(z_a, t_a)\} \subset \mathcal{R}_X, \quad z_a \in \{p_1, p_2, \dots, p_r, \infty\}, \quad t_a = \Psi_X(z_a),$$

the subindex \mathbf{a} will be very useful in several constructions. The next result clearly explains the singularities of Ψ_X^{-1} .

Lemma 4.1 (The existence of finitely ramified and logarithmic branch points). *Let $\Psi_X : \mathbb{C}_z \rightarrow \widehat{\mathbb{C}}_t$ be a structurally finite entire function of type (r, d) . Then*

- 1) Ψ_X has r critical values $\{\tilde{p}_\iota\} \subset \mathbb{C}_t$ (counted with multiplicity),
- 2) Ψ_X^{-1} has d direct singularities corresponding to d logarithmic branch points over d finite asymptotic values $\{a_\sigma\} \subset \mathbb{C}_t$ of Ψ_X , and
- 3) Ψ_X^{-1} has d direct singularities corresponding to d logarithmic branch points over $\infty \in \widehat{\mathbb{C}}_t$.

Furthermore, Ψ_X^{-1} has no indirect singularities.

Proof. Case (r, d) with $d \geq 1$ can be found as lemma 8.4 in [2] with a proof that relies heavily on the work of M. Taniguchi [45], [46]. \square

4.2. Branch point enumeration. As motivation, let $T\widehat{\mathbb{C}}_z$ be the holomorphic tangent bundle of $\widehat{\mathbb{C}}_z$. For $X \in \mathcal{E}(r, 0)$, the divisor of the meromorphic section $X : \widehat{\mathbb{C}}_z \rightarrow T\widehat{\mathbb{C}}_z$ is the assignment²

$$(24) \quad X \mapsto (\infty, r+2) \cup \{(p_\iota, -\nu_\iota)\}_{\iota=1}^n,$$

where $\sum_{\iota=1}^n \nu_\iota = r$ and $n \leq r$, the equality holds if and only if all the poles of X are simple. A very useful result for meromorphic vector fields on $\widehat{\mathbb{C}}_z$ of the so called Brill–Noether theory in algebraic geometry (or the Poincaré–Hopf theory if you prefer); the zeros and poles determine a meromorphic vector field on \mathbb{C}_Z up to scalar factor.

Lemma 4.2. *Let $\nu_j, \nu_\iota \in \mathbb{N}$, a divisor*

$$\{(q_j, \nu_j)\}_{j=1}^s \cup \{(p_\iota, -\nu_\iota)\}_{\iota=1}^n \subset \widehat{\mathbb{C}}_z \times \mathbb{Z}^*$$

determines a family of meromorphic vector fields $\{\lambda Y \mid \lambda \in \mathbb{C}^\}$ on $\widehat{\mathbb{C}}_z$ if and only if*

$$\sum_{j=1}^s \nu_j - \sum_{\iota=1}^n \nu_\iota = s - r = 2.$$

\square

We would like to extend Lemma 4.2 to the case of $X \in \mathcal{E}(r, d)$, $d \geq 1$. Of course the divisor (24) is not well defined since X is not meromorphic on $\widehat{\mathbb{C}}_z$.

In order to accomplish this an accurate enumeration of the branch points $\{(z_a, t_a)\} \subset \mathcal{R}_X$ in (23) is required. In what follows, the reader might find it helpful to follow along with Figures 7–8, 11–17 in §8.

²A formal sum of pairs (p, ν) denoting a point in $\widehat{\mathbb{C}}_z$ and its order in \mathbb{Z}^* , positive for a zero of the vector field, negative for a pole.

Enlarging the pairs in the divisor, we enumerate the corresponding finitely ramified branch points using *triplets*

Abusing notation, we say that the triplets are in \mathcal{R}_X .

Definition 4.3. The *non-Hausdorff closure*

is the sphere with $2d \geq 2$ infinities, that is the disjoint union of $2d$ copies of the Riemann sphere $\widehat{\mathbb{C}}$ with the equivalence relation $(z, \sigma) \sim (z, \eta)$ for all $\sigma, \eta \in \{1, \dots, 2d\}$ when $z \neq \infty$.

$$(27) \quad \{\infty_\sigma \doteq (\infty, \sigma)\}_{\sigma=1}^{2d} \subset \overline{\mathbb{T}}_z.$$
$$(28) \quad \begin{array}{ll} \{a_j\}_{j=1}^m \subset \mathbb{C}_t & \text{with multiplicities } \{\mathfrak{m}_j \geq 1\}_{j=1}^m, \sum_{j=1}^m \mathfrak{m}_j = d \text{ and} \\ a_{m+1} = \infty \in \widehat{\mathbb{C}}_t & \text{with multiplicity } d. \end{array}$$
$$(29) \quad \begin{array}{c} \sigma \in \underbrace{1, \dots, m_1}_1, \underbrace{m_1 + 1, \dots, m_1 + m_2}_2, \dots, \underbrace{d - m_m + 1, \dots, d}_m, \underbrace{d + 1, \dots, 2d}_{m+1}, \\ j = j(\sigma) \in \end{array}$$

Remark 4.4. 1. The asymptotic paths $\alpha_\sigma(\tau)$ lie in the non-Hausdorff closure $\overline{\mathbb{C}}_z$. If $\alpha_\sigma(\tau) : (0, \infty) \rightarrow \overline{\mathbb{C}}_z$ is an asymptotic path approaching $\infty_\sigma \in \overline{\mathbb{C}}_z$ associated to the asymptotic value $a_{j(\sigma)}$ then we may assume that $\alpha_\sigma(\tau)$ is restricted to one exponential tract (the one containing $\infty_\sigma \in \overline{\mathbb{C}}_z$). The actual choice of $\alpha_\sigma(\tau)$ inside the exponential tract $U_\sigma(\rho)$ will be made explicit in Proposition 4.8.4 and Remark 4.9.1.

2. Each asymptotic path $\alpha_\sigma(\tau)$ together with the distinguished parameter Ψ_X gives rise to the asymptotic value

$$(30) \quad a_{j(\sigma)} = \lim_{\substack{z \rightarrow \infty_\sigma \\ z \in \alpha_\sigma}} \Psi_X(z) = \lim_{\tau \rightarrow \infty} \int_{z_0}^{\alpha_\sigma(\tau)} P(\zeta) e^{-E(\zeta)} d\zeta \in \widehat{\mathbb{C}}_t.$$

3. Because of the multiplicity of $a_{j(\sigma)}$, when $j(\sigma) \neq m+1$ there are exactly \mathfrak{m}_j asymptotic paths $\alpha_\sigma(\tau)$ and \mathfrak{m}_j exponential tracts for each of the m distinct finite asymptotic values $a_{j(\sigma)} \in \mathbb{C}_t$, see Figure 2. Moreover, there are d asymptotic paths and d exponential tracts for the asymptotic value $a_{m+1} = \infty \in \widehat{\mathbb{C}}_t$.

Recalling that logarithmic branch points are infinitely ramified, and using the notation provided by Equation (27), we will denote the logarithmic branch points over the asymptotic values $a_{j(\sigma)} \in \mathbb{C}_t$ of Ψ_X , as *triplets*

$$(31) \quad \bigcirc_{n+\sigma} \doteq (\infty_\sigma, a_{j(\sigma)}, -\infty) \in \mathcal{R}_X, \quad \text{for } \sigma \in \{1, \dots, 2d\}.$$

Abusing notation, we say that the triplets are in \mathcal{R}_X .

Note that the above discussion proves the following.

Lemma 4.5. *For $X \in \mathcal{E}(r, d)$, there is a correspondence between:*

- the $2d$ logarithmic branch points $\bigcirc_{n+\sigma}$ in \mathcal{R}_X ,
- the $2d$ asymptotic values a_σ of Ψ_X (counted with multiplicities) in $\widehat{\mathbb{C}}_t$,
- the $2d$ exponential tracts $U_\sigma(\rho)$ in $\widehat{\mathbb{C}}_z$ and
- the $2d$ asymptotic paths $\alpha_\sigma(\tau)$ in $\overline{\mathbb{C}}_z$.

□

Remark 4.6. 1. An immediate advantage of the correspondence observed in Lemma 4.5 is that the index σ simultaneously enumerates all of the objects in question. In particular, from now on we agree that

$$a_\sigma \text{ is referring to } a_{j(\sigma)} \in \widehat{\mathbb{C}}_t, \text{ as in (29).}$$

For instance $\{a_{j(\sigma)}\}$ corresponds to one point in \mathbb{C}_t for $\sigma = \mathfrak{m}_1 + 1, \dots, \mathfrak{m}_1 + \mathfrak{m}_2$.

2. Each exponential tract when considered in $\widehat{\mathbb{C}}_z$ is an angular sector about ∞ . Hence the exponential tracts have a natural counterclockwise ordering about $\infty \in \widehat{\mathbb{C}}_z$ arising from $S^1 = \{e^{i\theta}\}$. The ordering will be made explicit in Proposition 4.8.3; see also Figure 2 and the last row in Figure 3.

We have the following *ad hoc* notion, that expands the notion of the divisor of X as meromorphic section, Equation (24).

Definition 4.7. Let $X \in \mathcal{E}(r, d)$, $d \geq 1$, the assignment

$$(32) \quad X \mapsto \underbrace{\left\{ \bigcirc_l = (p_l, \tilde{p}_l, -\nu_l) \right\}_{l=1}^n}_{\text{pole vertices}} \cup \underbrace{\left\{ \bigcirc_{n+\sigma} = (\infty_\sigma, a_\sigma, -\infty) \right\}_{\sigma=1}^d}_{\text{essential vertices}} \cup \underbrace{\left\{ \bigcirc_{n+\sigma} = (\infty_\sigma, \infty, -\infty) \right\}_{\sigma=d+1}^{2d}}_{\text{vertices over } \infty}$$

is the *divisor* of X .

The notations in Equation (32) will be useful at several stages of the proof of the main result. The following section explains the equidistribution of the exponential tracts and thus provides a natural ordering/enumeration for the asymptotic values.

4.3. Approximation of $X \in \mathcal{E}(r, d)$, $d \geq 1$, via rational vector fields X_n . The vector fields $X \in \mathcal{E}(r, d)$, $d \geq 1$ can be approximated by rational vector fields of the form $X_n(z) = \frac{1}{P_n(z)} \frac{\partial}{\partial z}$. Analogous ideas for other differential equations are applied in [35]. Moreover, as will be shown, the construction behaves nicely providing insight into the combinatorial/geometrical structure of X , Ψ_X and \mathcal{R}_X .

Let X be as in (6) and recall Euler's formula

$$(33) \quad e^{-E(z)} = \lim_{n \rightarrow \infty} \left(1 - \frac{E(z)}{n}\right)^n.$$

Thus

$$(34) \quad X_n(z) = \frac{1}{P(z) \left(1 - \frac{E(z)}{n}\right)^n} \frac{\partial}{\partial z} \quad \text{and} \quad \Psi_n(z) = \int_{z_0}^z P(\zeta) \left(1 - \frac{E(\zeta)}{n}\right)^n d\zeta$$

converge to

$$(35) \quad X(z) = \frac{e^{E(z)}}{P(z)} \frac{\partial}{\partial z} \quad \text{and} \quad \Psi_X(z) = \int_{z_0}^z P(\zeta) e^{-E(\zeta)} d\zeta$$

uniformly on compact sets of \mathbb{C}_z , while

$$\mathcal{R}_{X_n} = \{(z, \Psi_n(z)) \mid z \in \mathbb{C}_z\}$$

converges to \mathcal{R}_X , in the Caratheodory topology; see K. Biswas *et al.* [13], [14] for details on Caratheodory convergence.

Because of the Dictionary Proposition 2.5 (see also Remarks 3.7 and 3.8), as $n \rightarrow \infty$, the successions $\{X_n\}$, $\{\Psi_n\}$ and $\{\mathcal{R}_{X_n}\}$ enjoy the following analogous features:

Each X_n has:

- r poles at the roots $\{p_i\}_{i=1}^r$ of $P(z)$ with orders $\{-\nu_i\}$,
- d poles at the roots $\{\widehat{e}_\sigma = \widehat{e}_\sigma(n)\}_{\sigma=1}^d$ of $n - E(z)$, each of order $-n$ and
- a zero of order $r + dn + 2$ at $\infty \in \widehat{\mathbb{C}}_z$.

In consequence, each Ψ_n has:

- r critical points $\{p_i\}_{i=1}^r$ at the roots of $P(z)$, with r critical values $\{\widetilde{p}_i(n) \doteq \Psi_n(p_i)\}_{i=1}^r$,
- d critical points $\{\widehat{e}_\sigma = \widehat{e}_\sigma(n)\}_{\sigma=1}^d$ at the roots of $n - E(z)$ with critical values $\{\widetilde{e}_\sigma(n) \doteq \Psi_n(\widehat{e}_\sigma)\}_{\sigma=1}^d$ and
- a pole of order $-(r + dn + 2)$ at $\infty \in \widehat{\mathbb{C}}_z$.

Each \mathcal{R}_{X_n} has:

- r finitely ramified branch points $\{(p_i, \widetilde{p}_i(n), -\nu_i)\}_{i=1}^r$ with ramification index corresponding to $\nu_i + 1$ where $-\nu_i$ is the order of the pole p_i ,
- d finite ramification points $\{(\widehat{e}_\sigma(n), \widetilde{e}_\sigma(n), -n)\}_{\sigma=1}^d$ with ramification index $n + 1$ and
- a finite ramification point $(\infty, \infty, r + dn + 2)$ with ramification index $r + dn + 3$.

Clearly the critical points p_i do not change as $n \rightarrow \infty$, however the critical values $\widetilde{p}_i(n) \in \mathbb{C}_t$ do, but remain finite without changing their ramification index, thus each finitely ramified branch point $(p_i, \widetilde{p}_i(n), -\nu_i)$ converges to the finitely ramified branch point $(p_i, \widetilde{p}_i, -\nu_i) = (p_i, \Psi_X(p_i), -\nu_i)$.

As the critical points $\{\widehat{e}_\sigma(\mathbf{n})\}$ approach $\infty \in \widehat{\mathbb{C}}_z$, the corresponding critical values $\{\widehat{e}_\sigma(\mathbf{n})\}$ converge to the finite asymptotic values $\{a_\sigma\}$ of Ψ_X , as follows.

In $\widehat{\mathbb{C}}_z$, arguments (directions) and angular sectors at ∞ are well defined. The succession $\widehat{e}_\sigma(\mathbf{n})$ converges to a ray with constant argument θ_σ starting at $\infty \in \widehat{\mathbb{C}}_z$. Moreover, the rays θ_σ and $\theta_{\sigma+1}$ are exactly $2\pi/d$ radians apart.

A key point is the careful examination of the phase portraits of the rational vector fields $\Re(X_n)$ (for the description of the phase portrait in the vicinity of poles and zeros, recall Proposition 3.9 and Figure 1), having the following features:

- i) the zero at ∞ of X_n determines $2r + 2nd + 2$ elliptic sectors, and the same number of separatrices,
- ii) the d poles at \widehat{e}_σ of X_n determine $2n + 2$ hyperbolic sectors, and the same number of separatrices.

The above is summarized in Figure 2 and the following.

Proposition 4.8. *Let $d \geq 1$ and $X \in \mathcal{E}(r, d)$. Then, the sequence of polynomial distinguished parameters Ψ_{X_n} given by (34), converges to Ψ_X . Furthermore:*

- 1) *Each of the r sequences of finitely ramified branch points $(p_i, \tilde{p}_i(\mathbf{n}), -\nu_i) \in \mathcal{R}_{X_n}$ converges to the finitely ramified branch point $(p_i, \tilde{p}_i, -\nu_i) \in \mathcal{R}_X$.*
- 2) *Each of the d sequences of finitely ramified branch points $(\widehat{e}_\sigma(\mathbf{n}), \tilde{e}_\sigma(\mathbf{n}), -\mathbf{n}) \in \mathcal{R}_{X_n}$ converges to the logarithmic branch point $(\infty_\sigma, a_\sigma, -\infty) \in \mathcal{R}_X$.*
- 3) *The $2d$ exponential tracts of Ψ_X are angular sectors of angle π/d about $\infty \in \widehat{\mathbb{C}}_z$ and they alternate so that each exponential tract corresponding to a finite asymptotic value is in between two exponential tracts corresponding to the asymptotic value $\infty \in \widehat{\mathbb{C}}_t$.*
- 4) *There exist $2d$ asymptotic paths $\alpha_\sigma(\tau)$ associated to the asymptotic values $\{a_\sigma\}_{\sigma=1}^{2d}$ of Ψ_X which are angularly equidistributed about $\infty \in \widehat{\mathbb{C}}_z$. \square*

Remark 4.9. 1. By recalling that

$$E(z) = \mu(z^d + c_1 z^{d-1} + \dots + c_d) \text{ in (33),}$$

a simple calculation shows that:

a) for the finite asymptotic values $a_\sigma \in \mathbb{C}_t$ of Ψ_X , without loss of generality we can choose asymptotic paths $\alpha_\sigma(\tau)$ arriving at $\infty \in \widehat{\mathbb{C}}_z$ with angle $\theta_\sigma = \text{Arg}(\mu^{1/d}) + \frac{2\pi}{d}\sigma$ for $\sigma = 1, \dots, d$;

b) likewise, the asymptotic paths $\alpha_\sigma(\tau)$ corresponding to the asymptotic value $\infty \in \widehat{\mathbb{C}}_t$ arrive at $\infty \in \widehat{\mathbb{C}}_z$ with angle $\theta_\sigma = \text{Arg}(\mu^{1/d}) + \frac{2\pi}{d}(\sigma - d) + \frac{\pi}{d}$ for $\sigma = d+1, \dots, 2d$.

2. Figure 2 shows the angular equidistribution of the exponential tracts around ∞ for $X \in \mathcal{E}(r, d)$.

Example 4.2. Let

$$X(z) = \frac{e^{z^d}}{z^r} \frac{\partial}{\partial z} \in \mathcal{E}(r, d), \quad \text{for } d \geq 1.$$

Euler's formula provides the approximation of X by the vector fields

$$X_n(z) = \frac{1}{z^r \left(1 - \frac{z^d}{n}\right)^n} \frac{\partial}{\partial z}, \quad \text{for } n \geq 1,$$

so

$$\Psi_n(z) = \int_0^z \zeta^r \left(1 - \frac{\zeta^d}{n}\right)^n d\zeta = \frac{z^{r+1} {}_2F_1\left(-n, \frac{r+1}{d}; \frac{r+1}{d} + 1; \frac{z^d}{n}\right)}{r+1},$$

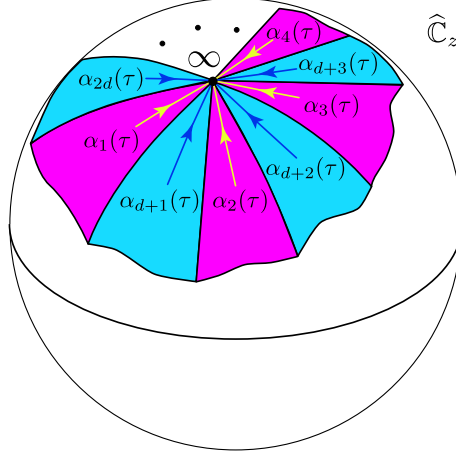


FIGURE 2. Angular equidistribution of the $2d$ exponential tracts about $\infty \in \widehat{\mathbb{C}}_z$, corresponding to the asymptotic values of $\Psi_X(z)$ for $X \in \mathcal{E}(r, d)$, $d \geq 1$. Purple angular sectors represent exponential tracts corresponding to finite asymptotic values $a_\sigma \in \mathbb{C}_t$, in yellow their asymptotic paths $\alpha_\sigma(\tau)$, for $\sigma = 1, \dots, d$. Blue angular sectors represent exponential tracts corresponding to the asymptotic value $\infty \in \widehat{\mathbb{C}}_t$, in dark blue their asymptotic paths, $\alpha_\sigma(\tau)$, for $\sigma = d+1, \dots, 2d$. Once again, the $2d$ asymptotic paths are equally distributed about $\infty \in \widehat{\mathbb{C}}_z$. Note that for the family $\mathcal{E}(r, d)$ this equidistribution property is independent of r .

where ${}_2F_1$ is the classical Gauss's hypergeometric function (see for instance [1] ch. 15).

The poles of X_n are 0, of order $-r$, and $\{\widehat{e}_\sigma(n) \doteq e^{\frac{2i\pi\sigma}{d}} n^{1/d}\}_{\sigma=1}^d$, of order $-n$. Of course the poles of X_n are the critical points of Ψ_n ,

On the other hand, the critical values of Ψ_n are given by $\Psi_n(0) = 0$ and

$$(36) \quad \widetilde{e}_\sigma(n) \doteq \Psi_n(e^{\frac{2i\pi\sigma}{d}} n^{1/d}) = e^{2i\pi\sigma \frac{(r+1)}{d}} \frac{\Gamma\left(\frac{r+1}{d} + 1\right)}{(r+1)} \frac{n^{(r+1)/d} \Gamma(n+1)}{\Gamma\left(n + \frac{r+1}{d} + 1\right)},$$

for $\sigma = 1, \dots, d$.

Furthermore X_n has a unique zero at $\infty \in \widehat{\mathbb{C}}_z$ of order $r + nd + 2$.

Hence each Riemann surface

$$\mathcal{R}_{X_n} = \{(z, \Psi_n(z)) \mid z \in \mathbb{C}_z\}$$

has $(0, 0, -r) \in \mathcal{R}_X$ as a branch point with ramification index $r+1$ and d branch points

$$(\widehat{e}_\sigma(n), \widetilde{e}_\sigma(n, -n)) \in \mathcal{R}_X, \quad \text{for } \sigma = 1, \dots, d,$$

with ramification index $n+1$.

Letting $n \rightarrow \infty$ and since

$$\lim_{n \rightarrow \infty} \frac{\Gamma(n+1) n^{\frac{r+1}{d}}}{\Gamma\left(n + \frac{r+1}{d} + 1\right)} = 1,$$

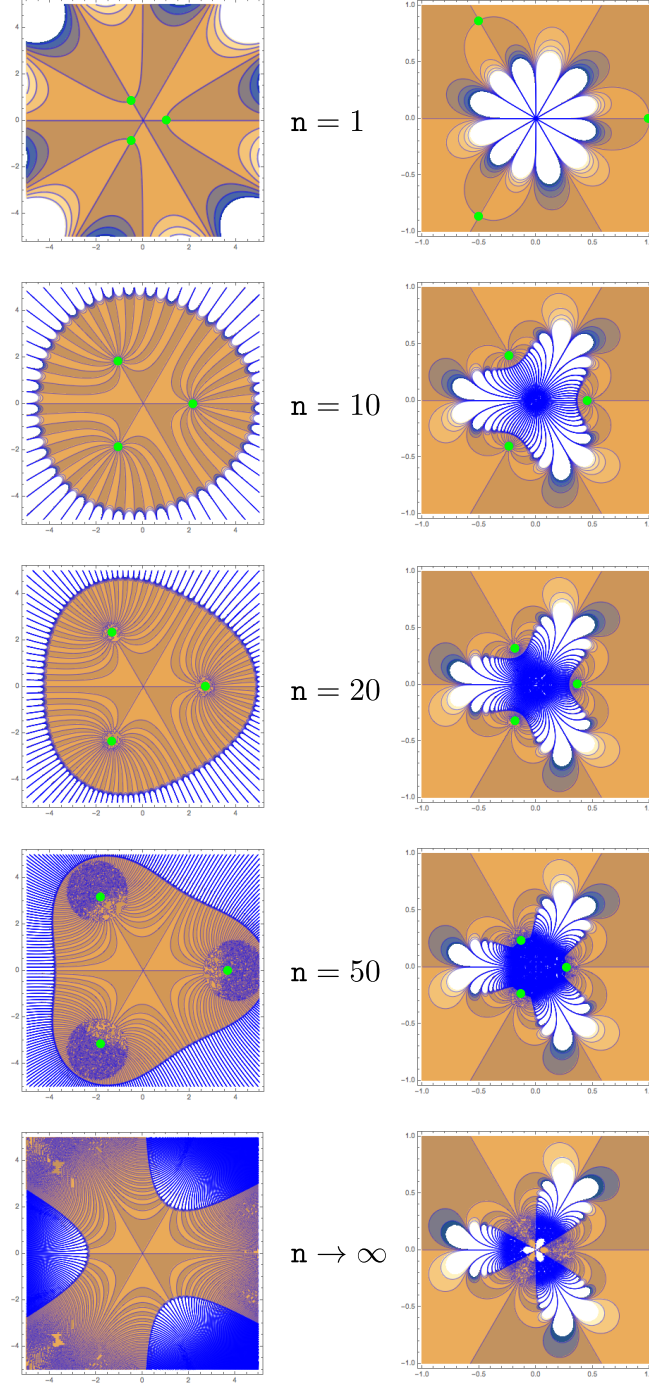


FIGURE 3. Phase portrait of $\Re(X_n)$ for $n = 1, 10, 20, 50$ converging to $\Re(X)$ with $X \in \mathcal{E}(2, 3)$ as in Example 4.2. Left hand side portrays a neighborhood of the origin, and the right hand side a neighborhood of $\infty \in \hat{\mathbb{C}}_z$. Note that by approaching $\infty \in \hat{\mathbb{C}}_z$ along paths that avoid the poles $\{e^{\frac{2i\pi\sigma}{d}} n^{1/d}\}_{\sigma=1}^d$ (green dots), the value of $\Psi_n(z)$ converges to $\infty \in \hat{\mathbb{C}}_t$.

we conclude that the critical values $\tilde{e}_\sigma(\mathbf{n})$ converge, along the asymptotic paths $\alpha_\sigma(\tau) = \tau e^{2i\pi\sigma/d}$ suggested by the sequence of critical points $\{\hat{e}_\sigma(\mathbf{n})\}_{\mathbf{n}=1}^\infty$, to the finite asymptotic values a_σ of $\Psi_X(z) = \int_0^z \zeta^r e^{-\zeta^d} d\zeta$, given by

$$(37) \quad a_\sigma = e^{2i\pi\sigma \frac{(r+1)}{d}} \frac{\Gamma\left(\frac{r+1}{d} + 1\right)}{(r+1)} \in \mathbb{C}_t, \quad \text{for } \sigma = 1, \dots, d.$$

Furthermore, traveling along the asymptotic paths $\alpha_\sigma(\tau) = \tau e^{2i\pi(\sigma-d)/d} e^{i\pi/d}$, that arrive at $\infty \in \widehat{\mathbb{C}}_z$ with angle $\frac{2\pi}{d}(\sigma-d) + \frac{\pi}{d}$, for $\sigma = d+1, \dots, 2d$, we see that $\Psi_{\mathbf{n}}(z)$ converges to $\infty \in \widehat{\mathbb{C}}_t$, thus there are d (classes of) asymptotic paths that give rise to the asymptotic value $\infty \in \widehat{\mathbb{C}}_t$.

In Figure 3 we visualize (using the techniques presented in [4]), for $r = 2$, $d = 3$, the phase portraits of $\Re(X_{\mathbf{n}})$, for $\mathbf{n} = 1, 10, 20, 50$, and $\Re(X)$. The poles $\{e^{\frac{2i\pi\sigma}{d}} \mathbf{n}^{1/d}\}_{\sigma=1}^d$ are portrayed as green dots. Note that at $\infty \in \widehat{\mathbb{C}}_z$ there is a zero of $X_{\mathbf{n}}$ of order exactly $r + d\mathbf{n} + 2 = 3\mathbf{n} + 4$.

5. THE GEOMETRY OF THE RIEMANN SURFACE \mathcal{R}_X ; SETUP FOR THE PROOF OF MAIN THEOREM

This section has two goals: understanding the geometry of the Riemann surface \mathcal{R}_X for $X \in \mathcal{E}(r, d)$ and setting up the geometrical/combinatorial elements in order to define vertices, edges and weights of the (r, d) -configuration trees.

5.1. Branch points of \mathcal{R}_X as vertices. Since the branch points of \mathcal{R}_X over $\infty \in \widehat{\mathbb{C}}_t$ are independent of $X \in \mathcal{E}(r, d)$, they will not enter the proof of the Main Theorem, thus the following concept is natural.

Definition 5.1. For $d \geq 1$, the *reduced divisor* of $X \in \mathcal{E}(r, d)$ is

$$(38) \quad X \mapsto \underbrace{\left\{ \textcircled{\iota} = (p_\iota, \tilde{p}_\iota, -\nu_\iota) \right\}_{\iota=1}^n}_{\text{pole vertices}} \cup \underbrace{\left\{ \textcircled{n+\sigma} = (\infty_\sigma, a_\sigma, -\infty) \right\}_{\sigma=1}^d}_{\text{essential vertices}} = \left\{ \textcircled{\mathbf{a}} = (z_{\mathbf{a}}, t_{\mathbf{a}}, -\nu_{\mathbf{a}}) \right\}_{\mathbf{a}=1}^{n+d}.$$

Remark 5.2. The corresponding critical points of Ψ_X (and transcendental singularities of Ψ_X^{-1}) are

$$(39) \quad z_{\mathbf{a}} \in \{p_1, \dots, p_\iota, \dots, p_n, \infty_1, \dots, \infty_\sigma \dots \infty_d\} \subset \overline{\mathbb{C}}_z$$

once again $n \leq r$, with equality if and only if all the poles of X are simple. Recalling Remark 4.6.2, their $n + m$ critical and finite asymptotic values of Ψ_X are to be denoted by

$$(40) \quad t_{\mathbf{a}} \in \{\tilde{p}_1, \dots, \tilde{p}_\iota, \dots, \tilde{p}_n, a_1, \dots, a_{j(\sigma)}, \dots, a_m\} \subset \mathbb{C}_t,$$

where $m \leq d$, with equality if and only if all the finite asymptotic values of Ψ_X are of multiplicity one.

The main features of $\textcircled{\mathbf{a}}$ are summarized in Table 1.

TABLE 1. Branch points of \mathcal{R}_X .

Branch point $(z_a, t_a) \in \mathcal{R}_X$	Vertex $\textcircled{a} = (z_a, t_a, -\nu_a)$	Notation in (r, d) -configuration trees; meaning
(p_l, \tilde{p}_l) (25)	$\textcircled{l} = (p_l, \tilde{p}_l, -\nu_l)$	Pole vertices if $r \geq 1$; $\tilde{p}_l = \Psi_X(p_l)$ is a critical value of Ψ_X , p_l is a pole of X having order $-\nu_l \leq -1$, hence (p_l, \tilde{p}_l) is a branch point with ramification index $\nu_l + 1 \geq 2$.
(∞, ∞)	(∞, ∞, s)	Zero vertex when $d = 0$, $r \geq 1$ in which case $s = 2 + r$; $\infty \in \hat{\mathbb{C}}_z$ is a zero of X having order s .
$(\infty_\sigma, a_\sigma)$ (31)	$\textcircled{n+\sigma} = (\infty_\sigma, a_\sigma, -\infty)$	Essential vertices if $d \geq 1$; $\infty \in \hat{\mathbb{C}}_z$ is an essential singularity of X , $a_\sigma \in \mathbb{C}_t$ being a finite asymptotic value of Ψ_X , with exponential tract $U_\sigma(\rho)$, so $(\infty_\sigma, a_\sigma, -\infty)$ is a logarithmic branch point in (the closure of) $\mathcal{R}_X \subset \overline{\mathbb{C}}_z \times \hat{\mathbb{C}}_t$.

5.2. The families of surfaces \mathcal{R}_X having only one vertex. We describe the families of vector fields avoided in the Main Theorem, *i.e.* those having exactly one branch point over \mathbb{C}_t .

Lemma 5.3. *Let $X \in \mathcal{E}(r, d)$. The associated Ψ_X has exactly one finite critical or asymptotic value $t_1 \in \mathbb{C}_t$ if and only if*

$$(r, d) = \begin{cases} (r \geq 1, 0) & \begin{aligned} &X \text{ has a unique pole of order } -r, \\ &\text{in which case } t_1 \text{ is the finite critical value,} \end{aligned} \\ (0, 1) & \begin{aligned} &X \text{ has an isolated essential singularity at } \infty \in \hat{\mathbb{C}}_z, \\ &\text{in which case } t_1 \text{ is the finite asymptotic value.} \end{aligned} \end{cases}$$

Proof. (\Leftarrow) The case X has a unique pole of order $-r$, is obvious: the required distinguished parameter is given by Equation (17) and the unique finite critical value is given by Equation (18).

When $(r, d) = (0, 1)$, the distinguished parameter is given by Equation (21) and the unique finite asymptotic value is given by Equation (22).

(\Rightarrow) By Lemma 4.1, Ψ_X^{-1} has d logarithmic branch points over d finite asymptotic values of Ψ_X , d logarithmic branch points over $\infty \in \hat{\mathbb{C}}_t$ and r critical values (counted with multiplicity).

Let $\{(z_a, t_1)\} \subset \pi_{X,2}^{-1}(t_1) \subset \mathcal{R}_X$ be all the branch points over t_1 . The set $\{(z_a, t_1)\}$ consists of

- exactly d logarithmic branch points over t_1 and
- n ($\leq r$) finitely ramified branch points (p_l, t_1) of ramification indices $\nu_l + 1$ with $r = \sum_{l=1}^{n \leq r} \nu_l$.

Note that there are $d + n \geq 1$ *distinct* branch points of \mathcal{R}_X .

Moreover, \mathcal{R}_X is a connected Riemann surface (it is the graph of Ψ_X). The restriction of the second projection over the punctured plane

$$\pi_{X,2} : \mathcal{R}_X \setminus \{\pi_{X,2}^{-1}(t_1)\} \longrightarrow \mathbb{C} \setminus \{t_1\}$$

is a holomorphic cover without ramification. The subgroups G of $\pi_1(\mathbb{C} \setminus \{t_1\}) \cong \mathbb{Z}$ classify topologically these covers.

For $G = \mathbb{Z}_{r+1}$ with $r \geq 1$, the cover is finite cyclic and we can recognize that $\Psi_X(z)$ is as in (17), using Riemann's removable singularity Theorem. This implies $X \in \mathcal{E}(r, 0)$ has a unique pole as in the first assertion.

While for $G = \mathbb{Z}$, using Lemma 4.1 assertion 3 we can recognize $\Psi_X(z)$ as in (21), which in turn provides the corresponding $X \in \mathcal{E}(0, 1)$.

The case $G = id$, gives $\Psi_X(z) = \frac{1}{\lambda}(z - p_1)$ and the constant vector field $X(z) = \lambda \frac{\partial}{\partial z}$, that does not belong to $\mathcal{E}(r, d)$. \square

5.3. Diagonals of \mathcal{R}_X as edges. Because of Lemma 5.3 from now on, unless explicitly noted, we assume that there are two or more finite critical or asymptotic values $t_a \in \mathbb{C}_t$ of Ψ_X .

In order to completely describe \mathcal{R}_X , we also require information of the relative position of the branch points of the surface, recall Diagram 12 and Definition 4.7; let $\{\mathfrak{a} = (z_a, t_a, -\nu_a)\}_{a=1}^{n+d}$ as in Equation (38).

Consider the oriented straight line segment $\overline{t_a t_r} \subset \mathbb{C}_t$. The inverse image

$$\pi_{X,2}^{-1}(\overline{t_a t_r}) = \{\Delta_{\vartheta ar}\} \subset \mathcal{R}_X$$

is a set consisting of a finite (when $m = 0$, equivalently $d = 0$) or an infinite (when $m \geq 1$) number of copies of $\overline{t_a t_r}$. A priori, for each segment $\Delta_{\vartheta ar}$, the projection $\pi_{X,1}(\Delta_{\vartheta ar}) \subset \overline{\mathbb{C}_z}$ can have regular points at its end points.

Definition 5.4. 1. A segment $\Delta_{\vartheta ar}$ is a *diagonal of \mathcal{R}_X* when the interior of $\pi_{X,1}(\Delta_{\vartheta ar})$ is in \mathbb{C}_z and the endpoints of $\pi_{X,1}(\Delta_{\vartheta ar})$ are $z_a, z_r \in \{p_1, \dots, p_n, \infty_1, \dots, \infty_d\} \subset \overline{\mathbb{C}_z}$; critical points of Ψ_X or transcendental singularities of Ψ_X^{-1} .

2. A given diagonal

$$\Delta_{\vartheta ar}, \text{ starts at } \mathfrak{a} = (z_a, t_a, -\nu_a) \text{ and ends at } \mathfrak{r} = (z_r, t_r, -\nu_r).$$

We shall say that the branch points of $\pi_{X,2}$, \mathfrak{a} and \mathfrak{r} , share the same sheet $\mathbb{C}_{\Delta_{\vartheta ar}} \setminus \{\text{suitable branch cuts}\}$ in \mathcal{R}_X .

Remark 5.5. 1. By notational simplicity, if we drop the index ϑ from $\Delta_{\vartheta ar}$ we are specifying the unique diagonal Δ_{ar} . The following identification will be useful in the proof of the Main Theorem

$$(41) \quad \underbrace{\Delta_{ar} \subset \mathcal{R}_X \text{ with endpoints } \mathfrak{a}, \mathfrak{r}}_{\text{diagonal}} \longleftrightarrow \underbrace{\Delta_{ar}}_{\text{oriented edge}}.$$

2. Note that since Ψ_X is a uni-valued function, there can not be homoclinic trajectories of $\Re(X)$ from a pole p to itself; *i.e.* there does not exist a diagonal $\Delta_{\iota\kappa}$ whose endpoints are the finitely ramified branch points $(p_\iota, \tilde{p}_\iota, -\nu_\iota)$ and $(p_\kappa, \tilde{p}_\kappa, -\nu_\kappa)$, with $\pi_{X,1}(p_\iota) = \pi_{X,1}(p_\kappa) = p$.

3. The diagonals Δ_{ar} can have endpoints as follows:

- 1) $\Delta_{\iota\kappa}$ has as endpoints two finitely ramified branch points (corresponding to pole vertices): $(p_\iota, \tilde{p}_\iota, -\nu_\iota)$ and $(p_\kappa, \tilde{p}_\kappa, -\nu_\kappa)$, $\iota \neq \kappa$. For an example see Figure 8 in §8.
- 2) $\Delta_{\iota\sigma}$ has as endpoints a finitely ramified branch point and a logarithmic branch point (corresponding to a pole and an essential vertex) or viceversa: $(p_\iota, \tilde{p}_\iota, -\nu_\iota)$ and $(\infty_\sigma, a_\sigma, -\infty)$. For an example see Figure 14 in §8.

- 3) $\Delta_{\sigma\rho}$ has as endpoints two logarithmic branch points (corresponding to essential vertices) with finite asymptotic values a_σ and a_ρ with exponential tracts α_σ and α_ρ : $(\infty_\sigma, a_\sigma, -\infty)$ to $(\infty_\rho, a_\rho, -\infty)$, $\sigma \neq \rho$, where the subscripts are as in (29). For an example see Figure 13 in §8.

Following the notation in [24], for Δ_{ar} a diagonal the associated *semi-residue* is

$$(42) \quad S(\omega_X, z_a, z_\tau) \doteq \int_{z_a}^{z_\tau} P(\zeta) e^{-E(\zeta)} d\zeta = t_\tau - t_a.$$

Lemma 5.6 (Existence of diagonals in \mathcal{R}_X). *Suppose that there are at least two branch points $\{\textcircled{a} = (z_a, t_a, -\nu_a)\}_{a=1}^{n+d} \subset \mathcal{R}_X$. Then every branch point \textcircled{a} is an endpoint for at least two diagonals, an incoming diagonal and an outgoing diagonal.*

Proof. Consider any branch point $\textcircled{a} = (z_a, t_a, -\nu_a) \in \pi_{X,2}^{-1}(t_a)$, with t_a as in Equation (40). Suppose that there is no diagonal Δ_{ar} with endpoint \textcircled{a} . This implies that \textcircled{a} does not share a sheet, $\mathbb{C}_t \setminus \{\text{suitable branch cuts}\}$, with any other branch point $\textcircled{\tau} = (z_\tau, t_\tau, -\nu_\tau) \in \pi_{X,2}^{-1}(t_\tau)$, for some finite asymptotic or critical value $t_\tau \neq t_a$ (note that the existence of t_τ is guaranteed by Lemma 5.3). In other words the only sheets, $\mathbb{C}_t \setminus \{\text{suitable branch cuts}\}$, of \mathcal{R}_X containing the branch point \textcircled{a} are of the form $\mathbb{C}_t \setminus \{L_a\}$, for $L_a = [t_a, \infty)$. Hence by the same arguments as in Lemma 5.3, the Riemann surface \mathcal{R}_X will have at least 2 connected components (one containing \textcircled{a} and the other containing $\textcircled{\tau}$), leading to a contradiction. \square

5.4. Geometrical building blocks and the weights of edges. Our elementary building blocks are pairs, Riemann surface and singular complex analytic vector fields, as follows.

Definition 5.7. The pair $(\overline{\mathbb{H}}_\pm^2, \frac{\partial}{\partial t})$ will be called a *(closed) half plane*; the closure of $\overline{\mathbb{H}}_\pm^2$ is considered in \mathbb{C} , hence its boundary is \mathbb{R} .

Likewise, $(\{0 \leq \Im(t) \leq h\}, \frac{\partial}{\partial t})$ will be called a *(closed) finite height horizontal strip*.

In the flat surface category, surgery tools are widely used, *v.g.* [44] p. 56 “welding of surfaces”, [37], or [48] §3.2–3.3 for general discussion.

Corollary 5.8 (Isometric glueing). *Let (M^0, g_X) , (N^0, g_Y) be two flat surfaces arising from two singular complex analytic vector fields X and Y . Assume that both spaces M^0 , N^0 have as geodesic boundary components of the same length: the trajectories $\sigma_1(\tau)$, $\sigma_2(\tau)$ of $\Re(X)$ and $\Re(Y)$, $\tau \in I \subset \mathbb{R}$. The isometric glueing of them along these geodesic boundary, is well defined, and provides a new flat surface on $M^0 \cup N^0$ arising from a new complex analytic vector field.* \square

Lemma 5.9. *Let $X \in \mathcal{E}(r, d)$.*

- 1) *The Riemann surface \mathcal{R}_X can be constructed by isometric glueing of*
 - *half planes $(\overline{\mathbb{H}}_\pm^2, \frac{\partial}{\partial t})$ and*
 - *finite height horizontal strips $(\{0 \leq \Im(t) \leq h\}, \frac{\partial}{\partial t})$, where $h \geq 0$.*
- 2) *There exists a one-to-one correspondence*

$$\left\{ \begin{array}{c} \text{finite height horizontal strips} \\ (\{0 \leq \Im(z) \leq h\}, \frac{\partial}{\partial t}) \end{array} \right\} \longleftrightarrow \left\{ \begin{array}{c} \text{diagonals } \Delta_{\text{ar}} \text{ with} \\ |\Im\left(\int_{z_a}^{z_\tau} \omega_X\right)| = h \geq 0 \end{array} \right\},$$

here $\textcircled{a} = (z_a, t_a, -\nu_a)$ and $\textcircled{\tau} = (z_\tau, t_\tau, -\nu_\tau)$.

- 3) The case when $\Im \left(\int_{z_a}^{z_r} \omega_X \right) = 0$ corresponds to the finite height horizontal strip degenerating into a segment of trajectory of $\Re(X)$ between the branch points \mathfrak{a} and \mathfrak{r} , i.e. a horizontal diagonal $\Delta_{\mathfrak{ar}}$.

Proof. Assertion (1) follows by using Lemma 4.1, we can consider the pullback under $\pi_{X,2}$ of the vector field $\frac{\partial}{\partial t}$ to \mathcal{R}_X . Thus, the phase portrait of $\Re(X)$ determines the decomposition.

Assertion (2) and (3) follow directly from Definition 5.4. \square

Definitions 5.10, 5.12 below apply for singular flat Riemann surfaces (not necessarily of type \mathcal{R}_X).

Definition 5.10. Let $\{t_k\}_{k=1}^r \subset \mathbb{C}_t$ be a finite set of distinct points. A *sheet* is a copy of \mathbb{C}_t with $r \geq 1$ branch cuts L_k ; i.e. \mathbb{C}_t is cut along horizontal right segments $L_k = [t_k, \infty)$, remaining connected

$$(43) \quad \mathbb{C}_t \setminus \{L_k\}_{k=1}^r \doteq [\mathbb{C}_t \setminus (\cup_{k=1}^r [t_k, \infty))] \cup_{k=1}^r \{[t_k, \infty)_+, [t_k, \infty)_-\},$$

having $2r$ horizontal boundaries where the subscripts \pm refer to the obvious upper or lower boundary using $\Im(t)$.

See Figure 4 for examples of sheets.

Remark 5.11. 1. The sheets $\mathbb{C}_t \setminus \{L_k\}_{k=1}^r$ include the upper and lower boundaries $[t_k, \infty)_\pm$.
2. Note that cuts (and the corresponding boundaries) need not be to the right, they could be more general simple paths, however for notational simplicity and ease of the proofs we shall only use right cuts $[t_k, \infty)_\pm$ as in (43).

Definition 5.12. A *diagonal of the sheet* $\mathbb{C}_t \setminus \{L_k\}_{k=1}^r$ is an oriented straight line segment

$$(44) \quad \Delta_{\mathfrak{ar}} = \overline{t_{\mathfrak{a}} t_{\mathfrak{r}}} \subset \mathbb{C}_t \setminus \{L_k\}_{k=1}^r,$$

starting at $t_{\mathfrak{a}}$ and ending at $t_{\mathfrak{r}}$, here $\mathfrak{r}, \mathfrak{a}$ are as in Equation (40).

The abuse of notation in Equations (41), (42), and (44), will be cleared in the proof of the main Theorem. See Figures 4.b, 4.c and Figure 8 for examples of diagonals of sheets.

We introduce, four non elementary building blocks, pictured in Figure 4, their Definitions 5.13, 5.15, 5.17 include a geometrical and a combinatorial framework.

Recalling Example 4.1 we propose the following.

Definition 5.13. A *semi-infinite helicoid* is the Riemann surface of

$$\int_{z_0}^z e^{-\mu(\zeta+c_1)} d\zeta - a_\sigma = -\frac{1}{\mu} e^{-\mu(z+c_1)} : \overline{\mathbb{H}}_\pm^2 \subset \mathbb{C}_z \longrightarrow \mathbb{C}_t$$

having a horizontal boundary $[a_\sigma, \infty)_\pm$, geometrically it is an infinite succession of half-planes

$$\left((\overline{\mathbb{H}}_\pm^2 \cup \overline{\mathbb{H}}_\mp^2 \cup \dots), \frac{\partial}{\partial t} \right).$$

glued in the usual way, Corollary 5.8. See Figure 4.a.

Remark 5.14. In the combinatorial framework, for $X \in \mathcal{E}(r, d)$, each essential vertex $\bigcirc_{n+\sigma} = (\infty_\sigma, a_\sigma, -\infty)$ has associated two semi-infinite helicoids, up and down, respectively.

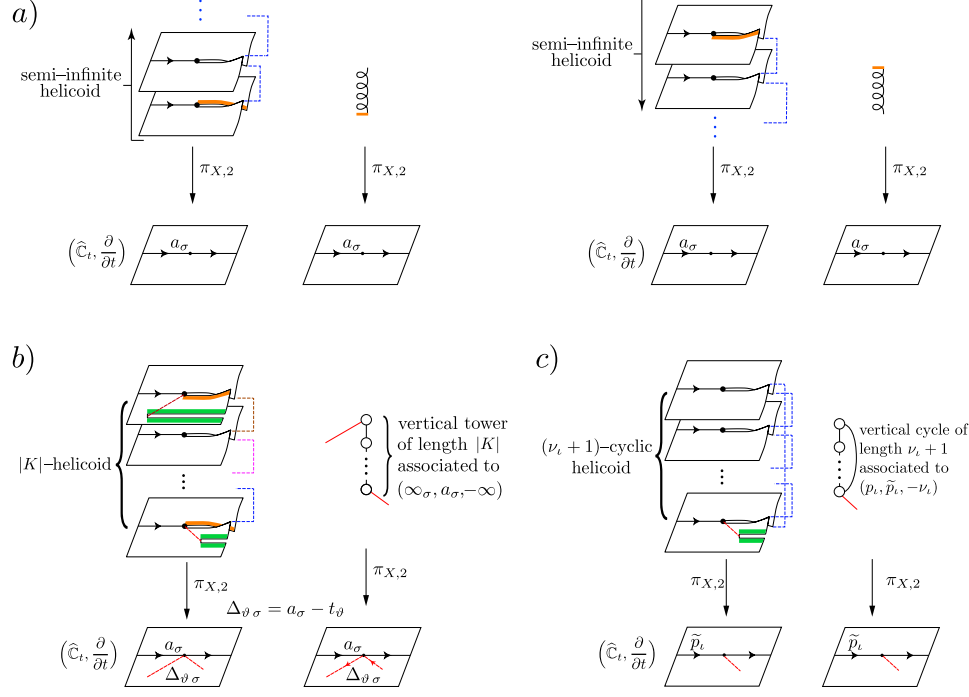


FIGURE 4. In this figure we have the representation of the non elementary building blocks as sheets with branch cuts glued appropriately in \mathcal{R}_X , and schematically as a graph. (a) On the top row we have the semi-infinite (up and down) helicoids. On the bottom row we have (b) on the left a $|K|$ -helicoid and (c) on the right an $(\nu_l + 1)$ -cyclic helicoid, for $(\nu_l + 1) \geq 2$. In the $|K|$ -helicoids and $(\nu_l + 1)$ -cyclic helicoids the red segments are diagonals.

Pictorially, we will represent each one by a small coil in our figures. However, the semi-infinite helicoids and their coils do not appear in the formal (r, d) -configuration trees.

Geometric characteristics: a semi-infinite helicoid

- lies over the finite asymptotic value $a_\sigma \in \mathbb{C}_t$,
- has an infinite number of sheets,
- its horizontal boundary is coloured in orange,
- is up or down (resp. the domain of its integral is $\overline{\mathbb{H}}_+^2$ or $\overline{\mathbb{H}}_-^2$).

Recalling the Example 4.1, we have the following.

Definition 5.15. For $K \in \mathbb{Z}$, a $|K|$ -helicoid is the Riemann surface of

$$\int_{z_0}^z e^{-\mu(\zeta+c_1)} d\zeta - a_\sigma = -\frac{1}{\mu} e^{-\mu(z+c_1)} : \mathcal{D} \subset \mathbb{C}_z \longrightarrow \mathbb{C}_t$$

where

$$\mathcal{D} = \begin{cases} \{0 \leq \Im(\mu z) \leq 2\pi(K+1)\}, & K \geq 0 \\ \{2\pi K \leq \Im(\mu z) \leq 2\pi\}, & K < 0, \end{cases}$$

having a finite number $\ell \geq 2$ of branch cuts $\{L_k\}_{k=2}^\ell$, geometrically it as a succession of $2(|K| + 1)$ half-planes

$$\left((\overline{\mathbb{H}}_\pm^2 \cup \overline{\mathbb{H}}_\mp^2 \cup \dots \cup \overline{\mathbb{H}}_\mp^2), \frac{\partial}{\partial t} \right)$$

glued in the usual way, with 2ℓ horizontal boundaries.

In the combinatorial framework, for $X \in \mathcal{E}(r, d)$, the following objects are equivalent:

a $|K|$ -helicoid,

a *vertical tower of length* $|K|$.

See Figure 4.b.

Remark 5.16. Each essential vertex $\bigcirc_{n+\sigma} = (\infty_\sigma, a_\sigma, -\infty)$ determines at least one $|K(\sigma)|$ -helicoid.

Geometric characteristics: a $|K|$ -helicoid

- lies over the finite asymptotic value $a_\sigma \in \mathbb{C}_t$,
- has $|K| + 1$ sheets and there are three subcases.

If $K > 0$ or $K < 0$, the $|K|$ -helicoid:

- goes up or down depending on the sign of $K \neq 0$,
- has $\ell \geq 2$ diagonals with common extreme points over $a_\sigma \in \mathbb{C}_t$,
- in particular, there are always 2 diagonals present: one on the image of the strip $\{0 \leq \Im(z) \leq 2\pi\}$,

and the other on the image of the strip

$$\{2\pi K \leq \Im(z) \leq 2\pi(K + 1)\}$$

K sheets above/below,

- has $2\ell \geq 4$ horizontal boundaries (arising from diagonals, colored green) and 2 horizontal boundaries (orange),

If $K = 0$, the $|K|$ -helicoid:

- has $\ell \geq 0$ diagonals having common extreme points over $a_\sigma \in \mathbb{C}_t$,
- has $2\ell \geq 0$ horizontal boundaries from diagonals (green) and 2 horizontal boundaries (orange).

Recalling the case of a pole, Example 3.1, we have the following.

Definition 5.17. A $(\nu_\iota + 1)$ -cyclic helicoid is the Riemann surface of

$$\frac{1}{\lambda} \int_{z_0}^z (\zeta - p_\iota)^{\nu_\iota} d\zeta + \tilde{p}_\iota = \frac{1}{\lambda} \frac{(z - p_\iota)^{\nu_\iota + 1}}{\nu_\iota + 1} : \mathbb{C}_z \longrightarrow \mathbb{C}_t$$

having a finite number $\{L_k\}_{k=0}^\ell$, $\ell \in \mathbb{N} \cup \{0\}$, of branch cuts, geometrically it is a finite succession of $2\nu_\iota + 2$ half-planes

$$\left((\overline{\mathbb{H}}_\pm^2 \cup \overline{\mathbb{H}}_\mp^2 \cup \dots \cup \overline{\mathbb{H}}_\mp^2), \frac{\partial}{\partial t} \right)$$

glued in the usual way, with $2\ell \geq 0$ horizontal boundaries.

In the combinatorial framework for $X \in \mathcal{E}(r, d)$, the following three objects are equivalent:

a $(\nu_\iota + 1)$ -cyclic helicoid,

a *vertical cycle of length* $\nu_\iota + 1$,

a pole vertex $\bigcirc_\iota = (p_\iota, \tilde{p}_\iota, -\nu_\iota)$.

See Figure 4.c.

Geometric characteristics: a $(\nu_\iota + 1)$ -cyclic helicoid

- lies over the finite critical value $\tilde{p}_\iota \in \mathbb{C}_t$,
- has $\nu_\iota + 1$ sheets,
- has $\ell \geq 0$ diagonals with common extreme points over \tilde{p}_ι .

Remark 5.18 (Cut and paste of the different geometric pieces for $X \in \mathcal{E}(r, d)$). The paste of a semi-infinite helicoid and a cyclic helicoid is forbidden; and the paste of two semi-infinite helicoids will appear essentially only for $X \in \mathcal{E}(0, 1)$, as in Example 4.1.

Semi-infinite helicoids and $|K|$ -helicoids are glued along their orange horizontal boundaries, see Figure 4.

Remark 5.19 (The weights of the edges). 1. In order to construct the surface \mathcal{R}_X by glueing the geometric pieces described in Lemma 5.9, we shall need to specify not only the branch points $\{\mathfrak{a} = (z_a, t_a, -\nu_a)\}_{a=1}^{n+d}$ and the corresponding diagonals $\{\Delta_{ar}\}$ of the sheets, but also how many sheets each geometric piece has. 2. In what follows, the term “vertical” refers to the z -direction in $\overline{\mathbb{C}}_z \times \mathbb{C}_t$. Let $(z_a, t_a, -\nu_a) \in \mathcal{R}_X$ be a fixed branch point, we consider the usual lifting

$$\beta(\theta) = \pi_{X,2}^{-1}(t_a + \rho e^{i2\pi\theta}) \subset \mathcal{R}_X \quad \text{where } \theta \in [\theta_{min}, \theta_{max}] \subset \mathbb{R},$$

for appropriate $\theta_{min}, \theta_{max}$ and small enough $\rho > 0$.

3. As is usual, three cases appear:

- i) Going around a branch point counterclockwise corresponds to going *up* on the ramified surface \mathcal{R}_X and hence the number that separates the sheets is positive.
 - ii) Similarly going around the branch point clockwise corresponds to going *down*.
 - iii) Furthermore going K times around a finitely ramified branch point of \mathcal{R}_X of ramification index ν is equivalent to going around it $K \pmod{\nu}$ times.
4. Whenever there are two (or more) diagonals sharing the same branch point, the number of sheets that separate the diagonals in question can be counted on the Riemann surface \mathcal{R}_X as number of planes traversed by a small enough circular path $\beta(\theta)$ around the common branch point. In this way, by choosing a *local zero level sheet* for each branch point of \mathcal{R}_X , we will be able to assign a weight to each edge/diagonal attached to the branch point (relative to the local zero level sheet).

6. WHY IS THE GEOMETRICAL DESCRIPTION OF $\mathcal{E}(r, d)$ DIFFICULT?

Let X be in $\mathcal{E}(r, d)$. The graph of Ψ_X is the flat Riemann surface \mathcal{R}_X . In order to get an accurate combinatorial description of \mathcal{R}_X for the family $\mathcal{E}(r, d)$, we shall need to specify two basic sets:

i) the vertices or branch points

$$\{\odot = (p_l, \tilde{p}_l, -\nu_l)\}_{l=1}^n \cup \left\{ \bigcirc = (\infty_\sigma, a_\sigma, -\infty) \right\}_{\sigma=1}^d = \left\{ \mathfrak{a} = (z_a, t_a, -\nu_a) \right\}_{a=1}^{n+d}$$

of \mathcal{R}_X , *i.e.* the reduced divisor of X , Definition 5.1,

ii) a subset of the diagonals $\{\Delta_{ar}\}$, Equation (41), connecting the branch points (in particular it will be useful to know which branch points share specific sheets of \mathcal{R}_X).

The implicit combinatorial obstacles are:

- D.1 No canonical choice for the initial integration point of $\Psi_X(z) = \int_{z_0}^z \omega_X$ can be given.
- D.2 There is no preferred/canonical *global zero level*, denoted (GZL),
 $\mathbb{C}_{\Delta_{ar}} \setminus \{\text{suitable branch cuts}\} \subset \mathcal{R}_X$,
that is to be chosen to start the description of \mathcal{R}_X as a combinatorial object.
- D.3 No canonical order can be given to the branch points $\{\mathfrak{a} = (z_a, t_a, -\nu_a)\}_{a=1}^{n+d}$ of \mathcal{R}_X .

D.4 *A priori*, the choice of minimal subset of the diagonals required to describe \mathcal{R}_X is non canonical.

In particular, note that difficulty D.1 will have a repercussion on the labeling of the vertices in Definition 7.7, while difficulties D.2 and D.3 are associated to the choice of a suitable root $\textcircled{1}$ in the reduced divisor. Difficulty D.4 will require a certain ordering of the subset of the diagonals on each sheet of \mathcal{R}_X (as will appear in Definition 7.6).

The resolution of these choices/conventions motivates the notion of equivalence classes $[\Lambda_X]$ as in our Main Theorem, see §9.4.

There are also analytical obstructions/obstacles:

D.5 Not all the vertices $\{\textcircled{\iota} = (p_\iota, \tilde{p}_\iota, -\nu_\iota)\}_{\iota=1}^n \cup \{\textcircled{n+\sigma} = (\infty_\sigma, a_\sigma, -\infty)\}_{\sigma=1}^d$ are possible as branch points for \mathcal{R}_X , only those that are a solution to the system of transcendental equations

$$(45) \quad \begin{cases} \Psi_X(p_\iota) = \tilde{p}_\iota \\ \Psi_X^{(\ell)}(p_\iota) = 0 & 1 \leq \ell \leq \nu_\iota, \quad \iota = 1, \dots, n, \\ \lim_{\tau \rightarrow \infty} \alpha_\sigma(\tau) = \infty_\sigma \\ \lim_{\tau \rightarrow \infty} \Psi_X(\alpha_\sigma(\tau)) = a_\sigma & \sigma = 1, \dots, d. \end{cases}$$

The last two equalities are analytical expressions of the geometrical structure of Figure 2. From a general point of view, we can consider abstract divisors (finite collection of triplets).

Definition 6.1. We shall say that an abstract collection of $n + d$ vertices

$$\{\textcircled{\iota} = (p_\iota, \tilde{p}_\iota, -\nu_\iota)\}_{\iota=1}^n \cup \{\textcircled{n+\sigma} = (\infty_\sigma, a_\sigma, -\infty)\}_{\sigma=1}^d$$

is *realizable* if it is a solution of (45), for some $\Psi_X, X \in \mathcal{E}(r, d)$.

7. COMBINATORIAL OBJECTS: (r, d) -CONFIGURATION TREES

In order to make precise the choices required to resolve the issues D.1, D.3, D.4 and D.5 cited in §6, we introduce the following auxiliary concepts: weighted directed zero-rooted trees and (r, d) -configuration trees, which can be understood as associated to some \mathcal{R}_X (even though they are abstract graphs, a priori not necessarily associated to the Riemann surface \mathcal{R}_X).

To accomplish the above, we shall use some basic notions of graph theory, namely trees, oriented or not, with and without roots and weights, see [31] pp. 46, 379 for standard concepts. It is natural to use the branch points of \mathcal{R}_X , described by the reduced divisor, Definition 5.1,

$$\{\textcircled{\mathfrak{a}} = (z_{\mathfrak{a}}, t_{\mathfrak{a}}, -\nu_{\mathfrak{a}})\}_{\mathfrak{a}=1}^{n+d} \quad \text{with} \quad z_{\mathfrak{a}} \in \overline{\mathbb{C}}_z, t_{\mathfrak{a}} \in \mathbb{C}_t \text{ and } \nu_{\mathfrak{a}} \in \mathbb{N} \cup \{\infty\},$$

as vertices of our graphs, **with a possible re-labelling when needed.**

To resolve issue D.1, we introduce *directed rooted trees* which have one vertex designated as the *root* $\textcircled{\varrho}$ and its edges are assigned an orientation

$$(46) \quad \Lambda = \left\{ \underbrace{\textcircled{1}, \dots, \textcircled{\mathfrak{r}}, \dots, \textcircled{\mathfrak{a}}, \dots, \textcircled{\mathfrak{m}}}_{\text{vertices}}; \underbrace{\textcircled{\varrho}}_{\text{root}}; \underbrace{\Delta_{\mathfrak{a}\mathfrak{r}}, \dots}_{\substack{\mathfrak{m}-1 \\ \text{oriented edges}}} \right\},$$

where $\mathfrak{m} \leq n + d$, *i.e.* not all vertices in Definition 5.1 are necessarily considered. We shall consider directed rooted trees that have an orientation away from the root

and convene that $\Delta_{\mathfrak{a}\mathfrak{r}}$ denotes the edge starting at \mathfrak{a} and ending at \mathfrak{r} . The *tree-order* is the partial ordering on the vertices of (46) such that, $\mathfrak{l} < \mathfrak{r}$ if and only if the unique path from the root \mathfrak{r} to \mathfrak{r} passes through \mathfrak{l} . The *depth* of the vertex \mathfrak{r} is the length of the path (number of edges) from the root.

As noted in Remark 5.19, the building blocks provide weights for the edges of the directed rooted trees.

Definition 7.1. Given a directed rooted tree as in (46), by assigning a weight $K(\mathfrak{a}, \mathfrak{r}) \in \mathbb{Z}$ to each edge $\Delta_{\mathfrak{a}\mathfrak{r}}$, we obtain a *weighted directed rooted tree*

$$\left\{ \underbrace{\mathfrak{1}, \dots, \mathfrak{m}}_{\text{vertices}}; \underbrace{\mathfrak{r}}_{\text{root}}; \underbrace{(\Delta_{\mathfrak{r}\mathfrak{a}}, K(\mathfrak{r}, \mathfrak{a})), \dots}_{\substack{\mathfrak{m}-1 \\ \text{weighted edges}}} \right\}.$$

A *zero parent* of a vertex $\mathfrak{a} \neq \mathfrak{r}$ is the unique vertex \mathfrak{r} connected to \mathfrak{a} on the path to the root, whose edge $(\Delta_{\mathfrak{r}\mathfrak{a}}, K(\mathfrak{r}, \mathfrak{a}))$ has in addition $K(\mathfrak{r}, \mathfrak{a}) = 0$.

For some weighted directed rooted trees the root is not a zero parent.

Example 7.1. For the weighted directed rooted tree with all its weights equal to 1, namely

$$\left\{ \mathfrak{1}, \dots, \mathfrak{m}; \mathfrak{r}; (\Delta_{\mathfrak{r}\mathfrak{1}}, 1), \dots, (\Delta_{\mathfrak{r}\mathfrak{m}}, 1) \right\},$$

none of the vertices is a zero parent.

Definition 7.2. A weighted directed rooted tree

$$(47) \quad \Lambda_{\mathfrak{r}} = \left\{ \underbrace{\mathfrak{1}, \dots, \mathfrak{m}}_{\text{vertices}}; \underbrace{\mathfrak{r}}_{\text{root}}; \underbrace{(\Delta_{\mathfrak{r}\mathfrak{a}}, K(\mathfrak{r}, \mathfrak{a})), \dots}_{\substack{\mathfrak{m}-1 \\ \text{weighted edges}}} \right\},$$

whose root \mathfrak{r} is a zero parent will be called a *weighted directed zero-rooted tree*.

Definition 7.3. A *zero child* of a vertex \mathfrak{r} is a vertex \mathfrak{a} of which \mathfrak{r} is the zero parent. A *zero descendant* of a vertex \mathfrak{r} is any vertex which is either the zero child of \mathfrak{r} or is (recursively) the zero descendant of any of the zero children of \mathfrak{r} .

From the above definitions we immediately obtain the following.

Lemma 7.4. Let $\Lambda_{\mathfrak{r}}$ be a weighted directed zero-rooted tree.

1. The zero descendants of the root \mathfrak{r} form the horizontal rooted subtree of the root, denoted by $\Lambda_{H(\mathfrak{r})}$. Note that the root of $\Lambda_{H(\mathfrak{r})}$ is once again \mathfrak{r} .

2. Each weighted edge $(\Delta_{\mathfrak{r}\mathfrak{a}}, K(\mathfrak{r}, \mathfrak{a}))$ with $K(\mathfrak{r}, \mathfrak{a}) \neq 0$, defines a horizontal rooted subtree $\Lambda_{H(\mathfrak{r}, \mathfrak{a})}$, with root \mathfrak{r} , of the incoming edge $(\Delta_{\mathfrak{r}\mathfrak{a}}, K(\mathfrak{r}, \mathfrak{a}))$, with vertices

$$V_{H(\mathfrak{r}, \mathfrak{a})} = \{\mathfrak{r}, \mathfrak{a}\} \cup \{\mathfrak{l} \mid \mathfrak{l} \text{ is a zero descendant of } \mathfrak{a}\}$$

and edges

$$E_{H(\mathfrak{r}, \mathfrak{a})} = \{(\Delta_{\mathfrak{r}\mathfrak{a}}, K(\mathfrak{r}, \mathfrak{a}))\} \cup \{\text{edges that end on the zero descendants of } \mathfrak{a}\}.$$

□

Note that, on each horizontal rooted subtree, the incoming edges are the only edges with non-zero weight.

Example 7.2. Consider the weighted directed zero-rooted tree

$$(48) \quad \Lambda_{\textcircled{1}} = \left\{ \textcircled{1}, \dots, \textcircled{12}; \textcircled{1}; \right. \\ \left. (\Delta_{12}, 0), (\Delta_{24}, 0), (\Delta_{47}, -3), (\Delta_{712}, 0), (\Delta_{711}, 4), \right. \\ \left. (\Delta_{13}, 1), (\Delta_{35}, 0), (\Delta_{36}, 0), (\Delta_{69}, 0), (\Delta_{610}, 0), (\Delta_{58}, 1) \right\}.$$

The root is $\textcircled{1}$, and the incoming edges are Δ_{13} , Δ_{47} , Δ_{711} and Δ_{58} . Then

$$\Lambda_{\textcircled{1}} = \Lambda_{H(1)} \cup \Lambda_{H(1,3)} \cup \Lambda_{H(4,7)} \cup \Lambda_{H(7,11)} \cup \Lambda_{H(5,8)},$$

provides the decomposition into horizontal rooted subtrees as in Lemma 7.4.

In Figure 5, the horizontal rooted subtree of the root is colored red; the horizontal rooted subtrees, corresponding to the incoming edges, are colored orange, blue, green, purple respectively. Note that the weight of each of the incoming edges could be any non-zero integer. The vertices $\textcircled{1}$, $\textcircled{4}$, $\textcircled{5}$ and $\textcircled{7}$ belong to more than one horizontal subtree.

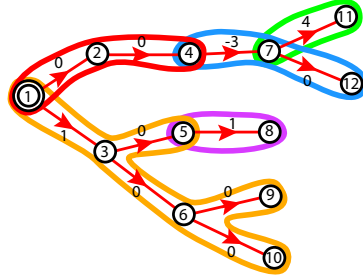


FIGURE 5. The decomposition into horizontal rooted subtrees of the weighted directed rooted tree of Example 7.2. The weights are placed beside the corresponding edges. The rooted subtree colored red is by definition the *global zero level subtree*. Recalling that the vertices correspond to branch points of \mathcal{R}_X , each of the horizontal subtrees is to represent the sheets of \mathcal{R}_X that contain the corresponding subset of branch points.

Remark 7.5. The decomposition of $\Lambda_{\textcircled{g}}$, given by Lemma 7.4, provides a disjoint partition on the set of edges. This relates to the fact that on \mathcal{R}_X the diagonals between branch points are partitioned into disjoint sets according to the sheet they share.

In order to overcome difficulty D.4, we shall need one more concept. Consider the linear (weighted) directed tree

$$G = \{\mathcal{V}; \mathfrak{E}\}$$

with m vertices

$$\mathcal{V} = \{\textcircled{a} \doteq (z_a, t_a, -\nu_a)\}_{a=1}^m, \quad z_a \in \overline{\mathbb{C}}_z, t_a \in \mathbb{C}_t, \nu_a \in \mathbb{N} \cup \{\infty\},$$

where $\{t_a\}$ are different points, labelled so that

$$\Im(t_a) \geq \Im(t_{a+1}), \quad \Re(t_a) \leq \Re(t_{a+1}),$$

and $m-1$ oriented weighted edges

$$\mathfrak{E} = \{(\Delta_{(a-1)a}, K(a-1, a))\}_{a=2}^m,$$

where $\Delta_{(\mathfrak{a}-1)\mathfrak{a}} \doteq (t_{\mathfrak{a}} - t_{\mathfrak{a}-1})$, and $K(\mathfrak{a} - 1, \mathfrak{a}) \in \mathbb{Z}$.

In particular, G can be understood as embedded in \mathbb{C}_t .

Note that the vertices are connected from left to right and top to bottom; starting with the top-&-left-most vertex and ending at the bottom-&-right-most vertex.

Definition 7.6. 1. The G constructed as above, is the *left-right-top-bottom linear (weighted) directed tree of the vertices \mathcal{V}* . The underlying undirected linear graph will be called the *undirected left-right-top-bottom linear (weighted) tree of the vertices \mathcal{V}* .

2. Moreover, for any choice of $\textcircled{\mathfrak{r}} \in \mathcal{V}$, the rooted tree

$$G_{\textcircled{\mathfrak{r}}} = \left\{ \mathcal{V}; \textcircled{\mathfrak{r}}; \widehat{\mathfrak{E}} \right\}$$

where

$\widehat{\mathfrak{E}} = \{\Delta_{\textcircled{\mathfrak{r}}\textcircled{\mathfrak{r}+1}}, \Delta_{\textcircled{\mathfrak{r}+1}\textcircled{\mathfrak{r}+2}}, \dots, \Delta_{\textcircled{\mathfrak{m}-1}\textcircled{\mathfrak{m}}}, \Delta_{\textcircled{\mathfrak{r}}\textcircled{\mathfrak{r}-1}}, \Delta_{\textcircled{\mathfrak{r}-1}\textcircled{\mathfrak{r}-2}}, \dots, \Delta_{21}\}$,
is called a *linear (weighted) directed rooted tree with incoming vertex $\textcircled{\mathfrak{r}}$* .

Note that G and $G_{\textcircled{\mathfrak{r}}}$ have the same vertices, however different oriented edges \mathfrak{E} and $\widehat{\mathfrak{E}}$. Figure 6 provides an example with seven vertices.

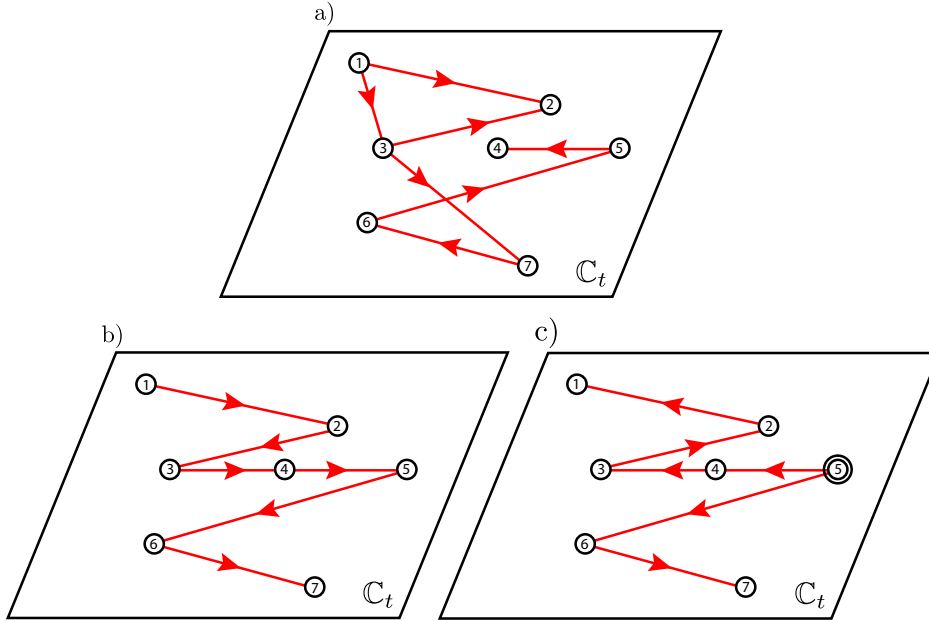


FIGURE 6. In (a) we have a directed graph with 7 vertices $\mathcal{V} = \{\textcircled{1}, \dots, \textcircled{7}\}$. In (b) we have eliminated and added some edges to obtain a left-right-top-bottom linear directed tree G of vertices \mathcal{V} with edges $\mathfrak{E} = \{\Delta_{12}, \Delta_{23}, \Delta_{34}, \Delta_{45}, \Delta_{56}, \Delta_{67}\}$. In (c) we have the linear directed rooted tree $G_{\textcircled{5}}$ where $\textcircled{5}$ is both the incoming vertex and the root, having edges $\widehat{\mathfrak{E}} = \{\Delta_{56}, \Delta_{67}, \Delta_{54}, \Delta_{43}, \Delta_{32}, \Delta_{21}\}$, note the change of directions of the edges.

3. As will be seen in the proof of the Main Theorem, condition (7) of Definition 7.7 provides, for each sheet of \mathcal{R}_X , a choice of the diagonals that connect the branch

points that share the same sheet. This choice will enable us to define appropriately the class $[\Lambda_X]$ of (r, d) -configuration trees.

4. In case that there is only one horizontal rooted subtree for Λ , Lemma 7.4 ensures that the only horizontal rooted subtree is $\Lambda_{H(\rho)}$.

5. When $r = 0$, Definition 7.7 reduces to the definition of a d -configuration tree presented in §8.3 of [2], for $X \in \mathcal{E}(0, d)$. The equivalence becomes explicit by observing that the essential vertices $\textcircled{\vartheta} = (\infty_\sigma, a_\sigma, -\infty)$ of $(0, d)$ -configuration trees correspond to the vertices $(\infty_\sigma, a_\sigma)$, pairs in [2], of d -configuration trees.

8. LOW DEGREE SIGNIFICATIVE EXAMPLES, FROM X TO Λ_X

We provide examples of the correspondence from vector fields to Riemann surfaces and configuration trees

$$X \longmapsto \mathcal{R}_X \longmapsto \Lambda_X,$$

using the basic geometric/combinatorial pieces described in Figure 4.

About the meaning of the different data of Λ_X .

- 1) The vertices of Λ_X are in bijection with the reduced divisor of X (recall Definition 5.1, Table 1), and with the branch points of \mathcal{R}_X with respect to $\pi_{X,2}$, restricted over \mathbb{C}_t , recall Diagram 12.
- 2) The edges correspond to a subset of the diagonals, connecting the branch points, necessary to describe completely the Riemann surface \mathcal{R}_X , recall Definition 5.4.1.
- 3) The root vertex $\textcircled{\vartheta} = (z_\varrho, t_\varrho, -\nu_\varrho)$, as usual in graph theory, means the initial vertex in order to construct a tree, as in (46). From the analytic and geometric point of view, the root determines the initial point of $\Psi_X(z) = \int_{z_1}^z \omega_X$.
- 4) The weights $K(\mathfrak{a}, \mathfrak{r}) \in \mathbb{Z}$ in Definition 7.7: If we can describe all the branch points of \mathcal{R}_X using only one sheet (Definition 5.10), then $K(\mathfrak{a}, \mathfrak{r}) = 0$. If several sheets are required, the weight of the edge $K(\mathfrak{a}, \mathfrak{r}) \in \mathbb{Z} \setminus \{0\}$ tells us the relative number of sheets of \mathcal{R}_X , we must go “up or down” on the surface in order to find another sheet containing other branch points. Vector fields having $K(\mathfrak{a}, \mathfrak{r}) \neq 0$ appear in Example 8.7 and §8.2.

In particular, if there are only two branch points then there is no need to go up or down at the starting branch point, so the weight of the only edge is 0.

- 5) The *global zero level sheet* denoted *GZL* (which is in general non canonical), indicates a subset of the branch points that share the same sheet as the root

$\textcircled{1}$.

Remark 8.1. The notion of *skeleton* associated to Λ_X will be described in Definition 9.5 and the notion of (r, d) -*soul* in Definition 9.7. They play an active role in the proof of the Main Theorem.

- For $X \in \mathcal{E}(r, d)$, $d \geq 1$, the (r, d) -soul is necessarily a flat Riemann surface with boundary, and is obtained from \mathcal{R}_X by removing its semi-infinite helicoids.
- In the case $X \in \mathcal{E}(r, 0)$, the (r, d) -soul coincides with \mathcal{R}_X .

8.1. $X \in \mathcal{E}(r, 0)$ has $r \geq 1$ poles on \mathbb{C}_z and Ψ_X is a polynomial map.

Example 8.1. Consider the vector field of Example 3.1,

$$X(z) = \frac{\lambda}{(z - p_1)^r} \frac{\partial}{\partial z}$$

and recall the notion of $(\nu_i + 1)$ -cyclic helicoid Definition 5.17. The $(r, 0)$ -configuration tree consists of one pole vertex and no edges

$$\Lambda_X = \left\{ \textcircled{1} = (p_1, \tilde{p}_1, -r); \textcircled{1}; \emptyset \right\},$$

where \tilde{p}_1 as in (18) is the critical value. In Figure 7 the case $r = 2$ is pictured: on the left hand side the phase portrait of X is shown, clearly there are 6 hyperbolic sectors each corresponding to a half plane; on the second column the Riemann surface is shown; finally on the rightmost column the combinatorial objects are portrayed. For the general case $-r \leq -1$ see Figure 4.c.

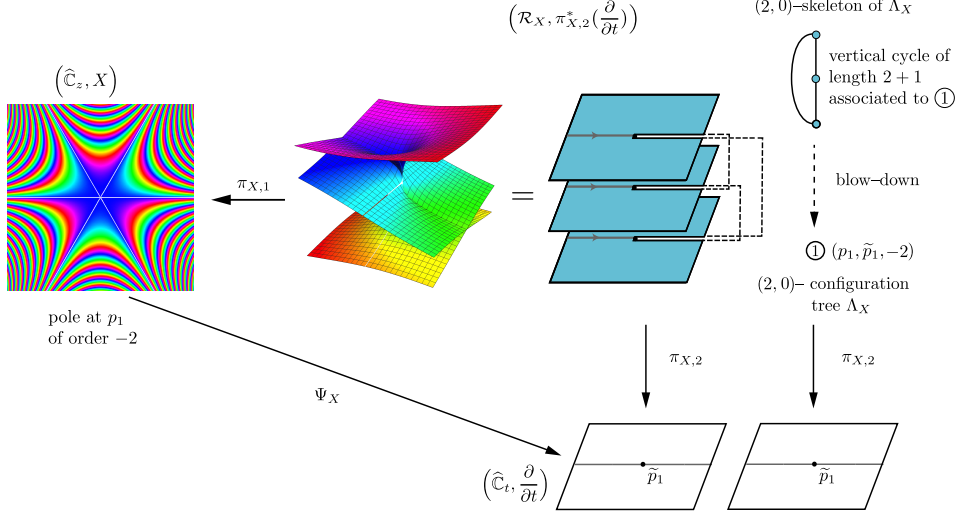


FIGURE 7. **Vector field** $X(z) = \frac{1}{(z-p_1)^2} \frac{\partial}{\partial z}$ **with a pole of order -2 at $p_1 \in \mathbb{C}_z$.** The surface \mathcal{R}_X consists of three sheets with a branch cut, glued together to form a $(2+1)$ -cyclic helicoid. On the right column, the $(2,0)$ -configuration tree consisting of one vertex, and its corresponding $(2,0)$ -skeleton are portrayed; see §9.2 and Definition 9.5.

In the next examples we shall consider (r, d) -configuration trees with two or more vertices, hence weighted edges shall appear.

Example 8.2. Consider the vector field

$$(49) \quad X(z) = \frac{\lambda}{(z-p_1)^{\nu_1}(z-p_2)^{\nu_2}} \frac{\partial}{\partial z} \in \mathcal{E}(r, 0), \quad \nu_1 + \nu_2 = r, \quad \nu_1, \nu_2 \geq 1,$$

and its distinguished parameter

$$\Psi_X(z) = \frac{1}{\lambda} \int_{z_0}^z (\zeta - p_1)^{\nu_1} (\zeta - p_2)^{\nu_2} d\zeta.$$

Without loss of generality, we assume that the critical values $\tilde{p}_j = \Psi_X(p_j)$, $j = 1, 2$, satisfy $\Im(\tilde{p}_1) \geq \Im(\tilde{p}_2)$. In this case the $(r, 0)$ -configuration tree has two pole vertices and one edge

$$\Lambda_X = \left\{ \textcircled{1} = (p_1, \tilde{p}_1, -\nu_1), \textcircled{2} = (p_2, \tilde{p}_2, -\nu_2); \textcircled{\textcircled{1}}; (\Delta_{12}, 0) \right\},$$

where the edge Δ_{12} is the semi-residue $S(\omega_X, p_1, p_2, \gamma) = \tilde{p}_2 - \tilde{p}_1$, which according to (42) is equivalent to the diagonal with the same name. Finally, the weight of the edge is 0, since Δ_{12} is in the global zero level sheet. See Figure 8 and 4.c.

If $\Im(\tilde{p}_1) > \Im(\tilde{p}_2)$, then the semi-residue $\Delta_{12} = S(\omega_X, p_1, p_2, \gamma) = \tilde{p}_2 - \tilde{p}_1 \in \mathbb{C} \setminus \mathbb{R}$, giving origin to a finite height horizontal strip, see left drawing in Figure 8. If $\Im(\tilde{p}_1) = \Im(\tilde{p}_2)$, then the diagonal Δ_{12} coincides, up to orientation, with a saddle connection of the real vector field $\Re(X)$.

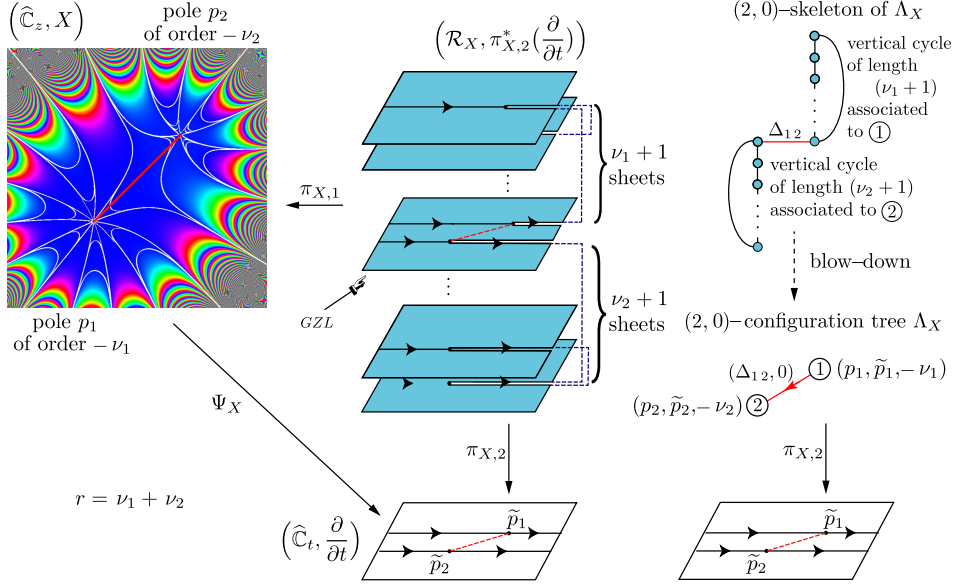


FIGURE 8. **Vector field** $X(z) = \frac{\lambda}{(z-p_1)^{\nu_1}(z-p_2)^{\nu_2}} \frac{\partial}{\partial z}$ **with two poles** p_i **of order** $-\nu_i$. The diagonal $\Delta_{12} \subset \mathcal{R}_X$ associated to the finitely ramified branch points and its projections via $\pi_{X,1}$ and $\pi_{X,2}$ are coloured red. The two branch points are the endpoints of the diagonal $\Delta_{12} \subset \mathcal{R}_X$ on the global zero level sheet. The phase portrait (left drawing) is the case with poles of orders $-3 = -\nu_2$ and $-5 = -\nu_1$. See Example 8.2, and §9.2 for the drawing on the right.

8.2. Vector fields in $\mathcal{E}(3,0)$ with three simple poles. Consider vector fields $X \in \mathcal{E}(3,0)$ with simple poles,

- we fix two finite ramification values $\tilde{p}_1 = 0$, $\tilde{p}_2 = 1$, and
- leave free the third \tilde{p}_3 in the twice punctured plane $\mathbb{C} \setminus \{0,1\}$.

This gives origin to a suitable family of vector fields \mathfrak{F} . It is to be noted that there is a strong analytical and combinatorial dependence on the choice of the ramification values of the involved distinguished parameters Ψ_X .

We shall study the general problem of compute Ψ_X starting with a configuration of preassigned critical values $\{\tilde{p}_1, \dots, \tilde{p}_r\}$ in §14, Corollary 14.1.

Proposition 8.2. *Let \mathfrak{F} be the family of vector fields defined by*

$$(50) \quad \begin{aligned} X(p_3, z) : (\mathbb{C} \setminus \{0, 1/2, 1\}) \times \mathbb{C} &\longrightarrow \mathcal{E}(3,0) \\ (p_3, z) &\longmapsto \frac{2p_3 - 1}{12z(z-1)(z-p_3)} \frac{\partial}{\partial z}. \end{aligned}$$

1) The corresponding distinguished parameters are the polynomials

$$(51) \quad \Psi(p_3, z) = \frac{12}{2p_3 - 1} \left(\frac{1}{4}z^4 + \frac{-p_3 - 1}{3}z^3 + \frac{p_3}{2}z^2 \right) \in \mathbb{C}[z].$$

2) The corresponding reduced divisors are

$$(52) \quad X(p_3, z) \longmapsto (0, 0, -1) + (1, 1, -1) + \left(p_3, \frac{p_3^3(2 - p_3)}{2p_3 - 1}, -1 \right).$$

3) The $(3, 0)$ -configuration trees $\Lambda_{X(p_3, z)}$ for $X(p_3, z)$ are given by Equations (58)–(76).

In simple words, each $\Lambda_{X(p_3, z)}$ describes the relative position of the branch points

$$\textcircled{1} = (0, 0, -1), \quad \textcircled{2} = (1, 1, -1), \quad \textcircled{3} = (p_3, \tilde{p}_3, -1)$$

on the Riemann surface $\mathcal{R}_{X(p_3, z)}$.

Remark 8.3. Motivation for the family \mathfrak{F} . Let $X \in \mathcal{E}(r, d)$ be a vector field with at least two different poles p_1, p_2 (so $r \geq 2$), the choice of

$$(p_1, \tilde{p}_1) = (0, 0), \quad (p_2, \tilde{p}_2) = (1, 1) \in \mathbb{C}^2$$

as in (49) and (52) can be explained as follows.

1. We consider the complex analytic action

$$(53) \quad \mathcal{A} : \text{Aut}(\mathbb{C}) \times \mathcal{E}(r, d) \longrightarrow \mathcal{E}(r, d), \quad (T, X) \longmapsto T^*X,$$

of the affine transformation group $\text{Aut}(\mathbb{C})$ corresponding to those $T \in \text{Aut}(\widehat{\mathbb{C}}) = \text{PSL}(2, \mathbb{C})$ that fix ∞ , see [3] for general theory. Using suitable T , we obtain $p_1 = 0$ and $p_2 = 1$. (It is to be noted that the affine group $\text{Aut}(\mathbb{C})$ is the largest complex automorphism group that acts on $\mathcal{E}(r, d)$.)

2. If $\Psi_X(z) = \int_{p_1=0}^z \omega_X$ then $\Psi_X(0) = 0 = \tilde{p}_1$.

3. Considering $\{\lambda X \mid \lambda \in \mathbb{C}^*\}$ as a projective class, we normalize by a suitable λ_0 , thus

$$\int_0^1 \frac{1}{\lambda_0} \omega_X = 1 = \tilde{p}_2.$$

In the particular case $\mathcal{E}(3, 0)$, we get Equation (50).

Proof. First step. A suitable tessellation for the third critical point p_3 . The degree four rational map

$$(54) \quad \mathbb{C}_{p_3} \longrightarrow \mathbb{C}_{\tilde{p}_3}, \quad p_3 \longmapsto \frac{p_3^3(2 - p_3)}{2p_3 - 1} = \tilde{p}_3$$

determines the behaviour of the third branch point $(p_3, \tilde{p}_3, -1) \in \mathcal{R}_{X(p_3, z)}$. The rational map (54) has $\{0, 1, 1/2\}$ as critical points with critical values $\{0, 1, \infty\}$, respectively. The inverse image $\tilde{p}_3^{-1}(\mathbb{R})$ is drawn in Figure 9 using black, blue and orange segments to represent the inverse images of $(-\infty, 0)$, $[0, 1]$ and $(1, \infty)$ respectively. There are eight open connected components

$$\{U_j\}_{j=1}^8 = \mathbb{C}_{p_3} \setminus \tilde{p}_3^{-1}(\mathbb{R})$$

determining a tessellation of \mathbb{C}_{p_3} . The regions U_j with even index j , coloured white, are the inverse image of the lower half plane \mathbb{H}_-^2 and the odd index regions, coloured gray, are the inverse image of the upper half plane \mathbb{H}_+^2 .

The meaning and suitability of the tessellation of (54) in \mathbb{C}_{p_3} is as follows.

A description of the topological behavior of the third critical value \tilde{p}_3 in loops enclosing the other two critical values 0, 1.

1) The red circle α describes a loop of \tilde{p}_3 enclosing the ramification value 0, but not 1.

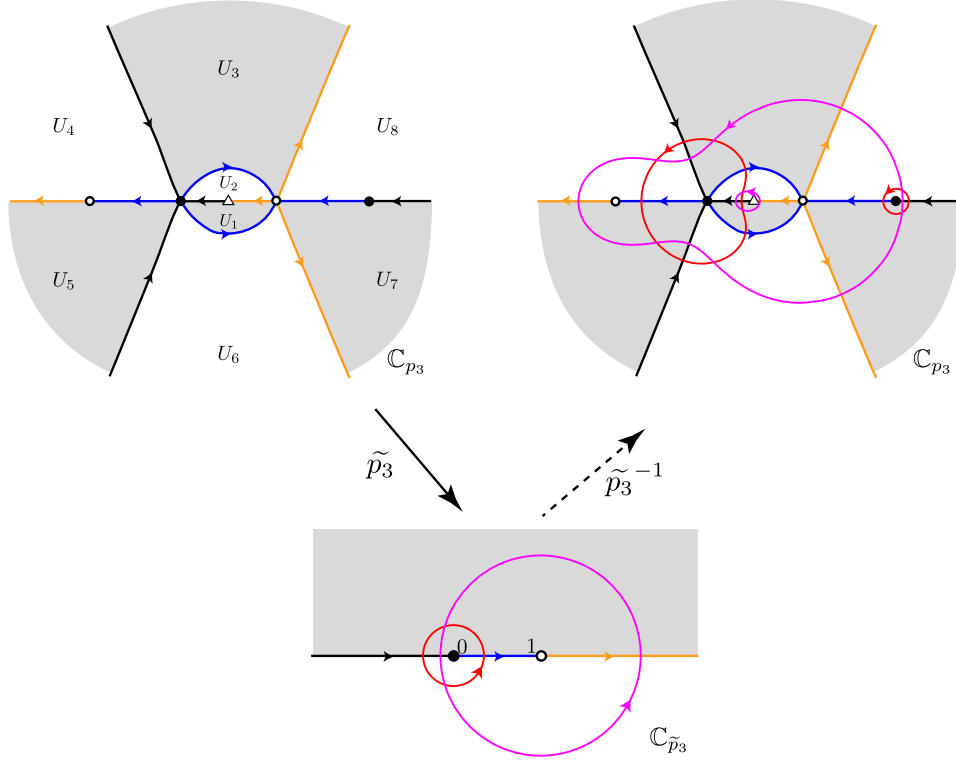


FIGURE 9. The degree four rational map $p_3 \mapsto \tilde{p}_3$ gives origin to eight open regions U_j , forming a tessellation of \mathbb{C}_{p_3} , see upper left figure. The points $0, 1, 1/2 \in \mathbb{C}_{p_3}$, coloured black, white, triangle vertices, correspond to the preimages of $0, 1, \infty \in \mathbb{C}_{\tilde{p}_3}$, respectively. The upper right figure provides a description of the lift of the red α and magenta β circles under \tilde{p}_3^{-1} . The blue tree $\tilde{p}_3^{-1}([0, 1])$ is the *dessin d'enfant* of the map \tilde{p}_3 .

- 2) The magenta circle β describes a loop of \tilde{p}_3 enclosing the ramification values 0 and 1.

These loops generate the fundamental group $\pi_1(\mathbb{C}_{\tilde{p}_3} \setminus \{0, 1\})$. The lifts of the circles α, β are described in Figure 9.

In order to proceed with the proof, the idea is as follows. If we determine the $(3, 0)$ -configuration trees of $X(p_3, z)$ at one point $p_3 \in U_j$, then by a continuity argument the analogous configuration tree remains valid for all $p_3 \in U_j$.

Second step. Computation of the $(3, 0)$ -configuration trees.

We shall need to consider the boundaries between the regions U_j , $j = 1, \dots, 8$. Let U_i and U_j denote two adjacent regions with common boundary (as open segments)

$$\partial U_{i,j} \doteq (\overline{U_i} \cap \overline{U_j}) \setminus \{\tilde{p}_3^{-1}(\{0, 1, \infty\})\}.$$

Moreover, we assign colors to the vertices and edges in Figure 10, as follows

$$\begin{aligned} \textcircled{1} &= (0, 0, -1) \text{ in red, } \textcircled{2} = (1, 1, -1) \text{ in green, } \textcircled{3} = (p_3, \tilde{p}_3, -1) \text{ in blue,} \\ \Delta_{12} &= \overline{(0, 0, -1), (1, 1, -1)}, \Delta_{21} = \overline{(1, 1, -1), (0, 0, -1)} \text{ in dashed black line,} \\ \Delta_{13} &= \overline{(0, 0, -1), (p_3, \tilde{p}_3, -1)}, \Delta_{31} = \overline{(p_3, \tilde{p}_3, -1), (0, 0, -1)} \text{ in red,} \\ \Delta_{23} &= \overline{(1, 1, -1), (p_3, \tilde{p}_3, -1)}, \Delta_{32} = \overline{(p_3, \tilde{p}_3, -1), (1, 1, -1)} \text{ in green.} \end{aligned}$$

Because of Definition 7.7.4 there are two possible cases for the root.

1) If $\tilde{p}_3 \in \mathbb{H}_+^2 \cup (-\infty, 0)$ then the vertex $\textcircled{3}$ is the root, by Equation (54), this is equivalent to

$$(55) \quad p_3 \in U_1 \cup U_3 \cup U_5 \cup U_7 \\ \cup \partial U_{3,4} \cup \partial U_{5,6} \cup (\partial U_{1,2} \cap (0, 1/2)) \cup (\partial U_{7,8} \cap (2, \infty)).$$

2) If $\tilde{p}_3 \notin \mathbb{H}_+^2 \cup (-\infty, 0)$ then the vertex $\textcircled{1}$ is the root, once again by (54)

$$(56) \quad p_3 \in U_2 \cup U_4 \cup U_6 \cup U_8 \\ \cup \partial U_{2,3} \cup \partial U_{1,6} \cup \partial U_{4,5} \cup \partial U_{3,8} \cup \partial U_{6,7} \\ \cup (\partial U_{1,2} \cap (1/2, 1)) \cup (\partial U_{7,8} \cap (1, 2)).$$

In either case, the diagonals/edges satisfy

$$(57) \quad \Delta_{ij} = -\Delta_{ji}, \quad i, j \in \{1, 2, 3\}, \quad i \neq j, \\ \Delta_{12} + \Delta_{23} + \Delta_{31} = 0.$$

The $(3, 0)$ -configuration trees can be deduced upon careful consideration of the phase portraits portrayed in Figure 10.

Case (1), the root is $\textcircled{3}$ and colored blue. From Equation (55), when

• $p_3 \in U_1$, the $(3, 0)$ -configuration tree is

$$(58) \quad \Lambda_{X(p_3, z)} = \left\{ \textcircled{1}, \textcircled{2}, \textcircled{3}; \textcircled{\textcircled{3}}; (\Delta_{32}, 0), (\Delta_{31}, 1) \right\}, \text{ with } \Delta_{32}, \Delta_{31} \in \mathbb{H}_+^2;$$

• $p_3 \in U_3$, the $(3, 0)$ -configuration tree is

$$(59) \quad \Lambda_{X(p_3, z)} = \left\{ \textcircled{1}, \textcircled{2}, \textcircled{3}; \textcircled{\textcircled{3}}; (\Delta_{31}, 0), (\Delta_{12}, 0) \right\}, \text{ with } \Delta_{12} = 1 \text{ and } \Delta_{31} \in \mathbb{H}_+^2;$$

• $p_3 \in U_5$, the $(3, 0)$ -configuration tree is

$$(60) \quad \Lambda_{X(p_3, z)} = \left\{ \textcircled{1}, \textcircled{2}, \textcircled{3}; \textcircled{\textcircled{3}}; (\Delta_{31}, 0), (\Delta_{12}, 1) \right\}, \text{ with } \Delta_{12} = 1 \text{ and } \Delta_{31} \in \mathbb{H}_+^2;$$

• $p_3 \in U_7$, the $(3, 0)$ -configuration tree is

$$(61) \quad \Lambda_{X(p_3, z)} = \left\{ \textcircled{1}, \textcircled{2}, \textcircled{3}; \textcircled{\textcircled{3}}; (\Delta_{32}, 0), (\Delta_{21}, 1) \right\}, \text{ with } \Delta_{21} = -1 \text{ and } \Delta_{32} \in \mathbb{H}_+^2;$$

• $p_3 \in \partial U_{1,2} \cap (0, 1/2)$, the $(3, 0)$ -configuration tree is

$$(62) \quad \Lambda_{X(p_3, z)} = \left\{ \textcircled{1}, \textcircled{2}, \textcircled{3}; \textcircled{\textcircled{3}}; (\Delta_{31}, 0), (\Delta_{32}, 1) \right\}, \text{ with } \Delta_{32} > 0 \text{ and } \Delta_{32} > 1;$$

• $p_3 \in \partial U_{7,8} \cap (2, \infty)$, the $(3, 0)$ -configuration tree is

$$(63) \quad \Lambda_{X(p_3, z)} = \left\{ \textcircled{1}, \textcircled{2}, \textcircled{3}; \textcircled{\textcircled{3}}; (\Delta_{32}, 0), (\Delta_{21}, 1) \right\}, \text{ with } \Delta_{21} = -1 \text{ and } \Delta_{32} > 1;$$

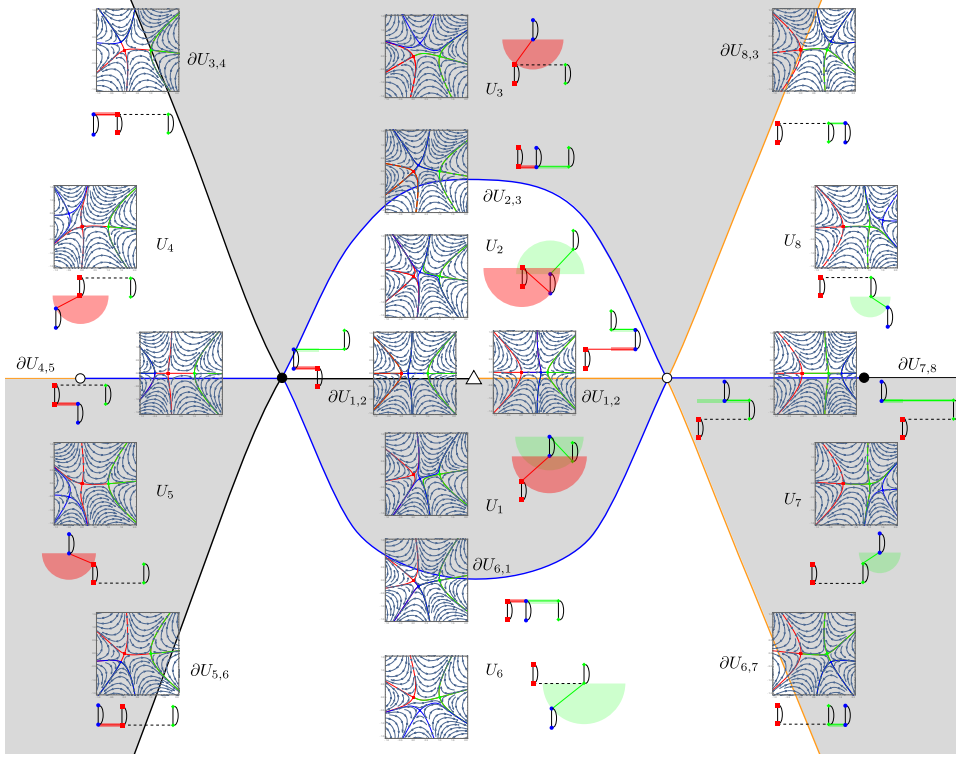


FIGURE 10. The plane \mathbb{C}_{p_3} as vector field atlas of $X(p_3, z)$ and their corresponding $(3, 0)$ -skeletons of $\Lambda_{X(p_3, z)}$. This provides a bifurcation diagram for the phase portraits, there appear 12 non equivalent (topologically, orientation preserving), real vector fields $\Re(X(p_3, z))$. The shaded red and green areas represent the half planes or segments where the diagonal corresponding to \tilde{p}_3 can move, its total winding number is 4 coinciding with the degree of the map \tilde{p}_3 in (54).

- $p_3 \in \partial U_{3,4}$, the $(3, 0)$ -configuration tree is (64)

$$\Lambda_{X(p_3, z)} = \left\{ \textcircled{1}, \textcircled{2}, \textcircled{3}; \textcircled{\textcircled{3}}; (\Delta_{31}, 0), (\Delta_{12}, 0) \right\}, \text{ with } \Delta_{12} = 1 \text{ and } \Delta_{31} > 0;$$

- $p_3 \in \partial U_{5,6}$, the $(3, 0)$ -configuration tree is (65)

$$\Lambda_{X(p_3, z)} = \left\{ \textcircled{1}, \textcircled{2}, \textcircled{3}; \textcircled{\textcircled{3}}; (\Delta_{31}, 0), (\Delta_{12}, 0) \right\}, \text{ with } \Delta_{12} = 1 \text{ and } \Delta_{31} > 0;$$

Case (2), the root is $\textcircled{\textcircled{1}}$ and colored red. From Equation (56), when

- $p_3 \in U_2$, the $(3, 0)$ -configuration tree is

$$(66) \quad \Lambda_{X(p_3, z)} = \left\{ \textcircled{1}, \textcircled{2}, \textcircled{3}; \textcircled{\textcircled{1}}; (\Delta_{13}, 0), (\Delta_{32}, 1) \right\}, \text{ with } \Delta_{13}, \Delta_{32} \in \mathbb{H}_-^2;$$

- $p_3 \in U_4$, the $(3, 0)$ -configuration tree is
(67)

$$\Lambda_{X(p_3, z)} = \left\{ \textcircled{1}, \textcircled{2}, \textcircled{3}; \textcircled{1}; (\Delta_{12}, 0), (\Delta_{13}, 1) \right\}, \text{ with } \Delta_{13} \in \mathbb{H}_-^2, \Delta_{32} \in \mathbb{H}_+^2;$$

- $p_3 \in U_6$, the $(3, 0)$ -configuration tree is
(68)

$$\Lambda_{X(p_3, z)} = \left\{ \textcircled{1}, \textcircled{2}, \textcircled{3}; \textcircled{1}; (\Delta_{12}, 0), (\Delta_{23}, 0) \right\}, \text{ with } \Delta_{12} = 1 \text{ and } \Delta_{23} \in \mathbb{H}_-^2;$$

- $p_3 \in U_8$, the $(3, 0)$ -configuration tree is
(69)

$$\Lambda_{X(p_3, z)} = \left\{ \textcircled{1}, \textcircled{2}, \textcircled{3}; \textcircled{1}; (\Delta_{12}, 0), (\Delta_{23}, 1) \right\}, \text{ with } \Delta_{12} = 1 \text{ and } \Delta_{23} \in \mathbb{H}_-^2;$$

- $p_3 \in \partial U_{4,5}$, the $(3, 0)$ -configuration tree is
(70)

$$\Lambda_{X(p_3, z)} = \left\{ \textcircled{1}, \textcircled{2}, \textcircled{3}; \textcircled{1}; (\Delta_{12}, 0), (\Delta_{13}, 1) \right\}, \text{ with } \Delta_{12} = 1 \text{ and } \Delta_{13} > 0;$$

- $p_3 \in \partial U_{1,2} \cap (1/2, 1)$, the $(3, 0)$ -configuration tree is
(71)

$$\Lambda_{X(p_3, z)} = \left\{ \textcircled{1}, \textcircled{2}, \textcircled{3}; \textcircled{1}; (\Delta_{13}, 0), (\Delta_{32}, 1) \right\}, \text{ with } \Delta_{13} > 1 \text{ and } \Delta_{32} < 0;$$

- $p_3 \in \partial U_{7,8} \cap (1, 2)$, the $(3, 0)$ -configuration tree is
(72)

$$\Lambda_{X(p_3, z)} = \left\{ \textcircled{1}, \textcircled{2}, \textcircled{3}; \textcircled{1}; (\Delta_{12}, 0), (\Delta_{23}, 1) \right\}, \text{ with } \Delta_{12} = 1 \text{ and } -1 < \Delta_{23} < 0;$$

- $p_3 \in \partial U_{1,6}$, the $(3, 0)$ -configuration tree is
(73)

$$\Lambda_{X(p_3, z)} = \left\{ \textcircled{1}, \textcircled{2}, \textcircled{3}; \textcircled{1}; (\Delta_{13}, 0), (\Delta_{32}, 0) \right\}, \text{ with } 0 < \Delta_{13} < 1 \text{ and } 0 < \Delta_{32} < 1;$$

- $p_3 \in \partial U_{3,8}$, the $(3, 0)$ -configuration tree is
(74)

$$\Lambda_{X(p_3, z)} = \left\{ \textcircled{1}, \textcircled{2}, \textcircled{3}; \textcircled{1}; (\Delta_{12}, 0), (\Delta_{23}, 0) \right\}, \text{ with } \Delta_{12} = 1 \text{ and } \Delta_{23} > 0;$$

- $p_3 \in \partial U_{2,3}$, the $(3, 0)$ -configuration tree is
(75)

$$\Lambda_{X(p_3, z)} = \left\{ \textcircled{1}, \textcircled{2}, \textcircled{3}; \textcircled{1}; (\Delta_{13}, 0), (\Delta_{32}, 0) \right\}, \text{ with } 0 < \Delta_{13} < 1 \text{ and } \Delta_{13} > 0;$$

- $p_3 \in \partial U_{6,7}$, the $(3, 0)$ -configuration tree is
(76)

$$\Lambda_{X(p_3, z)} = \left\{ \textcircled{1}, \textcircled{2}, \textcircled{3}; \textcircled{1}; (\Delta_{12}, 0), (\Delta_{23}, 0) \right\}, \text{ with } \Delta_{12} = 1 \text{ and } \Delta_{23} > 0.$$

□

As an advantage of Proposition (8.2), recalling the complex analytic action (53), then the quotient map

$$\begin{aligned} \Pi : \mathcal{E}(r, d) &\longrightarrow \frac{\mathcal{E}(r, d)}{\text{Aut}(\mathbb{C})} \\ X &\longmapsto [X] \end{aligned}$$

determines the analytic classes of vector fields. In particular, $\mathcal{E}(3, 0)/\text{Aut}(\mathbb{C})$ is a complex analytic space of complex dimension two, having singularities originated

from the vector fields in $\mathcal{E}(3, 0)$ with non trivial isotropy group under the $\text{Aut}(\mathbb{C})$ -action. See [3] for general theory on $\mathcal{E}(r, d)$ and [24], [34] for the rational case. Hence the family \mathfrak{F} gives origin to a curve $\Pi \circ X(p_2, z)$ of $\text{Aut}(\mathbb{C})$ -classes of vector fields.

Corollary 8.4. 1) *The complex analytic curve*

$$\Pi \circ X(p_3, z) : \mathbb{C} \setminus \{-1, 0, 1/2, 1, 2\} \longrightarrow \frac{\mathcal{E}(3, 0)}{\text{Aut}(\mathbb{C})}$$

is injective.

2) *The parameter plane $\mathbb{C}_{p_3} \setminus \{0, 1/2, 1\}$ provides a bifurcation diagram for the phase portraits of $\Re(X(p_3, z))$, there appear 12 non equivalent (topologically, orientation preserving).*

The notion of topological equivalence is Definition 11.1. We shall study the general problem of the number of topological classes of $\Re(X)$, for $X \in \mathcal{E}(r, d)$, in §11, see Theorem 11.3.

Proof. We want to describe the $\text{Aut}(\mathbb{C})$ -equivalent the vector fields $X(p_3, z)$. Consider the action $(T, X(p_3, z)) \mapsto T^*X(p_3, z)$, then it lifts to the action on distinguished parameters, as

$$(T, \Psi(p_3, z)) \mapsto T^*\Psi(p_3, z) = \Psi(p_3, z) \circ T^{-1}(z).$$

The polynomial $\Psi(p_3, z)$ has critical points $\{(0, 0), (1, 1), (p_3, \tilde{p}_3)\} \subset \mathbb{C}^2$. For $T \neq \text{Id} \in \text{Aut}(\mathbb{C})$, $\Psi(p_3, z) \circ T^{-1}(z)$ gives rise to a permutation of $\{(0, 0), (1, 1), (p_2, \tilde{p}_3)\}$. This is possible if and only if $\tilde{p}_3 = 0$ or 1. Using the definition of \tilde{p}_3 , Equation (54), we have $p_3 = -1$ or 2. In fact $\Psi(-1, z)$ and $\Psi(2, z)$ are $\text{Aut}(\mathbb{C})$ -equivalent (using the translation map T^{-1} that sends $\{-1, 0, 1\}$ to $\{0, 1, 2\}$).

The assertion (2) uses careful inspection of Figure 10. We convene that \sim means topologically equivalence, for p_3 the topologies correspond to:

- U_1, \dots, U_8 eight topologies; clearly the topology remains without change for p_3 on each open set. For example, U_1, U_2 determine two horizontal strip flows for the corresponding $\Re(X(p_3, z))$, however the orientation of the flows make it different.
- $\partial U_{1,2} \cap (0, 1/2) \sim \partial U_{4,5}, \partial U_{7,8} \cap (1, 1/2) \sim \partial U_{7,8} \cap (2, \infty)$, two topologies; in fact the corresponding $\Re(X(p_3, z))$ have two saddle connections, the orientation determines two non equivalent cases.
- $\partial U_{3,4} \sim \partial U_{1,6} \sim \partial U_{3,8}, \partial U_{5,6} \sim \partial U_{2,3} \sim \partial U_{6,7}$, two topologies; the corresponding $\Re(X(p_3, z))$ have two saddle connections that have a common half plane as boundary (this is the difference respect to the above case), and the orientation determines two non equivalent cases.

Hence we have 12 different topological classes. \square

8.3. $X \in \mathcal{E}(0, d)$ has an isolated essential singularity at $\infty \in \hat{\mathbb{C}}_z$, no zeros or poles. The simplest example corresponds to a $(0, 1)$ -configuration tree; only one essential vertex and no edges.

Example 8.3. Consider once again Example 4.1, that is

$$X(z) = e^{\mu(z+c_1)} \frac{\partial}{\partial z} \in \mathcal{E}(0, 1),$$

with $\mu \in \mathbb{C}^*, c_1 \in \mathbb{C}$ as in (7). We then have an isolated essential singularity at $\infty \in \hat{\mathbb{C}}_z$ with finite asymptotic value a_1 given by (22).

The $(0, 1)$ -configuration tree consists of one essential vertex and no edges

$$\Lambda_X = \left\{ \textcircled{1} = (\infty_1, a_1, -\infty); \textcircled{1}; \emptyset \right\}.$$

See Figure 11 and 4.a. The vertices are branch points of the Riemann surface \mathcal{R}_X , and since there is only one branch point/vertex, then no weighted edges appear. The

soul of \mathcal{R}_X is a sheet, recall Remark 8.1, and coincides with the global zero level. It is to be noted that the semi-infinite helicoids, even though they are part of \mathcal{R}_X , are not necessary in the combinatorial description of the surface; the complete \mathcal{R}_X is described by making the natural convention to glue two semi-infinite helicoids to each vertical tower, one on the top and one on the bottom. Hence the semi-infinite helicoids will have no counterpart in the combinatorial description as graphs. However, to remind the reader of their existence in \mathcal{R}_X we have schematically represented them in the figures by the “springs” or “coils” attached to the vertical towers.

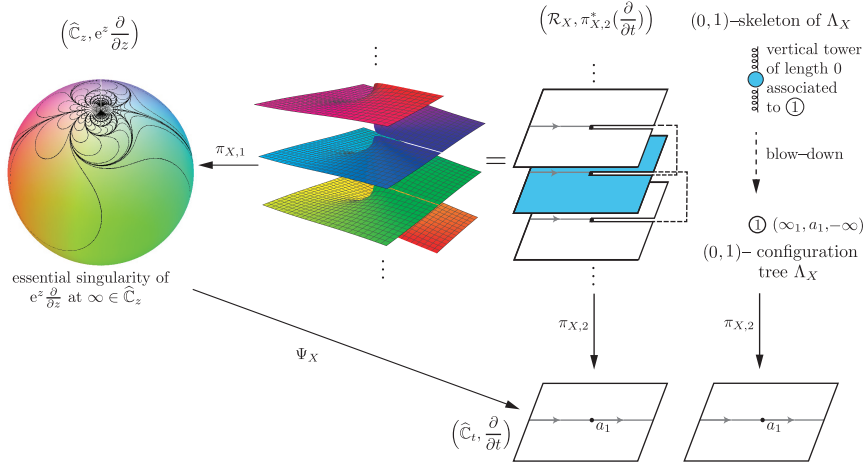


FIGURE 11. **Vector field $X(z) = e^{\mu(z+c_1)} \frac{\partial}{\partial z}$ with an essential singularity at $\infty \in \hat{\mathbb{C}}_z$.** The surface \mathcal{R}_X is a *logarithmic spiral* formed by two semi-infinite helicoids glued together. The soul, Definition 9.7, is shaded blue. See Example 8.3, and §9.2 for the drawing on the right.

In the following example there are $d \geq 2$ essential vertices and $d - 1$ edges, all sharing the same sheet.

Example 8.4. Consider the vector field

$$X(z) = e^{z^d} \frac{\partial}{\partial z} \in \mathcal{E}(0, d), \text{ for } d \geq 2.$$

If $z_0 = 0$, the distinguished parameter is

$$\Psi_X(z) = \int_0^z e^{-\zeta^d} d\zeta.$$

Note that $a_1 \doteq \int_0^\infty e^{-\zeta^d} d\zeta \in \mathbb{R}^+$. Moreover Ψ_X has d finite asymptotic values given by³ (see [40] p. 168)

$$a_\sigma = e^{i2\pi(\sigma-1)/d} a_1 \quad \text{for } \sigma = 1 \dots d,$$

each with multiplicity one, and a logarithmic branch point $(\infty_\sigma, a_\sigma, -\infty) \in \mathcal{R}_X$ over each finite asymptotic value. The exponential tracts A_σ for each of the finite asymptotic values a_σ are given by

³Our numbering of the indices σ differ from the ones in [40] so that they agree with the conventions outlined in Remark 4.6.3.

$$A_\sigma = \left\{ z \in \mathbb{C}_z \mid \left| \arg z - \frac{2\pi(\sigma-1)}{d} \right| < \frac{\pi}{d} \right\}, \quad \text{for } \sigma = 1, \dots, d.$$

Thus the $(0, d)$ -configuration tree Λ_X will have d essential vertices $V_H = \{\textcircled{\sigma} = (\infty_\sigma, a_\sigma, -\infty)\}_{\sigma=1}^d$ with root $\textcircled{1} = (\infty_1, a_1, -\infty)$. Recalling Definition 7.6.1, the $d-1$ edges E_H are selected such that we obtain a left-right-top-bottom linear directed tree of the vertices V_H , where the index σ_0 for the top and left most vertex will be given by the simple formula

$$\sigma_0 = \left\lceil \left\lfloor \frac{d}{2} \right\rfloor / 2 \right\rceil + 1,$$

where $\lceil \cdot \rceil$ and $\lfloor \cdot \rfloor$ are the ceiling and floor functions respectively. Recalling Definition 7.6.2, we obtain $\Lambda_{H, \textcircled{1}}$ the linear directed rooted tree with incoming vertex $\textcircled{1}$. Moreover, all d branch points share the same sheet in \mathcal{R}_X , hence by assigning weight 0 to each of the edges $\Delta_{\alpha\tau} \in \hat{E}_H$ we obtain the $(0, d)$ -configuration tree of X . In Figure 12 the case $d = 9$ is illustrated, the $(0, 9)$ -configuration tree is

$$(77) \quad \Lambda_X = \left\{ \textcircled{1}, \dots, \textcircled{9}; \textcircled{1}; (\Delta_{15}, 0), (\Delta_{52}, 0), (\Delta_{24}, 0), (\Delta_{43}, 0), \right. \\ \left. (\Delta_{16}, 0), (\Delta_{69}, 0), (\Delta_{97}, 0), (\Delta_{78}, 0) \right\}.$$

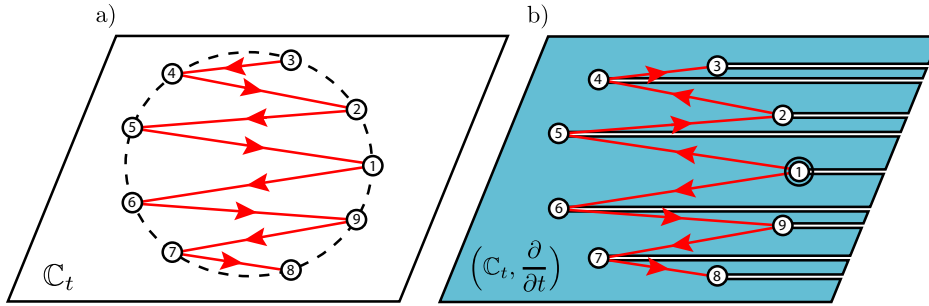


FIGURE 12. **Vector field $X(z) = e^{z^9} \frac{\partial}{\partial z}$ with essential singularity at ∞ and no poles.** In this case the top and left most vertex is $\textcircled{\sigma_0}$ with $\sigma_0 = \lceil \lfloor 9/2 \rfloor / 2 \rceil + 1 = 3$. (a) Represents the left-right-top-bottom linear directed tree of the vertices $V_H = \{\textcircled{1}, \dots, \textcircled{9}\}$. (b) Represents the $(0, 9)$ -configuration tree Λ_X where all the edges have weight 0. The soul, Definition 9.7, is shaded blue. The Riemann surface \mathcal{R}_X consists of gluing 18 semi-infinite helicoids, one above and one below each logarithmic branch point/vertex. All the branch points and diagonals belong to the global zero level sheet.

The soul of \mathcal{R}_X is a sheet and coincides with the global zero level.

The following example is a family of vector fields in $\mathcal{E}(0, 3)$ whose $(0, 3)$ -configuration trees have two edges, one of which can assume a non-zero weight. Recall that the weight of an edge indicates the number of sheets one has to go up or down, at the starting branch point, in order to reach the sheet that shares both the starting and ending branch point of the diagonal/edge (*i.e.* the sheet containing the diagonal).

Example 8.5. Consider the vector field

$$(78) \quad X(z) = 2\pi i \exp\left(-\frac{1}{3}z^3 + c_2 z\right) \frac{\partial}{\partial z}, \quad c_2 \in \mathbb{C}.$$

We shall need some background on Airy functions and integrals, for full details see [2], pp. 200–203 and references therein. Let

$$\mathcal{A}i(p, z) = \frac{1}{2\pi i} \int_{\mathcal{L}(z)} e^{\frac{1}{3}\zeta^3 - p\zeta} d\zeta,$$

be the *Airy integral*, where $A = \{z \in \mathbb{C} \mid \arg(z) \in (\pi/6, 3\pi/6)\}$ and $\mathcal{L}(z) := \mathcal{L}(z, \tau) : [0, 1] \rightarrow A$ is a simple C^1 path starting at 0 and ending at $z \in A$. The relationship between the Airy function Ai and the Airy integral is given by

$$(79) \quad \text{Ai}(p) = \mathcal{A}i(p) - e^{-i2\pi/3} \mathcal{A}i(e^{-i2\pi/3} p), \quad \mathcal{A}i(p) = \lim_{\substack{z \rightarrow \infty \\ z \in A}} \mathcal{A}i(p, z).$$

Choosing $z_0 = 0$, the distinguished parameter of X is

$$\Psi_X(z) = \int_0^z \omega_X = \frac{1}{2\pi i} \int_0^z e^{\frac{1}{3}\zeta^3 - c_2 \zeta} d\zeta,$$

so the 3 finite asymptotic values of $\Psi_X(z)$ are given by

$$(80) \quad a_{j+1}(c_2) = \eta^j \mathcal{A}i(\eta^j c_2), \quad j = 0, 1, 2, \quad \eta = e^{i2\pi/3},$$

with asymptotic paths ending in the exponential tracts $\eta^j A$, for $j = 0, 1$ and 2 respectively.

The $(0, 3)$ -configuration trees for X as in (78) are

$$(81) \quad \Lambda_X = \left\{ \textcircled{1} = (\infty_1, a_1, -\infty), \textcircled{2} = (\infty_2, a_2, -\infty), \textcircled{3} = (\infty_3, a_3, -\infty); \right. \\ \left. \textcircled{\textcircled{1}}; (\Delta_{12}, 0), (\Delta_{13}, K(1, 3)) \right\},$$

where

$$(82) \quad \begin{aligned} \Delta_{12} &= a_2 - a_1 = \eta \text{Ai}(\eta c_2), \\ \Delta_{13} &= a_3 - a_1 = -\text{Ai}(c_2), \end{aligned}$$

with $K(1, 3) \in \mathbb{Z}$. See Figure 13. The dependency of Δ_{12} and Δ_{13} on c_2 is clear from (82), however the dependency of $K(1, 3)$ on c_2 is much more intricate, any $K(1, 3) \in \mathbb{Z}$ appears: for a full description see [2] §8.6.1, particularly figure 14.

8.4. $X \in \mathcal{E}(r, d)$ has $r \geq 1$ poles on \mathbb{C}_z and an isolated essential singularity at $\infty \in \widehat{\mathbb{C}}_z$. The next example shows a simple case where the soul is non-trivial: it consists of more than one sheet.

Example 8.6. Consider the vector field

$$X(z) = \frac{e^z}{(z - p_1)(z - p_2)} \frac{\partial}{\partial z} \in \mathcal{E}(2, 1),$$

with $p_1 = 9i\frac{\pi}{2}$ and $p_2 = -i\frac{\pi}{2}$. Its distinguished parameter is then

$$\Psi_X(z) = \int_{z_0}^z \omega_X = \frac{e^{-z}}{4} (-8 - 9\pi^2 + 16i\pi(1 + z) - 4z(2 + z)).$$

The vector field X has an isolated essential singularity at $\infty \in \widehat{\mathbb{C}}_z$ and Ψ_X has one finite asymptotic value

$$a_1 = \Psi_X(\infty) = 0$$

with asymptotic path inside the exponential tract $\{z \in \mathbb{C}_z \mid \Re(z) > 0\}$. The poles p_1, p_2 have associated critical values $\tilde{p}_1 = -5\pi + 2i$ and $\tilde{p}_2 = -5\pi - 2i$ respectively.

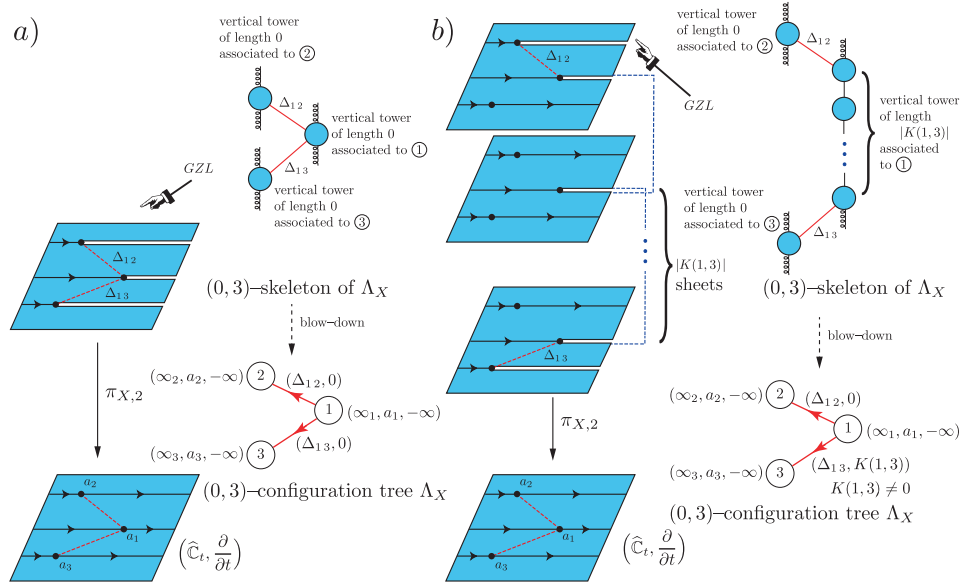


FIGURE 13. **Vector field** $X(z) = 2\pi i \exp\left(-\frac{1}{3}z^3 + c_2 z\right) \frac{\partial}{\partial z} \in \mathcal{E}(0,3)$ **with essential singularity at ∞ and no poles.** In (a) we have the case when $K(1,2) = K(1,3) = 0$ so the diagonals Δ_{12} and Δ_{13} share the same sheet of \mathcal{R}_X . Case (b) is when $K(1,2) = 0$ and $K(1,3) \in \mathbb{Z} \setminus \{0\}$, thus the diagonals Δ_{12} and Δ_{13} lie on two different sheets of \mathcal{R}_X . When starting on the global zero level sheet (the one that contains the diagonal Δ_{12}) one needs to go around the branch point $(\infty_1, a_1, -\infty)$ exactly $K(1,3)$ times (see Remark 5.19.4) in order to reach the sheet containing the diagonal Δ_{13} (thus in this figure $K(1,3) < 0$). Note that for case (b) the global zero level sheet is non canonical: if we instead choose as the global zero level sheet the one containing the diagonal Δ_{13} , then the integer parameters would be $K(1,3) = 0$ and $K(1,2) > 0$.

According to the labelling conventions in Definition 7.7, the $(2,1)$ -configuration tree

$$(83) \quad \Lambda_X = \left\{ \textcircled{1} = (p_1, \tilde{p}_1, -1), \textcircled{2} = (\infty_1, a_1, -\infty), \textcircled{3} = (p_2, \tilde{p}_2, -1); \right. \\ \left. \textcircled{1}; (\Delta_{12}, 0), (\Delta_{23}, -3) \right\},$$

has two pole vertices $\textcircled{1}, \textcircled{3}$, an essential vertex $\textcircled{2}$, and two edges

$$\Delta_{12} = a_1 - \tilde{p}_1 = 5\pi - 2i \quad \text{with weight } 0,$$

and

$$\Delta_{23} = \tilde{p}_2 - a_1 = -5\pi - 2i \quad \text{with weight } -3.$$

Note that the $(2,1)$ -soul of Λ_X is the Riemann surface consisting of 12 half planes, 2 finite height horizontal strips, two cone points with cone angle 4π (corresponding to the two simple poles), a cone point with cone angle 8π (corresponding to the

infinitely ramified branch point $(\infty_1, a_1, -\infty)$ and a horizontal branch cut starting at the branch point $(\infty_1, a_1, -\infty)$. See Figures 14 and 4.

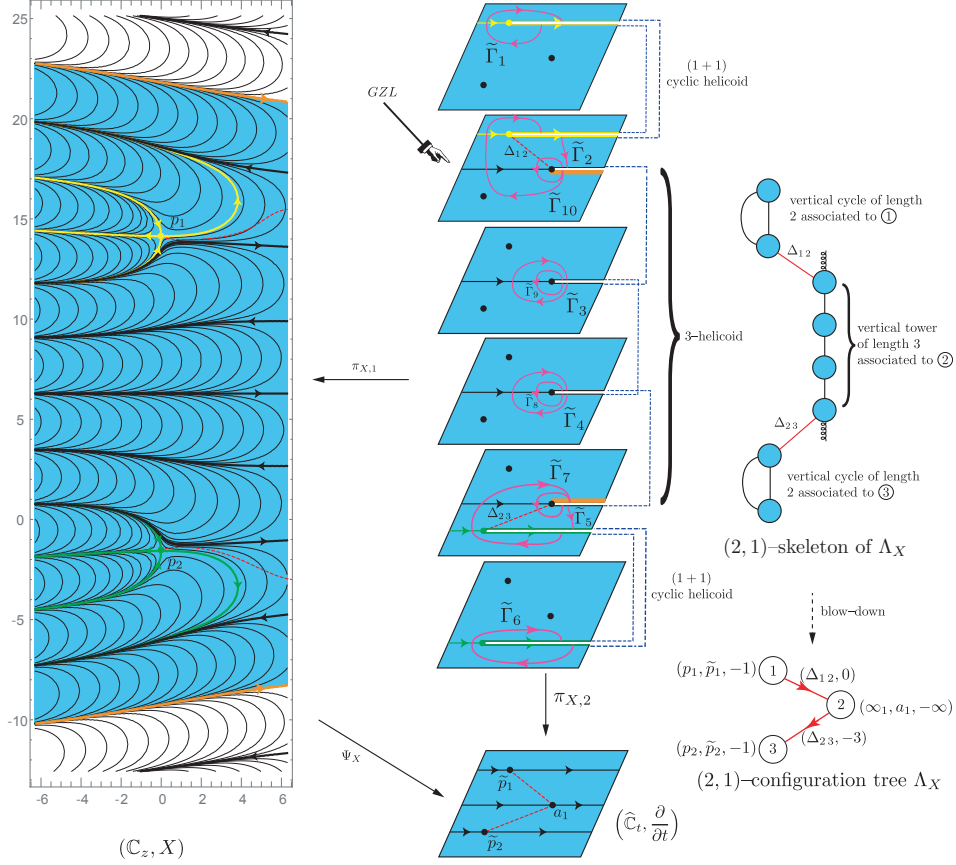


FIGURE 14. **Vector field** $X(z) = \frac{e^z}{(z - 9i\frac{\pi}{2})(z + i\frac{\pi}{2})} \frac{\partial}{\partial z}$ **with essential singularity at ∞ and two simple poles at $p_1 = 9i\frac{\pi}{2}$ and $p_2 = -i\frac{\pi}{2}$.** The Riemann surface \mathcal{R}_X consists of two semi-infinite helicoids, two $(1+1)$ -cyclic helicoids and a 3-helicoid. The soul, Definition 9.7, is shaded blue and consists of the Riemann surface \mathcal{R}_X minus the semi-infinite helicoids. The boundary (where the two semi-infinite helicoids should be glued) is coloured orange.

The next examples present (r, d) -configuration trees with more than one weighted edge.

Example 8.7. Consider the vector field

$$X(z) = -\frac{e^{z^3}}{3z^2} \frac{\partial}{\partial z} \in \mathcal{E}(2, 3).$$

If $z_0 = 0$ the distinguished parameter is

$$\Psi_X(z) = e^{-z^3} - 1.$$

Thus the pole $p_1 = 0$ has order $-\nu_1 = -2$ and critical value $\tilde{p}_1 = 0$, while the essential singularity at $\infty \in \widehat{\mathbb{C}}_z$ has finite asymptotic value $a_1 = -1$, with multiplicity 3. In order to distinguish each of the three finite asymptotic values, one has to consider the asymptotic path associated to each and see on which of the following exponential tracts each lies in

$$(84) \quad \begin{aligned} A_1 &= \{z \in \mathbb{C} \mid \arg(z) \in (-\pi/6, \pi/6)\}, & A_2 &= \{z \in \mathbb{C} \mid \arg(z) \in (\pi/2, 5\pi/6)\}, \\ A_3 &= \{z \in \mathbb{C} \mid \arg(z) \in (7\pi/6, 3\pi/2)\}. \end{aligned}$$

That is $(\infty_1, -1, -\infty), (\infty_2, -1, -\infty), (\infty_3, -1, -\infty) \in \mathcal{R}_X$ are 3 logarithmic branch points corresponding to the above exponential tracts as in Definition 4.3.

The $(2, 3)$ -configuration tree has three essential vertices, and one pole vertex. According to Definition 7.7.4, since $r \neq 0$ the root must be the unique pole vertex, so we conveniently label the vertices as follows

$$\begin{aligned} \textcircled{1} &= (z_1, t_1, -\nu_1) = (p_1, \tilde{p}_1, -2), & \textcircled{2} &= (z_2, t_2, -\nu_2) = (\infty_1, a_1, -\infty), \\ \textcircled{3} &= (z_3, t_3, -\nu_3) = (\infty_2, a_1, -\infty), & \textcircled{4} &= (z_4, t_4, -\nu_4) = (\infty_3, a_1, -\infty). \end{aligned}$$

In this way the $(2, 3)$ -configuration tree is

$$(85) \quad \Lambda_X = \left\{ \textcircled{1}, \textcircled{2}, \textcircled{3}, \textcircled{4}; \textcircled{\textcircled{1}}; (\Delta_{12}, 0), (\Delta_{13}, 1), (\Delta_{14}, -1) \right\}.$$

Once again the edges Δ_{12} , Δ_{13} and Δ_{14} correspond to the diagonals/semi-residues between the branch points associated to the corresponding vertices:

$$(86) \quad \begin{aligned} \Delta_{12} &= \int_{p_1}^{\infty_1} \omega_X = a_1 - \tilde{p}_1 = -1, & \Delta_{13} &= \int_{p_1}^{\infty_2} \omega_X = a_1 - \tilde{p}_1 = -1, \\ \Delta_{14} &= \int_{p_1}^{\infty_3} \omega_X = a_1 - \tilde{p}_1 = -1. \end{aligned}$$

The weight $K(1, 2) = 0$ since the branch points corresponding to the root $\textcircled{\textcircled{1}}$ and the vertex $\textcircled{2}$ share the same sheet in \mathcal{R}_X , $K(1, 3) = 1$ since in order to reach the diagonal Δ_{13} one has to go up one sheet, at the branch point corresponding to $\textcircled{1}$ (*i.e.* Δ_{13} is one sheet above the diagonal Δ_{12} in \mathcal{R}_X), and $K(1, 4) = -1$ since in order to reach the diagonal Δ_{14} one has to go down one sheet, at the branch point corresponding to $\textcircled{1}$ (*i.e.* Δ_{14} is one sheet below the diagonal Δ_{12} in \mathcal{R}_X).

Recalling Remark 7.8.2 and the definition of semi-residues (42), note that it is possible to calculate the weights $K(\mathbf{a}, \mathbf{r})$ by considering the phase portrait of X : the path of integration from p_1 to ∞_1 stays on the same angular sector about p_1 so $K(1, 2) = 0$, the path of integration from ∞_1 to ∞_2 necessarily crosses two angular sectors going counterclockwise around p_1 corresponding to going up a sheet in \mathcal{R}_X so $K(1, 3) = 1$, and the path of integration from ∞_1 to ∞_3 crosses two angular sectors going clockwise around p_1 corresponding to going down a sheet in \mathcal{R}_X so $K(1, 4) = -1$.

In this case the decomposition, provided by Lemma 7.4, into horizontal subtrees is

$$\Lambda_X = \Lambda_{H(1)} \cup \Lambda_{H(1,3)} \cup \Lambda_{H(1,4)},$$

where

$$\begin{aligned} \Lambda_{H(1)} &= \left\{ \textcircled{1}, \textcircled{2}; \textcircled{\textcircled{1}}; (\Delta_{12}, 0) \right\}, & \Lambda_{H(1,3)} &= \left\{ \textcircled{1}, \textcircled{3}; \textcircled{\textcircled{1}}; (\Delta_{13}, 1) \right\}, \\ \Lambda_{H(1,4)} &= \left\{ \textcircled{1}, \textcircled{4}; \textcircled{\textcircled{1}}; (\Delta_{14}, -1) \right\}. \end{aligned}$$

See Figure 15 and the left hand side of Figure 17.

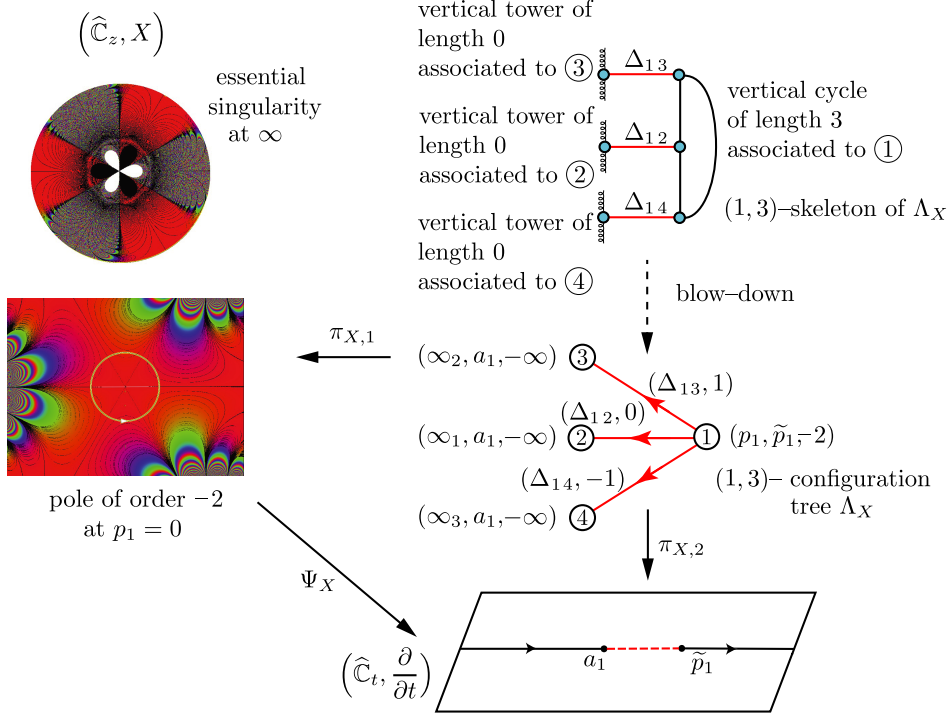


FIGURE 15. **Vector field** $X(z) = -\frac{e^{z^3}}{3z^2} \frac{\partial}{\partial z}$ **with an essential singularity at ∞ and pole $p_1 = 0$ of order -2 .** The diagonals Δ_{12} , Δ_{13} and Δ_{14} , and their projections are shown as red segments. The Riemann surface \mathcal{R}_X is not drawn. See Example 8.7, and §9.2 for the right drawing.

Example 8.8. In a similar vein as the previous example consider the vector field

$$X(z) = \frac{e^{z^3}}{3z^3 - 1} \frac{\partial}{\partial z} \in \mathcal{E}(3, 3),$$

with simple poles at $p_1 = \frac{1}{\sqrt[3]{3}}$, $p_2 = \frac{e^{i2\pi/3}}{\sqrt[3]{3}}$, $p_3 = \frac{e^{-i2\pi/3}}{\sqrt[3]{3}}$, and an essential singularity at $\infty \in \widehat{\mathbb{C}}_z$. Its distinguished parameter is

$$\Psi_X(z) = \int_0^z \omega_X = -ze^{-z^3}.$$

Thus the critical values corresponding to the poles are

$$\tilde{p}_1 = -\frac{1}{\sqrt[3]{3e}}, \quad \tilde{p}_2 = -\frac{e^{i2\pi/3}}{\sqrt[3]{3e}} \quad \text{and} \quad \tilde{p}_3 = -\frac{e^{-i2\pi/3}}{\sqrt[3]{3e}}.$$

The essential singularity at ∞ has $a_1 = 0$ as its finite asymptotic value with multiplicity 3, once again with the same exponential tracts as the previous example, see equation (84), hence $(\infty_1, 0, -\infty)$, $(\infty_2, 0, -\infty)$, $(\infty_3, 0, -\infty) \in \mathcal{R}_X$ are the 3 logarithmic branch points corresponding to the mentioned exponential tracts.

The $(3, 3)$ -configuration tree has three essential vertices and three pole vertices,

which we label as

$$(87) \quad \begin{aligned} \textcircled{1} &= (z_1, t_1, -\nu_1) = (p_2, \tilde{p}_2, -1), & \textcircled{2} &= (z_2, t_2, -\nu_2) = (p_1, \tilde{p}_1, -1), \\ \textcircled{3} &= (z_3, t_3, -\nu_3) = (p_3, \tilde{p}_3, -1), & \textcircled{4} &= (z_4, t_4, -\nu_4) = (\infty_1, a_1, -\infty), \\ \textcircled{5} &= (z_5, t_5, -\nu_5) = (\infty_2, a_1, -\infty), & \textcircled{6} &= (z_6, t_6, -\nu_6) = (\infty_3, a_1, -\infty). \end{aligned}$$

Thus the $(3, 3)$ -configuration tree (see Figure 16) is⁴

$$(88) \quad \Lambda_X = \left\{ \textcircled{1}, \textcircled{2}, \textcircled{3}, \textcircled{4}, \textcircled{5}, \textcircled{6}; \textcircled{\textcircled{3}}; \right. \\ \left. (\Delta_{36}, 0), (\Delta_{32}, 1), (\Delta_{24}, 1), (\Delta_{41}, 0), (\Delta_{15}, 1) \right\},$$

with edges given by the diagonals/semi-residues

$$(89) \quad \begin{aligned} \Delta_{36} &= \int_{p_3}^{\infty_3} \omega_X = a_1 - \tilde{p}_3 = \frac{e^{-i2\pi/3}}{\sqrt[3]{3e}}, \\ \Delta_{32} &= \int_{p_3}^{p_1} \omega_X = (\tilde{p}_1 - \tilde{p}_3) = -\left(\frac{1 - e^{-i2\pi/3}}{\sqrt[3]{3e}} \right), \\ \Delta_{24} &= \int_{p_1}^{\infty_1} \omega_X = a_1 - \tilde{p}_1 = \frac{1}{\sqrt[3]{3e}}, \\ \Delta_{41} &= \int_{p_1}^{p_2} \omega_X = \tilde{p}_2 - a_1 = -\frac{1}{\sqrt[3]{3e}} e^{i2\pi/3}, \\ \Delta_{15} &= \int_{p_2}^{\infty_2} \omega_X = a_1 - \tilde{p}_2 = \frac{e^{i2\pi/3}}{\sqrt[3]{3e}}, \end{aligned}$$

and weights $K(3, 6) = 0$, $K(3, 2) = 1$, $K(2, 4) = 1$, $K(4, 1) = 0$, $K(1, 5) = 1$.

Once again it is instructive to examine in detail how these weights are calculated, Figures 16 and 17 will facilitate the discussion.

Consider the phase portrait of X : for the calculation of the weight $K(3, 6) = 0$, consider the projection of the diagonal Δ_{36} onto \mathbb{C}_z , clearly this path remains on one angular sector about p_3 (that corresponds to the exponential tract A_3 containing $\infty_3 \in \overline{\mathbb{C}_z}$). Thus the logarithmic branch point $(\infty_3, a_1, -\infty)$ and the finitely ramified branch point $(p_3, \tilde{p}_3, -1)$ share the same sheet on \mathcal{R}_X .

Now consider the projection onto \mathbb{C}_z of the diagonals Δ_{36} and Δ_{32} : the projection of Δ_{36} lies on the exponential tract A_3 associated to ∞_3 while the projection of the diagonal Δ_{32} lies on the strip flow determined by p_1 and p_3 . In order to go from the exponential tract A_3 to the strip flow just mentioned, one must go through three half planes about p_3 . This is equivalent to going up (or down) one level on \mathcal{R}_X , hence $K(3, 2) = 1$.

Similarly, considering the projections of Δ_{32} and Δ_{24} we note that when coming from the pole p_3 to the pole p_1 and then to ∞_1 contained in A_1 we go around p_1 and touch upon three half planes (since ∞_1 lies on the real axis), thus $K(2, 4) = 1$. For $K(2, 1) = 0$, note that the projection of Δ_{41} lies entirely within the strip flow determined by p_1 and p_2 , thus the logarithmic branch point $(\infty_1, a_1, -\infty)$ and the finitely ramified branch point $(p_2, \tilde{p}_2, -1)$ share the same sheet on \mathcal{R}_X .

Finally, by considering the projections of Δ_{41} and Δ_{15} we see that the projection of Δ_{15} lies on the exponential tract associated to ∞_2 while the projection of the diagonal Δ_{41} lies on the exponential tract associated to ∞_1 . In order to go from one exponential tract to another one must cross at least three angular sectors (but

⁴The root is $\textcircled{\textcircled{3}}$ so as to agree with the conventions of Definition 7.7.

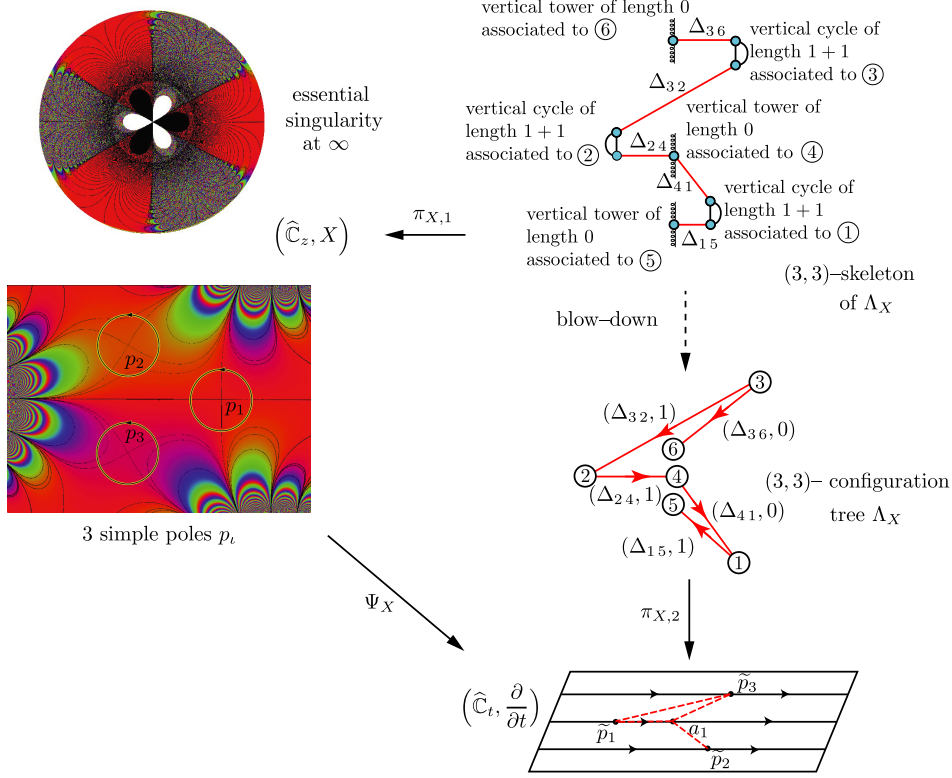


FIGURE 16. **Vector field** $X(z) = \frac{e^{z^3}}{3z^3 - 1} \frac{\partial}{\partial z}$ **with an essential singularity at ∞ and 3 simple poles p_i .** The five diagonals and their projections are shown in red. The Riemann surface \mathcal{R}_X is not drawn. See Example 8.8, and §9.2 for the drawing on the right.

no more than four), this is equivalent to the fact that one must go up or down one level on \mathcal{R}_X to get from the sheet containing Δ_{41} to the sheet containing Δ_{15} . Hence $K(1, 5) = 1$.

In this case the decomposition, provided by Lemma 7.4, into horizontal subtrees is

$$\Lambda_X = \Lambda_{H(3)} \cup \Lambda_{H(3,2)} \cup \Lambda_{H(2,4)} \cup \Lambda_{H(1,5)},$$

where

$$\begin{aligned} \Lambda_{H(3)} &= \{ \textcircled{3}, \textcircled{6}; \textcircled{\textcircled{3}}; (\Delta_{36}, 0) \}, & \Lambda_{H(3,2)} &= \{ \textcircled{2}, \textcircled{3}; \textcircled{\textcircled{3}}; (\Delta_{32}, 1) \}, \\ \Lambda_{H(2,4)} &= \{ \textcircled{1}, \textcircled{2}, \textcircled{4}; \textcircled{\textcircled{2}}; (\Delta_{24}, 1)(\Delta_{41}, 0) \}, & \Lambda_{H(1,5)} &= \{ \textcircled{1}, \textcircled{5}; \textcircled{\textcircled{1}}; (\Delta_{15}, 1) \}. \end{aligned}$$

Example 8.9. Recall Example 4.2, where the vector fields

$$X(z) = \frac{e^{z^d}}{z^r} \frac{\partial}{\partial z} \in \mathcal{E}(r, d), \quad \text{for } d \geq 1,$$

are approximated by the rational vector fields

$$X_n(z) = \frac{1}{z^r \left(1 - \frac{z^d}{n}\right)^n} \frac{\partial}{\partial z} \in \mathcal{E}(r + nd, 0), \quad \text{for } n \geq 1.$$

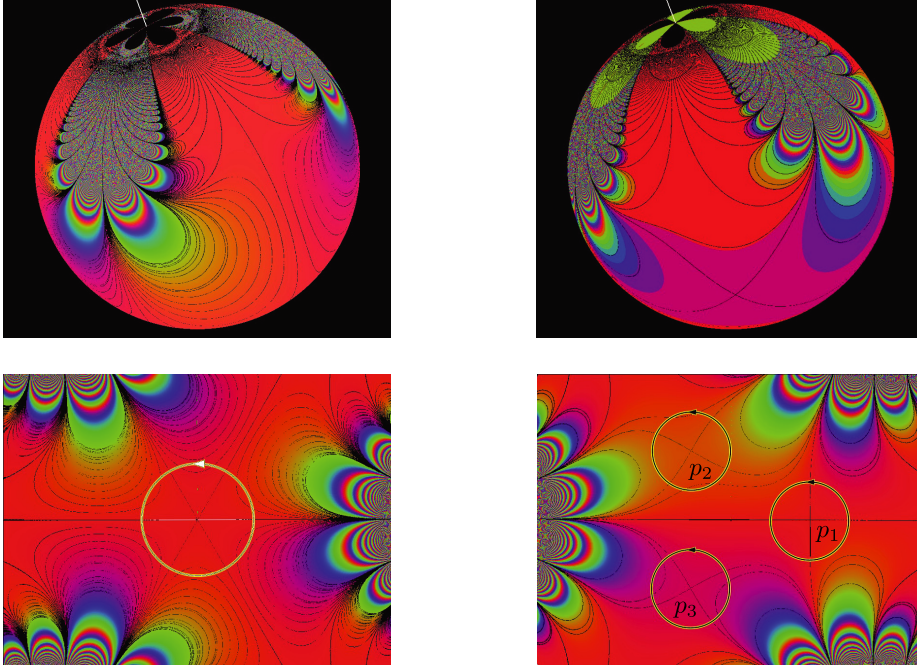


FIGURE 17. Detail of vector fields in Examples 8.7 and 8.8.

The left hand side shows the vector field $X(z) = -\frac{e^{z^3}}{3z^2} \frac{\partial}{\partial z}$, the right hand side the vector field $X(z) = \frac{e^{z^3}}{3z^3-1} \frac{\partial}{\partial z}$. Each angular sector around the poles corresponds to a half plane on \mathcal{R}_X . Note that the dynamics of $\Re(X)$ in a neighbourhood of $\infty \in \widehat{\mathbb{C}}$ are different. The images contain the information needed to construct the corresponding (r, d) -configuration trees, as explained in the text.

We wish to explore (some of) the (r, d) -configuration trees for X and X_n .

First note that the answer will heavily depend on the parameters r and d . For instance, (37) shows that there is only one finite asymptotic value a with multiplicity d (as in Example 8.7) if and only if $r = -1 \pmod{d}$, i.e. $(r+1)/d = k \in \mathbb{N}$.

In this case the unique finite asymptotic value is $a = (k-1)!/d$. Thus \mathcal{R}_X has a branch point at $\textcircled{1} = (p_1, \tilde{p}_1, -\nu_1) = (0, 0, -r)$ of ramification index $\nu_1 = r = kd - 1$ and logarithmic branch points at $\textcircled{1+\sigma} = (\infty_\sigma, a, -\infty) \in \mathcal{R}_X$, with asymptotic paths $\alpha_\sigma(\tau) = \tau e^{i2\pi\sigma/d}$ for $\sigma = 1, \dots, d$.

On the other hand the Riemann surfaces \mathcal{R}_{X_n} associated to $X_n(z)$ have a branch point at $\textcircled{1} = (p_1, \tilde{p}_1, -r) = (0, 0, -r)$ of ramification index $r+1 = kd$ and branch points at

$$\textcircled{1+\sigma}_n = (\widehat{e}_\sigma(\mathbf{n}), \tilde{e}_\sigma(\mathbf{n}), -\mathbf{n}) = (e^{i2\pi\sigma/d} \mathbf{n}^{1/d}, a \mathbf{n}^k \mathbf{n}! / (\mathbf{n}+k)!, -\mathbf{n})$$

of ramification index $\mathbf{n} + 1$, for $\sigma = 1, \dots, d$. Hence by examining the corresponding phase portraits we can see that the (r, d) -configuration trees are given by

$$(90) \quad \Lambda_{X_n} = \left\{ \textcircled{1}, \textcircled{2}_n, \dots, \textcircled{1+\sigma}_n, \dots, \textcircled{1+d}_n; \textcircled{\textcircled{1}}; \right. \\ \left. (\Delta_{12}, 0), (\Delta_{13}, k), \dots, (\Delta_{1(1+\sigma)}, (\sigma-1)k), \dots, (\Delta_{1(1+d)}, (d-1)k) \right\},$$

$$(91) \quad \Lambda_X = \left\{ \textcircled{1}, \textcircled{2}, \dots, \textcircled{1+\sigma}, \dots, \textcircled{1+d}; \textcircled{\textcircled{1}}; \right. \\ \left. (\Delta_{12}, 0), (\Delta_{13}, k), \dots, (\Delta_{1(1+\sigma)}, (\sigma-1)k), \dots, (\Delta_{1(1+d)}, (d-1)k) \right\},$$

whose skeletons are as in Figure 18.

Example 8.10. *A prototypical $(r, 4)$ -configuration tree.* Consider a vector field

$$(92) \quad X(z) = \frac{e^{E(z)}}{(z-p_1)^{\nu_1}(z-p_2)^{\nu_2}} \frac{\partial}{\partial z}, \quad r = \nu_1 + \nu_2,$$

$E(z)$ a polynomial of degree 4, and $\Im(p_1) > \Im(p_2)$. The singularity at $\infty \in \widehat{\mathbb{C}}_z$ has four finite asymptotic values (∞_1, a_1) , (∞_2, a_2) , (∞_3, a_2) and (∞_4, a_3) ; note that two of them differ exclusively by their exponential tract, sharing the asymptotic value $a_2 \in \mathbb{C}_z$. The existence of such a polynomial $E(z)$ will be proved in §9.3, in particular this involves solving the system of equations (45).

The following $(r, 4)$ -configuration tree Λ_X , will be used to exemplify some constructions and possible complexities that arise in the proof of the Main Theorem. Thus the $(r, 4)$ -configuration tree has three essential vertices and two pole vertices, which we label as follows

$$(93) \quad \begin{aligned} \textcircled{1} &= (p_1, \tilde{p}_1, -\nu_1), & \textcircled{2} &= (\infty_2, a_2, -\infty), & \textcircled{3} &= (\infty_1, a_1, -\infty), \\ \textcircled{4} &= (p_2, \tilde{p}_2, -\nu_2), & \textcircled{5} &= (\infty_3, a_2, -\infty), & \textcircled{6} &= (\infty_4, a_3, -\infty). \end{aligned}$$

Let

$$(94) \quad \Lambda_X = \left\{ \textcircled{1}, \textcircled{2}, \textcircled{3}, \textcircled{4}, \textcircled{5}, \textcircled{6}; \textcircled{\textcircled{1}}; \right. \\ \left. (\Delta_{12}, 0), (\Delta_{15}, -2), (\Delta_{23}, K(2, 3)), (\Delta_{24}, K(2, 4)), (\Delta_{26}, K(2, 6)) \right\},$$

with edges given by the diagonals/semi-residues

$$(95) \quad \begin{aligned} \Delta_{12} &= \int_{p_1}^{\infty_2} \omega_X = a_2 - \tilde{p}_1, & \Delta_{15} &= \int_{p_1}^{\infty_3} \omega_X = a_2 - \tilde{p}_1, \\ \Delta_{23} &= \int_{\infty_2}^{\infty_1} \omega_X = a_1 - a_2, & \Delta_{24} &= \int_{\infty_2}^{p_2} \omega_X = \tilde{p}_2 - a_2, \\ \Delta_{26} &= \int_{\infty_2}^{\infty_4} \omega_X = a_3 - a_2, \end{aligned}$$

and weights $K(1, 2) = 0$, $K(1, 5) = -2$, $K(2, 6) < K(2, 4) < K(2, 3) \leq -1$. Figure 19 shows the $(r, 4)$ -configuration tree Λ_X together with the corresponding $(r, 4)$ -skeleton. This figure will be used as a guide in the proof of the Main Theorem.

In this case the decomposition, provided by Lemma 7.4, into horizontal subtrees is

$$\Lambda_X = \Lambda_{H(1)} \cup \Lambda_{H(1,5)} \cup \Lambda_{H(2,3)} \cup \Lambda_{H(2,4)} \cup \Lambda_{H(2,6)},$$

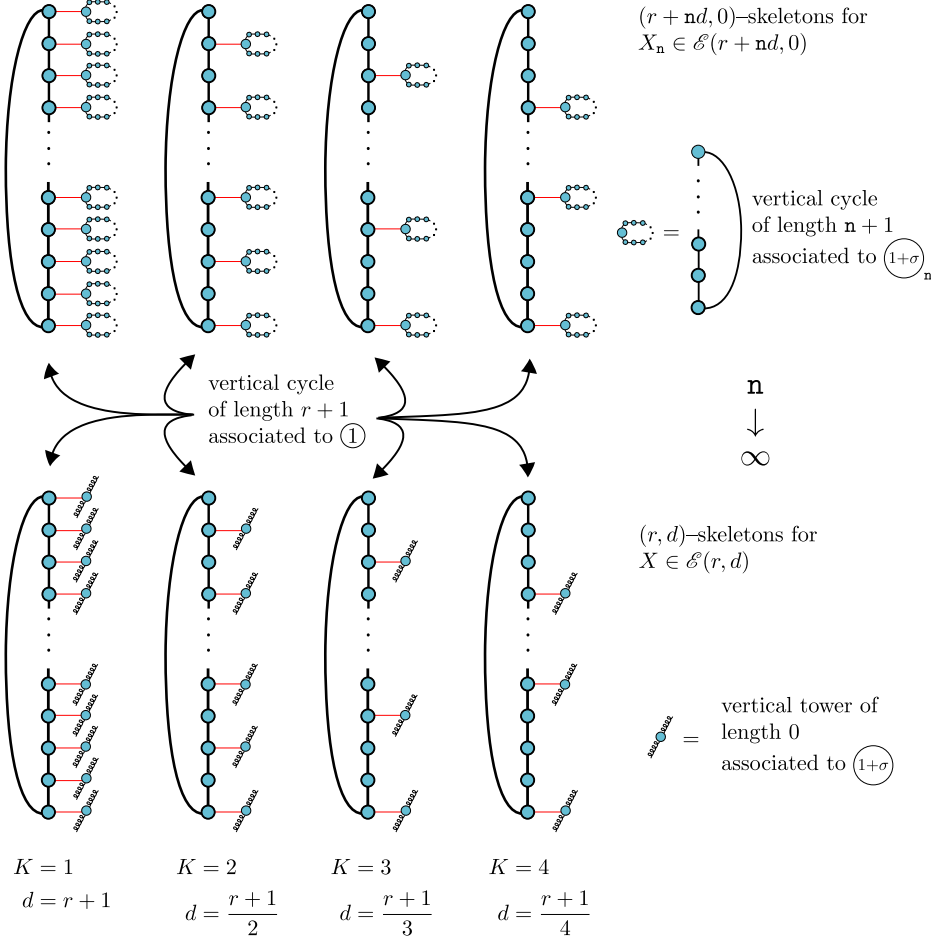


FIGURE 18. Regarding Example 8.9; the top figures are the $(r + nd, 0)$ -skeletons for $X_n \in \mathcal{E}(r + nd, 0)$ approximating $X \in \mathcal{E}(r, d)$, when $r = -1 \pmod{d}$. Bottom figures are the (r, d) -skeletons for $X \in \mathcal{E}(r, d)$. Note that for X_n the critical values are 0 and $a n^k n! / (n+k)!$ and for X the only critical value is 0 and the only finite asymptotic value is $a = (k-1)!/d$. Further note that $k = (r+1)/d$ is the number of sheets that separate the different diagonals both in \mathcal{R}_{X_n} and \mathcal{R}_X .

where

$$\begin{aligned}
 \Lambda_{H(1)} &= \left\{ \textcircled{1}, \textcircled{2}; \textcircled{\textcircled{1}}; (\Delta_{12}, 0) \right\}, & \Lambda_{H(1,5)} &= \left\{ \textcircled{1}, \textcircled{5}; \textcircled{\textcircled{1}}; (\Delta_{15}, -2) \right\}, \\
 \Lambda_{H(2,3)} &= \left\{ \textcircled{2}, \textcircled{3}; \textcircled{\textcircled{2}}; (\Delta_{23}, K(2,3)) \right\}, & \Lambda_{H(2,4)} &= \left\{ \textcircled{2}, \textcircled{4}; \textcircled{\textcircled{2}}; (\Delta_{24}, K(2,4)) \right\}, \\
 \Lambda_{H(2,6)} &= \left\{ \textcircled{2}, \textcircled{6}; \textcircled{\textcircled{2}}; (\Delta_{26}, K(2,6)) \right\}.
 \end{aligned}$$

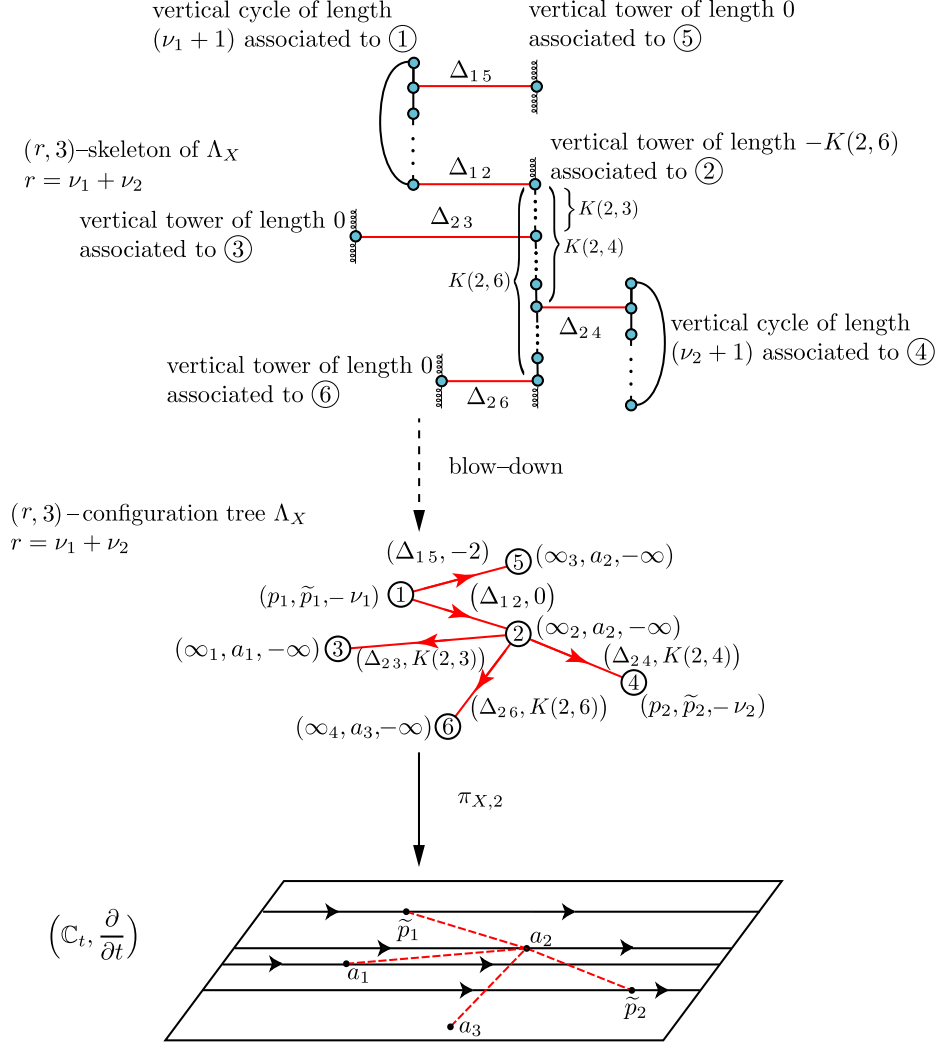


FIGURE 19. **The $(r, 4)$ -configuration tree Λ_X and its $(r, 4)$ -skeleton corresponding to Example 8.10.** The root is ①, the weight $K(1, 2) = 0$ (hence the branch points ①, ② which are the endpoints of the diagonal $\Delta_{12} \subset \mathcal{R}_X$, share the global zero level (GZL) sheet), $K(1, 5) = -2 \pmod{\nu_1 + 1}$, and $K(2, 6) < K(2, 4) < K(2, 3) \leq -1$. The information about how many sheets we have gone “up” or “down” on the Riemann surface is given by the weights. The asymptotic value a_2 has multiplicity 2.

9. PROOF OF MAIN THEOREM: DESCRIPTION OF THE FAMILY $\mathcal{E}(r, d)$ VIA COMBINATORIAL SCHEME

Plan for proof. That $\mathcal{E}(r, d)$ is a complex manifold of dimension $r + d + 1$ is obvious, see [3] for more general discussion.

The proof of the bijection $\mathcal{E}(r, d) \cong \{[\Lambda_X]\}$ shall procede as follows:

- 1) In §9.1 starting from Ψ_X , we construct the (r, d) -configuration tree Λ_X .
- 2) In §9.2, we start with an abstract (r, d) -configuration tree Λ_X Definition 7.7 and construct the (r, d) -skeleton of Λ_X (as an associated combinatorial object).
- 3) In §9.3 from the (r, d) -skeleton of Λ_X , we proceed to construct a Riemann surface \mathcal{R}_X in $\mathcal{E}(r, d)$.

Note that our Dictionary Proposition 2.5 provides the correspondence between \mathcal{R}_X , Ψ_X and $X \in \mathcal{E}(r, d)$.

The suitable equivalence class $[\Lambda_X]$ of (r, d) -configuration trees Λ_X will be explained in §9.4.

9.1. From $X \in \mathcal{E}(r, d)$ to an (r, d) -configuration tree Λ_X .

Recalling Definition 7.7 of (r, d) -configuration tree, we have:

- The trivial case: Ψ_X has exactly one finite asymptotic or critical value:

From Lemma 5.3, only the following two cases are possible,

$$1) X(z) = \frac{\mu}{(z-p_1)^r} \frac{\partial}{\partial z}, \text{ i.e. } (r, d) = (r, 0), \text{ or}$$

$$2) X(z) = \mu^{-1} e^z \frac{\partial}{\partial z}, \text{ i.e. } (r, d) = (0, 1),$$

where $p_1 \in \mathbb{C}_z$ and $\mu \neq 0$.

For (1), $\Lambda_X = \{\textcircled{1} = (p_1, \tilde{p}_1, -r); \textcircled{1}; \emptyset\}$, see Example 8.1.

For (2), $\Lambda_X = \{\textcircled{1} = (\infty_1, a_1, -\infty); \textcircled{1}; \emptyset\}$, see Example 8.3.

- The non-trivial case: Ψ_X has two or more finite asymptotic or critical values, i.e. $d + n \geq 2$:

Considering the surface \mathcal{R}_X , recall Equation (31) and the reduced divisor, Definition 5.1.

1. Vertices of Λ_X . Let the vertices be those obtained from the reduced divisor

$$(96) \quad V = \left\{ \textcircled{\iota} = (p_\iota, \tilde{p}_\iota, -\nu_\iota) \right\}_{\iota=1}^n \cup \left\{ \textcircled{n+\sigma} = (\infty_\sigma, a_\sigma, -\infty) \right\}_{\sigma=1}^d \\ = \left\{ \textcircled{\mathfrak{a}} = (z_\mathfrak{a}, t_\mathfrak{a}, -\nu_\mathfrak{a}) \right\}_{\mathfrak{a}=1}^{n+d}.$$

There are $n + d$ vertices.

Note that the essential vertices $\textcircled{n+\sigma}$ are labelled as in Remark 4.6.2, that is according to the natural counterclockwise order of the exponential tracts in S^1 about $\infty \in \widehat{\mathbb{C}}_z$. Root choice:

If $r = 0$ let the root be $\textcircled{\varrho} \doteq \textcircled{1} = (\infty_1, a_1, -\infty)$.

If $r \neq 0$ let the vertex $(p_\varrho, \tilde{p}_\varrho, -\nu_\varrho)$ be such that $\Im(\tilde{p}_\varrho) \geq \Im(\tilde{p}_\iota)$ and $\Re(\tilde{p}_\varrho) \leq \Re(\tilde{p}_\iota)$ for $1 \leq \iota \leq n$; i.e. $\tilde{p}_\varrho \in \mathbb{C}_t$ is the top & left-most critical value, following the root condition in Definition 7.7. In this case, choose the root to be $\textcircled{\varrho} \doteq (p_\varrho, \tilde{p}_\varrho, -\nu_\varrho)$.

2. Edges of Λ_X . From Definition 5.4, the diagonals, associated to different pairs $t_\mathfrak{a}, t_\mathfrak{r}$ of finite asymptotic or critical values, are *oriented* segments

$$\Delta_{\mathfrak{ar}} = \overline{(z_\mathfrak{a}, t_\mathfrak{a}, -\nu_\mathfrak{a})(z_\mathfrak{r}, t_\mathfrak{r}, -\nu_\mathfrak{r})} \text{ in } \mathcal{R}_X,$$

whose endpoints project down, via $\pi_{X,2}$, to the finite asymptotic or critical values $t_\mathfrak{a}, t_\mathfrak{r}$. From Lemma 5.6 it follows that there are at least two⁵ diagonals associated to each finite asymptotic or critical value. As a first step, we ignore orientation

⁵This is so because diagonals are oriented.

and consider the diagonals as undirected edges⁶, which without loss of generality we shall simply denote by $E = \{\Delta_{\text{ar}}\}$. In this way we obtain a connected graph, say $G = \{V; E\}$.

A subgraph formed by the set of vertices associated to branch points that share the same sheet in \mathcal{R}_X will be called a *horizontal subgraph*. Note that each horizontal subgraph, consisting of the vertices (branch points) sharing a same sheet of \mathcal{R}_X , say $\{\mathcal{L} = (z_\ell, t_\ell, -\nu_\ell)\}_{\ell=1}^s$ together with the corresponding set of edges (undirected diagonals) on the same sheet, forms a complete graph K_s with $s(s-1)$ edges. However, by eliminating appropriate edges from K_s we can always obtain an (undirected) left-right-top-bottom linear tree of the vertices $\{\mathcal{L} = (z_\ell, t_\ell, -\nu_\ell)\}_{\ell=1}^s$, recall Definition 7.6.

Now replace each of the horizontal subgraphs of G by the corresponding (undirected) left-right-top-bottom linear tree. As a consequence, the diagonals Δ_{ar} and finite height horizontal strips

$$\left(\{\Im(t_{\text{a}}) \leq \Im(t) \leq \Im(t_{\text{r}})\}, \frac{\partial}{\partial t}\right) \subset \mathcal{R}_X$$

are in bijective correspondence, as in Lemma 5.9.2–3.

This produces a connected (undirected) graph $\bar{\Lambda}_X$ whose horizontal subgraphs are (undirected) left-right-top-bottom linear subtrees. The next lemma shows its shape.

Lemma 9.1. *If $X \in \mathcal{E}(r, d)$ then the graph $\bar{\Lambda}_X$ is a tree.*

Proof. Recall the decomposition of \mathbb{C}_z in half planes and finite height horizontal strips, Lemma 5.9.

Assume that all the asymptotic and critical values t_{a} , associated to the branch points $(z_{\text{a}}, t_{\text{a}})$, lie on different horizontal trajectories of $(\mathbb{C}_t, \frac{\partial}{\partial t})$ (we leave the general case for the interested reader, see for instance the discussion preceding Proposition 9.8). Note that the intersection of the interior of any two finite height horizontal strips is empty.

Since \mathbb{C}_z is simply connected and each diagonal determines a finite height horizontal strip, there is no loop/cycle of diagonals. \square

Finally, assign an orientation to $\bar{\Lambda}_X$ by choosing the appropriate orientation so that the edges point away from the root vertex \mathcal{Q} .

We thus obtain a non-weighted, directed rooted tree

$$(97) \quad \left\{ \{\mathfrak{a} = (z_{\text{a}}, t_{\text{a}}, -\nu_{\text{a}})\}_{\text{a}=1}^{d+n}; \mathcal{Q}; \{\Delta_{\text{ar}}\} \right\},$$

satisfying conditions (1–6) of Definition 7.7.

By simple inspection, it is clear that each diagonal in (97) falls into one of the cases mentioned in Remark 5.5.

3. Weights of Λ_X . At this point of the description of the surface \mathcal{R}_X , the branch points correspond to vertices of a non-weighted tree whose edges correspond to the diagonals between branch points. However, as mentioned in Remark 5.19, an important part of the description of the Riemann surface \mathcal{R}_X as a pasting of geometric pieces, corresponds to the number of sheets in \mathcal{R}_X that separate the diagonals (pairwise). Recalling that in a rooted tree there is a unique (simple) path from each vertex to the root, allows us to assign a weight to each edge/diagonal of the tree.

⁶We agree to leave only one undirected edge for each pair of oriented edges.

As an aid, the reader can follow the construction by considering Example 8.10. [We will include such references inside square brackets.]

For the assignment of weights $\{K(\mathbf{a}, \mathbf{r})\}$ to the edges $\{\Delta_{\mathbf{a}\mathbf{r}}\}$ we shall proceed by induction on the depth of the vertices as follows.

- a) We start by considering the vertices contiguous to the root $\textcircled{\varrho}$ (*i.e.* vertices of depth 1 in (97)), say $\{\textcircled{\mathfrak{z}}\}$. Since all the branch points corresponding to $\{\textcircled{\mathfrak{z}}\}$ share a sheet with the branch point corresponding to the root $\textcircled{\varrho}$, any of the corresponding edges can be assigned a weight zero. Choose one, say $\textcircled{\mathfrak{z}_0}$, and assign the weight $K(\varrho, \mathfrak{z}_0) = 0$ to the edge $\Delta_{\varrho\mathfrak{z}_0}$ and call this sheet in \mathcal{R}_X the *global zero level (GZL) sheet*.

If there are more vertices in $\{\textcircled{\mathfrak{z}}\}$ whose branch points share the global zero level sheet then the corresponding edges are also assigned the weight 0.

[Referring to Example 8.10, our first edge is Δ_{12} with weight $K(1, 2) = 0$; note that the diagonal is as in case (3) of Remark 5.5. Moreover, there are no more vertices sharing the GZL sheet.]

- b) Now consider the vertices of depth 1 that do not share the GZL sheet, say $\{\textcircled{\mathfrak{v}}\} \subset \{\textcircled{\mathfrak{z}}\}$. For each of these vertices consider their edge $\Delta_{\varrho\mathfrak{r}}$: we assign the weight $K(\varrho, \mathfrak{r})$ such that

$2\pi K(\varrho, \mathfrak{r})$ is the *argument between the sheets containing $\Delta_{\varrho\mathfrak{z}_0}$ and $\Delta_{\varrho\mathfrak{r}}$* .

[Referring to Example 8.10, the vertex of depth 1 not sharing the GZL sheet is $\textcircled{5}$. In this case the weight $K(1, 5) = -2 \pmod{\nu_1 + 1}$.]

If (97) has only vertices contiguous to the root $\textcircled{\varrho}$, then we have completed the construction of Λ_X .

- c) We now consider the set of vertices of depth 2. Of course there is an edge from a vertex of depth 1, say $\textcircled{\mathfrak{z}}$ to a vertex of depth 2, say $\textcircled{\mathfrak{a}}$. The associated weight for the edge $\Delta_{\mathfrak{z}\mathfrak{a}}$ is defined as $K(\mathfrak{z}, \mathfrak{a})$ such that

$2\pi K(\mathfrak{z}, \mathfrak{a})$ is the *argument between the sheets containing $\Delta_{1\mathfrak{z}}$ and $\Delta_{\mathfrak{z}\mathfrak{a}}$* .

- d) Continue the assignment of weights as in (c) for all the edges that contain vertices of depth 2.

[Referring to Example 8.10, the weight $K(2, 3) \leq -1$ since on \mathcal{R}_X the diagonal Δ_{23} is $|K(2, 3)|$ sheets below the diagonal Δ_{12} ; similarly the weight $K(2, 4) \leq -2$, since on \mathcal{R}_X the diagonal Δ_{24} is $|K(2, 4)|$ sheets below the diagonal Δ_{12} .]

- e) Repeat (c) and (d) with vertices of depth ≥ 3 , assigning the weights until all the vertices are exhausted.

[Referring to Example 8.10, the last edge to be considered is Δ_{35} with corresponding weight $K(3, 5) = -2$.]

We have thus constructed an (r, d) -configuration tree

$$(98) \quad \Lambda_X = \left\{ \left\{ \textcircled{\mathfrak{a}} = (z_{\mathfrak{a}}, t_{\mathfrak{a}}, -\nu_{\mathfrak{a}}) \right\}_{\mathfrak{a}=1}^{d+n}; \textcircled{\varrho}; \{(\Delta_{\mathbf{a}\mathbf{r}}, K(\mathbf{a}, \mathbf{r}))\} \right\}$$

associated to Ψ_X .

Remark 9.2. [Remark 5.19 revisited.] The integer weight $K(\mathbf{a}, \mathbf{r})$ associated to the edge $\Delta_{\mathbf{a}\mathbf{r}}$ can be incorporated into a continuous “edge” by considering

$$\widetilde{\Delta}_{\mathbf{a}\mathbf{r}} \doteq \Delta_{\mathbf{a}\mathbf{r}} e^{i2\pi K(\mathbf{a}, \mathbf{r})} \in \widehat{\mathbb{C}}^*,$$

where $\widetilde{\mathbb{C}}^* = \{|z|e^{i\arg(z)}\}$ is the universal cover of \mathbb{C}^* and $\arg(z)$ is the multivalued argument. This will provide the compatibility of “continuous coordinates/parameters” for the manifold structure of $\mathcal{E}(r, d)$.

9.2. From an (r, d) -configuration tree Λ_X to the (r, d) -skeleton of Λ_X . Let Λ_X be an abstract (r, d) -configuration tree as in Definition 7.7. In fact, we want to show the existence of a vector field X . In order to achieve this goal, we construct the (r, d) -skeleton of Λ_X (as a certain “blow-up” of Λ_X , see Definition 9.5).

The (r, d) -skeleton of Λ_X will contain the same information as Λ_X .

- a) With the disadvantage of being more cumbersome to express.
- b) With the advantage that it will enable us to identify the equivalence classes of Λ_X in §9.4.
- c) Also note that the (r, d) -skeleton of Λ_X describes the “embedding” of Λ_X in $\overline{\mathbb{C}}_z \times \mathbb{C}_t$.

Figure 19 presents a particular example that will help the reader follow the construction.

A priori, Λ_X has two types of vertices: essential vertices $\bigcirc_{n+\sigma} = (\infty_\sigma, a_\sigma, -\infty)$ and pole vertices $\bigcirc_{\iota} = (p_\iota, \tilde{p}_\iota, -\nu_\iota)$.

Before proceeding to the construction of the (r, d) -skeleton of Λ_X , we shall need the following two definitions/constructions.

Associated to the pole vertices, recalling Definition 5.17, the following construction is natural. See right hand side of Figures 4.c, 7, 8 and the blow up of vertices ① and ④ in Figure 19.

Remark 9.3. For each pole vertex $\bigcirc_{\iota} = (p_\iota, \tilde{p}_\iota, -\nu_\iota)$ of Λ_X , the vertical cycle of length $\nu_\iota + 1$ associated to \bigcirc_{ι}

is a cyclic graph consisting of exactly $\nu_\iota + 1$ copies of the vertex \bigcirc_{ι} joined by $\nu_\iota + 1$ vertical edges (without weights). The vertices on the vertical cycle are also assigned a local level: in this case arithmetic modulo $(\nu_\iota + 1)$ is to be used.

The vertical cycle of length $\nu_\iota + 1$ will only have vertices of valence 2. Once again, call one direction of the vertical cycle *up* and the other direction *down*. To be precise, *up* corresponds to the anti-clockwise direction of $\beta(\theta) = \pi_{X,2}^{-1}(t_a + \rho e^{i2\pi\theta})$ considered in Remark 5.19.3.

Similarly, associated to essential vertices, recalling Definition 5.15, the following construction is natural.

Remark 9.4. For each essential vertex $\bigcirc_{n+\sigma} = (\infty_\sigma, a_\sigma, -\infty)$, of Λ_X , let

$$K_{\max}(\sigma) = \max_{\mathfrak{r}} \{0, K(\sigma, \mathfrak{r})\} \quad \text{and} \quad K_{\min}(\sigma) = \min_{\mathfrak{r}} \{0, K(\sigma, \mathfrak{r})\},$$

where the maximum and minimum are taken over all the edges that start at $\bigcirc_{n+\sigma}$ and end at the respective $\{\bigcirc_{\mathfrak{r}}\}$. Then by letting

$$K(\sigma) \doteq K_{\max}(\sigma) - K_{\min}(\sigma)$$

we shall say that the

vertical tower of length $K(\sigma)$ associated to $\bigcirc_{n+\sigma}$

is a linear graph consisting of exactly $K(\sigma) + 1 \geq 1$ copies of the vertex $\bigcirc_{n+\sigma}$ joined by $K(\sigma)$ vertical edges (without weights). Each of the vertices of the vertical tower will have a *local level* assigned to it: the local level assigned to the first vertex of the vertical tower will be $K_{\min}(\sigma)$, the local level assigned to the second vertex of the vertical tower will be $K_{\min}(\sigma) + 1$, continuing in this way the local level assigned to the last vertex of the vertical tower will be $K_{\max}(\sigma)$. We shall call the increasing direction, using $\beta(\theta) = \pi_{X,2}^{-1}(t_a + \rho e^{i2\pi\theta})$, of the local level *up* and the decreasing direction *down*.

The vertical tower will have vertices of valence 1 at the extreme local levels $K_{\min}(\sigma)$ and $K_{\max}(\sigma)$, otherwise of valence 2.

On the right hand side of Figure 4.b a simple example of a vertical tower is presented. However in Example 8.10 and Figure 19 a more complex $(r, 4)$ -skeleton is shown: vertex $\textcircled{2} \in \Lambda_X$ blows up into the vertical tower of length $-K(2, 6)$. Moreover, the local zero level is assigned to the vertex where the edge Δ_{12} is attached; the local $K(2, 3) \leq -1$ level is assigned to the vertex where the edge Δ_{23} is attached; the local $K(2, 4) \leq -2$ level is assigned to the vertex where the edge Δ_{24} is attached; and the local $K(2, 6) \leq -3$ level is assigned to the vertex where the edge Δ_{26} is attached.

We can now define the associated combinatorial object.

Definition 9.5. Let Λ_X be an (r, d) -configuration tree. The (r, d) -skeleton of Λ_X is the undirected graph obtained by:

- Replacing each essential and pole vertices $\textcircled{\mathfrak{a}} = (z_{\mathfrak{a}}, t_{\mathfrak{a}}, -\nu_{\mathfrak{a}}) \in \Lambda_X$, with their associated vertical tower or vertical cycle respectively.
- For each directed weighted edge, $(\Delta_{\mathfrak{a}\mathfrak{r}}, K(\mathfrak{a}, \mathfrak{r})) \in \Lambda_X$, eliminate the weight and consider it an undirected *horizontal edge* $\pm\Delta_{\mathfrak{a}\mathfrak{r}}$.
- The undirected $\pm\Delta_{\mathfrak{a}\mathfrak{r}}$ edge is to have as its ends the local level 0 vertex of the vertical tower or vertical cycle associated to $\textcircled{\mathfrak{r}}$, and the local level $K(\mathfrak{a}, \mathfrak{r})$ vertex of the vertical tower or vertical cycle associated to $\textcircled{\mathfrak{a}}$; noting that if $\textcircled{\mathfrak{a}}$ is a pole vertex, modular arithmetic is to be used.

Remark 9.6. The (r, d) -skeleton of Λ_X has the following properties (also see Diagram 99):

- The edges of the (r, d) -skeleton of Λ_X are divided in two sets:
 - the vertical edges (alluded to in Definitions 9.4 and 9.3 above), and
 - the *horizontal edges* $\pm\Delta_{\mathfrak{a}\mathfrak{r}}$, which form a finite set of connected subtrees, that correspond precisely to the horizontal subtrees of the (r, d) -configuration tree Λ_X (recall Definition 7.7.7).
- Consider two horizontal edges $\Delta_{\mathfrak{ja}}$ and $\Delta_{\mathfrak{ar}}$ in the (r, d) -skeleton of Λ_X that share the vertex $\textcircled{\mathfrak{a}}$ in the original (r, d) -configuration tree Λ_X . We shall say that:

In the (r, d) -skeleton of Λ_X , the (horizontal) edge $\Delta_{\mathfrak{ar}}$, relative to the (horizontal) edge $\Delta_{\mathfrak{ja}}$, is
$$\begin{cases} \text{at the same (global) level if } K(\mathfrak{a}, \mathfrak{r}) = 0, \\ K(\mathfrak{a}, \mathfrak{r}) \text{ levels up if } K(\mathfrak{a}, \mathfrak{r}) > 0, \\ K(\mathfrak{a}, \mathfrak{r}) \text{ levels down if } K(\mathfrak{a}, \mathfrak{r}) < 0. \end{cases}$$

Hence, using geometry and combinatorics, $K(\mathfrak{a}, \mathfrak{r})$ can be recognized as

- the number of sheets in \mathcal{R}_X separating the diagonals $\Delta_{\mathfrak{ja}}$ and $\Delta_{\mathfrak{ar}}$, or equivalently
 - the number of levels in the (r, d) -skeleton of Λ_X separating the edges $\Delta_{\mathfrak{ja}}$ and $\Delta_{\mathfrak{ar}}$.
- Note that even though one can recognize which is the GZL sheet on the (r, d) -skeleton of Λ_X , this is a property inherited from Λ_X : it is not intrinsic to the (r, d) -skeleton.
 - Roughly speaking, the (r, d) -configuration tree Λ_X is a *blow-down* of the (r, d) -skeleton of Λ_X , see Diagram 99 and Figure 19 for an example.

9.3. From the (r, d) -skeleton of Λ_X to the Riemann surface \mathcal{R}_X . We proceed in two steps: In the first step, from the (r, d) -skeleton of Λ_X we will construct a

connected Riemann surface with boundary, the (r, d) -soul of Λ_X (see Definition 9.7).

As the second and final step, we shall glue $2d$ infinite helicoids on the boundaries of the (r, d) -soul of Λ_X to obtain the simply connected Riemann surface \mathcal{R}_X (without boundary).

Definition 9.7. Given an (r, d) -skeleton of Λ_X as above, the associated (r, d) -soul of Λ_X is a flat Riemann surface

- 1) constructed from the gluing of half planes $(\mathbb{H}_\pm^2, \frac{\partial}{\partial t})$ and finite height horizontal strips $\{0 < \Im(z) < h\}, \frac{\partial}{\partial t}$,
- 2) having two families of cone points:
 - a) the first with n conic points $\{(p_\iota, \tilde{p}_\iota)\}_{\iota=1}^n$ each with cone angle $2(\nu_\iota + 1)\pi$ and $r = \sum_\iota \nu_\iota$,
 - b) the second with d conic points $\{(z_\sigma, a_\sigma)\}_{\sigma=1}^d$ each with cone angle $2(K(\sigma) + 1)\pi$, $K(\sigma) \geq 0$,
- 3) d horizontal branch cuts starting at the cone points of the second family.

The branch cuts determine the boundary of the (r, d) -soul, $2d$ horizontal boundaries, recall Equation (43).

For $X(z) = \frac{1}{P(z)} e^{E(z)} \frac{\partial}{\partial z} \in \mathcal{E}(r, d)$ the (r, d) -soul of the (r, d) -configuration tree Λ_X is a simply connected Riemann surface with n cone points $\{(p_\iota, \tilde{p}_\iota)\}_{\iota=1}^n$ each with cone angle $2(\nu_\iota + 1)\pi$, corresponding to the n finitely ramified branch points associated to the poles of X , where $-\nu_\iota$ is the order of the pole p_ι ; d cone points $\{(\infty_\sigma, a_\sigma)\}_{\sigma=1}^d$ each with cone angle $2(K(\sigma) + 1)\pi$, corresponding to the logarithmic branch points of X ; with boundary the $2d$ horizontal segments $[a_\sigma, \infty)_- \cup [a_\sigma, \infty)_+$.

1. Construction of the (r, d) -soul of Λ_X from the (r, d) -skeleton of Λ_X .

From Remark 9.6.2, we see that the (r, d) -skeleton of Λ_X has two types of vertices: those that do not share horizontal edges and those that share horizontal edges (the vertices that belong to a horizontal subtree).

Generic horizontal subtrees assumption. For simplicity, let us first assume that on any given horizontal subtree the asymptotic and critical values, associated to the vertices of the horizontal subtree, all lie on different horizontal trajectories of $(\mathbb{C}_t, \frac{\partial}{\partial t})$. Figure 12 illustrates this assumption.

Starting from the (r, d) -skeleton of Λ_X consider the following construction.

- a) Replace each vertex⁷ of the (r, d) -skeleton of Λ_X that does not share a horizontal edge with a sheet $\mathbb{C}_t \setminus L_{\mathbf{a}}$.
- b) Given a horizontal subtree with s vertices, say $\{(\mathbf{a}_1), \dots, (\mathbf{a}_s)\}$, replace the given horizontal subtree with a sheet

$$\mathbb{C}_t \setminus \{L_{\mathbf{a}_\ell}\}_{\ell=1}^s,$$

where each $L_{\mathbf{a}_\ell}$ is the horizontal branch cut associated to the vertex (\mathbf{a}_ℓ) , recall Equation (43). By the generic horizontal subtrees assumption, all the values $\{t_{\mathbf{a}_\ell}\}$ lie on different horizontal trajectories of $\frac{\partial}{\partial t}$, then none of the horizontal branch cuts $L_{\mathbf{a}_\ell}$ intersect in \mathbb{C}_t .

Continue this replacement process for every horizontal subtree.

⁷Recall that all the vertices of the (r, d) -skeleton of Λ_X are either the original vertices (\mathbf{a}) of the original (r, d) -configuration tree Λ_X , or copies of them. Thus any vertex in the (r, d) -skeleton of Λ_X projects to a unique vertex on Λ_X .

Note that we obtain stacked copies of $\mathbb{C}_t \setminus L_a$ and $\mathbb{C}_t \setminus \{L_{a_\ell}\}_{\ell=1}^s$, but they retain their relative position respect to the (r, d) -skeleton of Λ_X , by the fact that we still have not removed the vertical edges of the d -skeleton of Λ_X .

- c) We now replace the vertical towers and vertical cycles in the (r, d) -skeleton of Λ_X with $|K|$ -helicoids or $(\nu + 1)$ -cyclic helicoids respectively (recall Definitions 5.15 and 5.17). On each vertical tower or vertical cycle, say the one associated to the vertex \textcircled{a} , apply Corollary 5.8 to glue the horizontal branch cuts by alternating the boundaries of $\mathbb{C}_t \setminus L_a$; so as to form finite helicoids or cyclic helicoids over the vertex \textcircled{a} , making sure that all the finite helicoids go up when turning counter-clockwise around the vertex.

In the case where a vertical tower is involved, the finite helicoid has two boundaries consisting of $[t_a, \infty)_+$ and $[t_a, \infty)_-$; in the case where a vertical cycle is involved we obtain a cyclic helicoid, that is a finite helicoid whose boundaries have been identified/glued.

Non-generic (degenerate) horizontal subtrees. We now turn our attention to the particular case when on some horizontal subtree there are at least two asymptotic or critical values $\{t_a\}_{a=1}^{d+n} \subset (\mathbb{C}, \frac{\partial}{\partial t})$ arising from the vertices \textcircled{a} , that lie on the same horizontal trajectory of $\frac{\partial}{\partial t}$. Since there are only a finite set of asymptotic or critical values, then for any small enough angle $\theta > 0$, the set of values $\{t_a\} \subset (\mathbb{C}, e^{i\theta} \frac{\partial}{\partial t})$ lie on $m + n$ different trajectories of the rotated vector field $\Re(e^{i\theta} \frac{\partial}{\partial t})$. Proceed with the construction (a)–(e) as above but using $e^{i\theta} L_a$ instead of L_a for the construction. Note that for small enough $\theta > 0$ all the surfaces obtained are homeomorphic. Finally let $\theta \rightarrow 0^+$ and consider the limiting surface.

According to Definition 9.7 we have:

Proposition 9.8. *Every Λ_X has a canonically associated (r, d) -soul.*

Proof. The (r, d) -soul of the (r, d) -configuration tree Λ_X is the Riemann surface with boundary, described by (a)–(c) above. \square

Example 9.1. The (r, d) -soul is shaded blue in all the figures.

- 1) $X \in \mathcal{E}(r, 0)$, so Ψ_X is a polynomial, in which case the $(r, 0)$ -soul of Λ_X is \mathcal{R}_X . See Figure 8.
- 2) $X(z) = e^z \frac{\partial}{\partial z} \in \mathcal{E}(0, 1)$, so Ψ_X is an exponential, in which case the $(0, 1)$ -soul of Λ_X consists of $\mathbb{C}_t \setminus L_1$, a single sheet with exactly one branch cut. See Figure 11 and figure 11.a in [2].
- 3) $X(z) = e^{z^2} \frac{\partial}{\partial z} \in \mathcal{E}(0, 2)$, so Ψ_X is the error function, in which case the $(0, 2)$ -soul of Λ_X consists of $\mathbb{C}_t \setminus (L_1 \cup L_2)$, a single sheet with exactly two branch cuts. See Figure 22 and figure 11.b in [2].
- 4) An (r, d) -configuration tree has all $K(a, \mathbf{r}) \equiv 0$ if and only if on the corresponding Riemann surface \mathcal{R}_X all the diagonals share the same sheet $\mathbb{C}_t \setminus \{L_a\}_{a=1}^{d+n}$. In this case the (r, d) -soul of Λ_X is this sheet. See Figure 12.b.

2. Construction of \mathcal{R}_X from the (r, d) -soul of Λ_X . To each of the $2d$ boundaries of the (r, d) -soul of Λ_X , glue a semi-infinite helicoid to obtain a simply connected Riemann surface \mathcal{R}_X . This surface has exactly d logarithmic branch points over d finite asymptotic values of Ψ_X and n finitely ramified branch points with ramification indices that add up to $r + n$.

We can recognize that our isometric glueing Corollary 5.8 in the above cases coincides with the Maskit surgery as is defined by M. Taniguchi [45] p. 68, [46] p. 110–115. In fact, \mathcal{R}_X is realized via Maskit surgeries with

- d exp-blocks (in our language $2d$ semi-infinite helicoids) and
- r quadratic blocks,

hence following⁸ [45] theorem 1 and [46] theorem 2.14, there exist polynomials $E(z)$ of degree d and $P(z)$ of degree r arising from Λ_X , which characterize the function

$$\Psi_X \in SF_{r,d} = \left\{ \int_{z_0}^z P(\zeta) e^{-E(\zeta)} d\zeta + b \mid P, E \in \mathbb{C}[z], \deg P = r, \deg E = d \right\}.$$

Alternatively⁹, since \mathcal{R}_X is a log-Riemann surface with d logarithmic branch points over d finite asymptotic values and n finitely ramified branch points with ramification indices that add up to $r + n$ whose finite completion is simply connected, by theorem 1.1 of [14], it follows that $\Psi_X \in SF_{r,d}$.

Finally assign to \mathcal{R}_X a flat metric $(\mathcal{R}_X, \pi_{X,2}^*(\frac{\partial}{\partial t}))$ induced by $\pi_{X,2}$. By the Dictionary Proposition 2.5, our sought after vector field is

$$X(z) = \Psi_X^*(\frac{\partial}{\partial t})(z) = \frac{1}{P(z)} e^{E(z)} \frac{\partial}{\partial z} \in \mathcal{E}(r, d)$$

as required.

We have essentially proved the following.

Proposition 9.9. *Consider the following set of (r, d) -configuration trees*

$$\left\{ \begin{array}{l} \Lambda_X \text{ has at least two branch points} \\ \text{over different values in } \mathbb{C}_t \end{array} \right\},$$

then the (r, d) -soul of Λ_X determines a unique vector field $X \in \mathcal{E}(r, d)$.

Proof. If Λ_X has only one ramification value in \mathbb{C}_t , then by simple inspection it is

$$\Lambda_X = \left\{ \textcircled{1} = (p_1, \tilde{p}_1, -r); \textcircled{1}; \emptyset \right\} \text{ or } \Lambda_X = \left\{ \textcircled{1} = (\infty_1, a_1, -\infty); \textcircled{1}; \emptyset \right\},$$

see Examples 8.1, 8.3. The corresponding vector fields

$$X(z) = \frac{\mu}{(z-p_1)^r} \frac{\partial}{\partial z} \in \mathcal{E}(r, 0) \text{ and } X(z) = \mu^{-1} e^z \frac{\partial}{\partial z} \in \mathcal{E}(0, 1),$$

are not uniquely determined, since $\mu \neq 0$ is not unique.

On the other hand, if Λ_X has at least two branch points over different values, say $t_1, t_2 \in \mathbb{C}_t$, then the diagonal Δ_{12} satisfies the Equation (42),

$$\int_{z_1}^{z_2} P(\zeta) e^{-E(\zeta)} d\zeta = t_2 - t_1.$$

It allows us the computation of the factors λ, μ in Equation (8), obtaining the uniqueness of $P(z)$ and $E(z)$. \square

Remark 9.10. Note that the (r, d) -configuration tree Λ_X is a tree “embedded” in $\mathcal{R}_X \subset \widehat{\mathbb{C}}_z \times \widehat{\mathbb{C}}_t$; however it is an embedding as a subset of $\overline{\mathbb{C}}_z \times \widehat{\mathbb{C}}_t$. It is not a genuine embedding in \mathcal{R}_X since the logarithmic branch points are not in fact part of the surface $\mathcal{R}_X \subset \mathbb{C}_z \times \widehat{\mathbb{C}}_t$ (see also Definition 4.3). On the other hand, on the (r, d) -skeleton of Λ_X , the branch points of \mathcal{R}_X are replaced by a vertical tower or vertical cycle during the blow-up process of Λ_X (the vertical edges of the (r, d) -skeleton of Λ_X indicate how many sheets separate the diagonals). In this sense, both the (r, d) -configuration tree Λ_X and the (r, d) -skeleton of Λ_X project to a graph $\pi_{X,2}(\Lambda_X) \subset \mathbb{C}_t$. See Figures 8–16 and 19, in particular $\pi_{X,2}(\Lambda_X)$ need not be a tree as in Figure 16. This is represented by the diagram:

⁸It is to be noted that in the case of $X \in \mathcal{E}(r, 0)$, $r \geq 1$, there is no need to use M. Taniguchi’s results involving exponential blocks.

⁹Note that these results are classical, in particular R. Nevanlinna [40], [41] and G. Elfving [21] essentially proved the correspondence between \mathcal{R}_X and Ψ_X .

$$\begin{array}{c}
(r, d)\text{-skeleton of } \Lambda_X \\
\text{blow-up} \updownarrow \text{blow-down} \\
(99) \quad \widehat{\mathbb{C}}_z \times \widehat{\mathbb{C}}_t \leftarrow \mathcal{R}_X \text{ “} \leftarrow \text{” } (r, d)\text{-configuration tree } \Lambda_X \hookrightarrow \overline{\mathbb{C}}_z \times \widehat{\mathbb{C}}_t \\
\downarrow \pi_{X,2} \\
\pi_{X,2}(\Lambda_X) \subset \mathbb{C}_t.
\end{array}$$

9.4. The equivalence relation on (r, d) -configuration trees.

Remark 9.11. *Non-uniqueness of (r, d) -configuration trees Λ_X associated to Ψ_X .*

1. Even though condition (4) of Definition 7.7 provides a clear choice for the root $\textcircled{\varrho}$ of $\Lambda(r, d)$, if the branch point corresponding to the root shares more than one sheet with other branch points, then each of these sheets could be the global zero level sheet. Hence each choice provides a different global zero level subtree and thus a different (r, d) -configuration tree Λ_X .

2. The choice of the weight when considering an edge that connects a pole vertex with any other type of vertex is not unique because of the modular arithmetic involved. For instance, if we have a weighted edge $(\Delta_{\iota, \mathfrak{r}}, K(\iota, \mathfrak{r}))$ connecting a pole vertex $\textcircled{\iota} = (p_\iota, \tilde{p}_\iota, -\nu_\iota)$ to any other vertex $\textcircled{\mathfrak{r}}$, then changing $K(\iota, \mathfrak{r})$ to $K(\iota, \mathfrak{r}) + \ell\nu$ for $\ell \in \mathbb{Z}$, will give rise to a different (r, d) -configuration tree associated to the same Ψ_X .

3. However, recalling Remark 9.6.2-3, it is to be noted that for fixed $X \in \mathcal{E}(r, d)$, even though there are choices in the construction of Λ_X , up to re-labelling of the vertices, the (r, d) -skeletons associated to each choice will be the same as undirected graphs.

Following is an example that illustrates (1)–(3).

Example 9.2 (Example 8.8 revisited). Let us consider once again

$$X(z) = \frac{e^{z^3}}{3z^3 - 1} \frac{\partial}{\partial z} \in \mathcal{E}(3, 3).$$

However we shall now re-label the vertices, choose a different global zero level and assign different weights to some edges.

(100)

$$\begin{array}{llll}
\textcircled{1} = (z_1, t_1, \nu_1) & = & (p_2, \tilde{p}_2, -1), & \textcircled{4} = (z_4, t_4, \nu_4) = (p_1, \tilde{p}_1, -1), \\
\textcircled{5} = (z_5, t_5, \nu_5) & = & (p_3, \tilde{p}_3, -1), & \textcircled{2} = (z_2, t_2, \nu_2) = (\infty_1, a_1, -\infty), \\
\textcircled{3} = (z_3, t_3, \nu_3) & = & (\infty_2, a_1, -\infty), & \textcircled{6} = (z_6, t_6, \nu_6) = (\infty_3, a_1, -\infty).
\end{array}$$

Thus the $(3, 3)$ -configuration tree (see Figure 20) is

$$\begin{aligned}
(101) \quad \Lambda_X = & \left\{ \textcircled{1}, \textcircled{2}, \textcircled{3}, \textcircled{4}, \textcircled{5}, \textcircled{6}; \textcircled{\textcircled{5}}; \right. \\
& \left. (\Delta_{54}, 0), (\Delta_{56}, -5), (\Delta_{42}, -1), (\Delta_{21}, 0), (\Delta_{13}, -1) \right\},
\end{aligned}$$

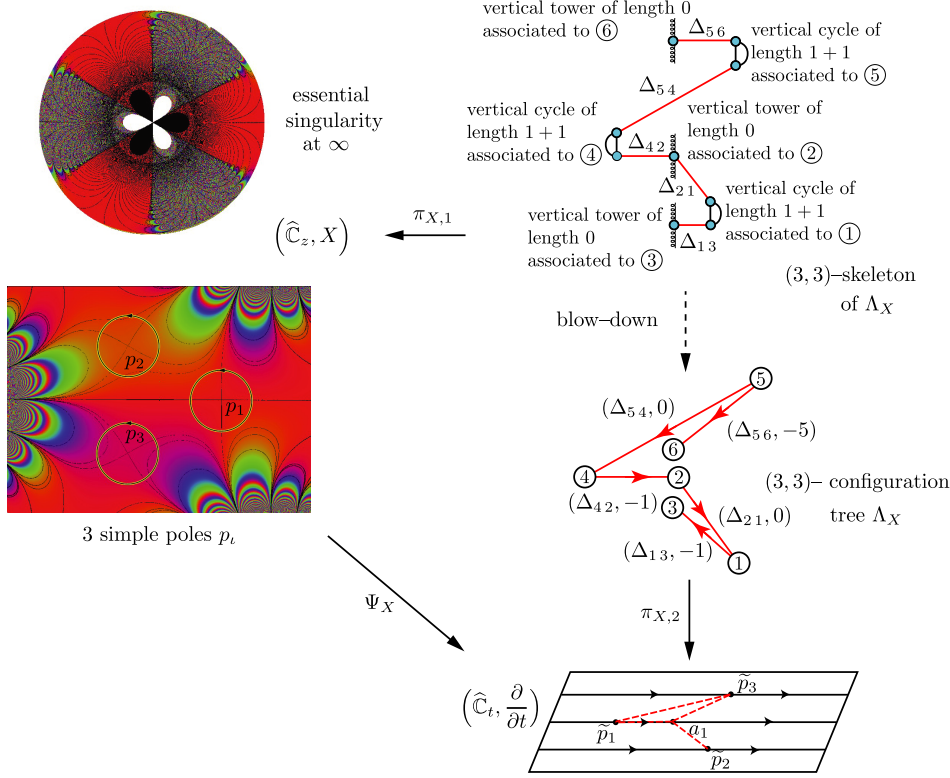


FIGURE 20. Vector field $\frac{e^{z^3}}{3z^3-1} \frac{\partial}{\partial z}$ with an essential singularity at ∞ and 3 simple poles p_i . The five diagonals and their projections are shown in red. The Riemann surface \mathcal{R}_X is not drawn. See Example 9.2.

Theorem 10.1. For $X \in \mathcal{E}(r, d)$, its phase portrait decomposes into $\Re(X)$ -invariant components as follows

$$\begin{aligned}
 (103) \quad (\mathbb{C}_z, X) &= \underbrace{\left(\overline{\mathbb{H}}_{\pm}^2, \frac{\partial}{\partial z} \right) \cup \dots \cup \left(\overline{\mathbb{H}}_{\mp}^2, \frac{\partial}{\partial z} \right)}_{2(r+1) \leq N_p \leq 4r} \\
 &\cup \left[\left(\left\{ 0 \leq |\Im(z)| \leq 2\pi(K_\sigma + 1) \right\}, e^z \frac{\partial}{\partial z} \right)_{a_\sigma} \right. \\
 &\quad \left. \cup \left(\overline{\mathbb{H}}_{\pm}^2, e^z \frac{\partial}{\partial z} \right)_{a_\sigma, \text{upper}} \cup \left(\overline{\mathbb{H}}_{\pm}^2, e^z \frac{\partial}{\partial z} \right)_{a_\sigma, \text{lower}} \right] \\
 &\quad \bigcup_{\ell}^{M \leq \infty} \left(\left\{ 0 \leq \Im(z) \leq h_\ell \right\}, \frac{\partial}{\partial z} \right),
 \end{aligned}$$

where $\{a_\sigma\}$ are the finite asymptotic values of Ψ_X , N_p is the number of half planes associated to the poles of X (equivalently the number of hyperbolic sectors around the poles of X) and M is the number of diagonals (equivalently the number of finite height strips in the phase portrait of $\Re(X)$).

There are an infinite number of half planes $(\overline{\mathbb{H}}_\pm^2, \frac{\partial}{\partial z})$ in the decomposition if and only if $d \geq 1$.

Proof. Decomposition (103) follows by recalling Definition 5.7, the biholomorphism $\pi_{X,1}$ presented in Diagram 5 and the fine structure of the (r, d) -skeleton of Λ_X . It is an accurate description of the phase portrait decomposition of $\Re(X)$:

The first row depicts the, at least $2(r+1)$ and at most $4r$, half planes associated to the r poles.

On the second row are the d finite helicoids arising from the d finite asymptotic values $\{a_\sigma\}$, where it is to be noticed that this can be an empty collection.

On the third row are the $2d$ semi-infinite helicoids.

Finally, on the fourth row the finite height strips associated to the diagonals in \mathcal{R}_X . \square

Corollary 10.2. *Let $X \in \mathcal{E}(r, d)$, $d \geq 1$. Then, the incomplete trajectories of $\Re(X)$ in $\widehat{\mathbb{C}}_z$ are infinite, numerable and Lebesgue measure zero.* \square

Obviously, the number of incomplete trajectories is finite if and only of $r \geq 1$ and $d = 0$. Compare with [33] and [32].

11. ON THE TOPOLOGY OF $\Re(X)$

Consider the group of orientation preserving homeomorphisms of \mathbb{C} ,

$$\text{Homeo}(\mathbb{C})^+ = \{h : \widehat{\mathbb{C}}_z \rightarrow \widehat{\mathbb{C}}_z \mid \text{preserving orientation and fixing } \infty \in \widehat{\mathbb{C}}\}.$$

Definition 11.1. Let $X_1, X_2 \in \mathcal{E}(r, d)$ be two singular analytic vector fields.

They are *topologically equivalent* if there exists $h \in \text{Homeo}(\mathbb{C})^+$ which takes the trajectories of $\Re(X_1)$ to trajectories of $\Re(X_2)$, preserving real time orientation, but not necessarily the parametrization.

A *bifurcation for $\Re(X_1)$ occurs*, when the topology of its phase portrait topologically changes under small deformation of X_1 in the family $\mathcal{E}(r, d)$, otherwise $\Re(X_1)$ is *structurally stable* in $\mathcal{E}(r, d)$.

Let $\Lambda_X = \left\{ \left\{ \textcircled{\mathbf{a}} = (z_{\mathbf{a}}, t_{\mathbf{a}}, -\nu_{\mathbf{a}}) \right\}_{\sigma=1}^{d+n}; \textcircled{\mathbf{q}}; \left\{ (\Delta_{\mathbf{ar}}, K(\mathbf{a}, \mathbf{r})) \right\} \right\}$ be a (r, d) -configuration tree. By simple inspection we have

Theorem 11.2 (Structural stability of $\Re(X)$ for $X \in \mathcal{E}(r, d)$).

The real vector field $\Re(X)$ is structurally stable in $\mathcal{E}(r, d)$ if and only if

- i) X has only simple poles and
- 2) $\Im(\Delta_{\mathbf{ar}}) \neq 0$ for all weighted edges of Λ_X .

Proof. A diagonal $\Delta_{\mathbf{ar}}$ has $\Im(\Delta_{\mathbf{ar}}) = 0$ and poles of X at its two extreme points, if and only if $\Delta_{\mathbf{ar}}$ determines a saddle connection of $\Re(X)$, see Lemma 5.9.3. This is the unique bifurcation scenario. \square

Recalling that an (r, d) -skeleton of Λ_X is a graph embedded in $\overline{\mathbb{C}}_z \times \mathbb{C}_t$, with a specific complex parameter associated to each edge and having horizontal and vertical attributes, we now make the following.

As a direct consequence of the structure of the (r, d) -skeleton of Λ_X we have.

Theorem 11.3 (Number of non topologically equivalent vector fields $\mathfrak{Re}(X)$ for $X \in \mathcal{E}(r, d)$).

Given a fixed pair (r, d) :

- 1) The number of topologies of $\mathfrak{Re}(X)$ is infinite when $(r, d) \in \{(r \geq 2, 1), (r \geq 1, 2), (r \geq 0, d \geq 3)\}$.
- 2) The number of topologies is
 - a) one when $(r, d) = (0, 1), (1, 0)$;
 - b) two when $(r, d) = (0, 2), (1, 1)$;
 - c) finite when $(r, 0)$.

For $X \in \mathcal{E}(r, 0)$, the phase portrait $\mathfrak{Re}(X)$ on \mathbb{C}_z only has a finite number $n \leq r$ of multiple saddle points. These phase portraits were first studied by W. M. Boothby [16], [17], showing that they appear as the real part of certain harmonic functions (non necessarily polynomials); in our framework, the imaginary part of $\Psi_X(z) = \int^z P(\zeta) e^{-E(\zeta)} d\zeta$.

Proof. For each $(r, d) \in \{(r \geq 2, 1), (r \geq 1, 2), (r \geq 0, d \geq 3)\}$ there will be at least one topological (r, d) -skeleton of Λ_X with at least one vertical tower with two horizontal subgraphs attached to the *same* vertical tower. These horizontal subgraphs are vertically separated from each other by an integer number $K(\sigma, \rho)$, of degree 2 vertices on a vertical tower. Hence there are an infinite number of different ways, described by $\{K(\sigma, \rho) \geq 1\}$, we can attach these two subgraphs to the vertical tower, each of which represents a different configuration in \mathcal{R}_X .

The remaining cases are $(r, d) \in \{(0, 1), (0, 2), (1, 1), (r \geq 1, 0)\}$. The cases $(0, 1), (1, 0)$ are trivial by Lemma 5.3. For cases $(0, 2)$ and $(1, 1)$: \mathcal{R}_X has two branch points hence they must share the same sheet. Thus each one of these cases have exactly two topologies. Case $(0, 2)$ is illustrated in Figure 22. Case $(r \geq 2, 0)$ corresponds to Ψ_X being a polynomial, hence the number of topologies is finite. \square

Table 2 presents a summary of the possible non topologically equivalent vector fields $\mathfrak{Re}(X)$, for $X \in \mathcal{E}(r, d)$, that arise for different pairs (r, d) .

Remark 11.4. As a side note, Theorem 11.3 and Proposition 8.2 show that the topological classification of functions is coarser than the topological classification of phase portraits of vector fields, even for Ψ_X and X in $\mathcal{E}(r, d)$.

12. THE ESSENTIAL SINGULARITY AT ∞

Our naive question;

how can we describe the essential singularity of X at $\infty \in \widehat{\mathbb{C}}_z$, for $X \in \mathcal{E}(r, d)$?, is answered in this section.

In [2] §5, germs of singular analytic vector fields X are studied; the Poincaré–Hopf index theory and a certain version of the decomposition in angular sectors for essential isolated singularities are established for the phase portrait of $\mathfrak{Re}(X)$. In fact, starting with a simple closed anticlockwise orientated path γ enclosing $z_\vartheta \in \{p_1, \dots, p_r, \infty\} \subset \widehat{\mathbb{C}}_z$ a pole, zero or essential singularity, the notion of an admissible cyclic word \mathcal{W}_X in the alphabet $\{H, E, P, \mathcal{E}\}$ is well defined,

$$(104) \quad ((\widehat{\mathbb{C}}, z_\vartheta), \mathfrak{Re}(X)) \mapsto \mathcal{W}_X.$$

TABLE 2. Topologies of $\mathfrak{R}\mathfrak{e}(X)$ for different pairs (r, d) .

r	d	# of topologies of $\mathfrak{R}\mathfrak{e}(X)$	(r, d) -configuration trees Λ_X chosen as a representative for the topological class
1	0	1	$\Lambda_X = \{(p_1, \tilde{p}_1, -1); \emptyset\}$
0	1	1	$\Lambda_X = \{(\infty_1, a_1, -\infty); \emptyset\}$
0	2	2	$\Lambda_X = \{(\infty_1, a_1, -\infty), (\infty_1, a_2, -\infty); (\Delta_{12}, K(1, 2))\}$, with $\Delta_{12} \in \mathbb{C}^*$, two topologies: $\Delta_{12} \in \mathbb{R}, \Delta_{12} \notin \mathbb{R}$
1	1	2	$\Lambda_X = \{(\infty_1, a_1, -\infty), (p_1, \tilde{p}_1, -1); (\Delta_{12}, K(1, 2))\}$, with $\Delta_{12} \in \mathbb{C}^*$, two topologies: $\Delta_{12} \in \mathbb{R}, \Delta_{12} \notin \mathbb{R}$
2	0	3	$\Lambda_X = \{(p_1, \tilde{p}_1, -2); \emptyset\}$, gives rise to one topology. $\Lambda_X = \{(p_1, \tilde{p}_1, -1), (p_2, \tilde{p}_2, -1); (\Delta_{12}, K(1, 2))\}$, with $\Delta_{12} \in \mathbb{C}^*$, two topologies: $\Delta_{12} \in \mathbb{R}, \Delta_{12} \notin \mathbb{R}$
$r \geq 3$	0	finite	$\Lambda_X = \{(p_1, \tilde{p}_1, -\nu_1), \dots, (p_n, \tilde{p}_n, -\nu_n);$ $\{(\Delta_{\iota\kappa}, K(\iota, \kappa)) \mid \iota, \kappa \in \{1, \dots, n-1\}\}\}$, $1 \leq n \leq r$ being the number of distinct poles
$r \geq 2$	1	infinite	$\Lambda_X = \{(\infty_1, a_1, -\infty),$ $(p_1, \tilde{p}_1, -\nu_1), \dots, (p_n, \tilde{p}_n, -\nu_n);$ $\{(\Delta_{\mathfrak{a}\mathfrak{r}}, K(\mathfrak{a}, \mathfrak{r})) \mid \mathfrak{a}, \mathfrak{r} \in \{1, \dots, n+1\}\}\}$, $1 \leq n \leq r$ being the number of distinct poles
$r \geq 1$	2	infinite	$\Lambda_X = \{(\infty_1, a_1, -\infty), (\infty_2, a_2, -\infty),$ $(p_1, \tilde{p}_1, -\nu_1), \dots, (p_n, \tilde{p}_n, -\nu_n);$ $\{(\Delta_{\mathfrak{a}\mathfrak{r}}, K(\mathfrak{a}, \mathfrak{r})) \mid \mathfrak{a}, \mathfrak{r} \in \{1, \dots, n+2\}\}\}$, $1 \leq n \leq r$ being the number of distinct poles
$r \geq 0$	$d \geq 3$	infinite	$\Lambda_X = \{(\infty_1, a_1, -\infty), (\infty_2, a_2, -\infty),$ $(\infty_3, a_3, -\infty), \dots, (\infty_d, a_d, -\infty),$ $(p_1, \tilde{p}_1, -\nu_1), \dots, (p_n, \tilde{p}_n, -\nu_n);$ $\{(\Delta_{\mathfrak{a}\mathfrak{r}}, K(\mathfrak{a}, \mathfrak{r})) \mid \mathfrak{a}, \mathfrak{r} \in \{1, \dots, d+n\}\}\}$, $0 \leq n \leq r$ being the number of distinct poles

Remark 12.1. The letters in the alphabet are the usual angular sectors for vector fields: hyperbolic H , elliptic E , parabolic P (see [5] p. 304, [6] p. 86) and Figure 21. A new *class 1 entire sector* \mathcal{E} based upon $e^z \frac{\partial}{\partial z}$ at infinity: recalling Diagram 12, \mathcal{E} can be thought as the image under $\pi_{X,1}$ of a semi-infinite helicoid contained in \mathcal{R}_X , see Example 8.3, Figures 4.a, 11 and 21. For full details see [2] p. 151.

Specific attributions encoded by the word \mathcal{W}_X in (104) are as follows.

- 1) *Equivalence classes.* The word \mathcal{W}_X is well defined up to the relations
$$E\mathcal{E}H \sim \mathcal{E} \quad \text{and} \quad H\mathcal{E}E \sim \mathcal{E},$$
according to [2] pp. 166–167. Under this equivalence the word becomes independent of the choice of the path γ enclosing the singularity.
- 2) *Poincaré–Hopf index.* If the number of letters H , E and \mathcal{E} that appear in a word \mathcal{W}_X at z_\emptyset , is denoted by h , e and ε respectively, then the Poincaré–Hopf

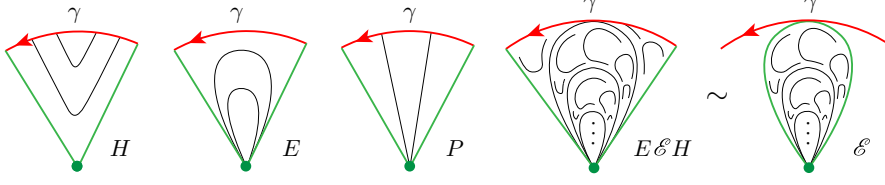


FIGURE 21. Hyperbolic H , elliptic E , parabolic P and entire \mathcal{E} sectors at a singular point $(\widehat{\mathbb{C}}_z, z_\vartheta)$ of a vector field $\Re(X)$. The point z_ϑ is green, the path γ is shown in red. The equivalent relation $E\mathcal{E}H \sim \mathcal{E}$ is illustrated on the right.

index formula is

$$(105) \quad PH(X, z_\vartheta) = 1 + \frac{e - h + \varepsilon}{2}.$$

Furthermore, in theorem A p. 130 and §6 of [2], the Poincaré–Hopf index theorem

$$(106) \quad \chi(\widehat{\mathbb{C}}) = \sum PH(X, z_\vartheta)$$

is extended to include germs of singular analytic vector fields X that determine an admissible cyclic word.

- 3) *Displacement of parabolic sectors.* As matter of record, each parabolic sector P_ν of \mathcal{W}_X has a displacement number $\nu \in \mathbb{C} \setminus \mathbb{R}$, see [2] pp. 149–150.
- 4) *The residue.* In fact the residue of the vector field germ is

$$Res(\omega_X) \doteq Res(X, z_\vartheta) = \frac{1}{2\pi i} \int_\gamma \omega_X,$$

recall that $\omega_X(X) = 1$, also see [2] p. 167.

Clearly for $X \in \mathcal{E}(r, d)$ all the residues are zero, since $\omega_X = P(z)e^{-E(z)}dz$ is holomorphic on \mathbb{C}_z .

The action (53),

$$\mathcal{A} : Aut(\mathbb{C}) \times \mathcal{E}(r, d) \longrightarrow \mathcal{E}(r, r), \quad (T, X) \longmapsto T^*X,$$

is a valuable tool, see [3].

Clearly, for each singularity $z_\vartheta \in \{p_1, \dots, p_r, \infty\}$ of X , the germ $((\widehat{\mathbb{C}}_z, z_\vartheta), X(z))$ is

- a local analytic invariant (under the local biholomorphisms of $(\widehat{\mathbb{C}}_z, z_\vartheta)$), and
- an analytic invariant under the above action of $Aut(\mathbb{C})$.

Example 12.1 (Cyclic words at poles). For $X(z) = \frac{1}{(z-p_\iota)^{\nu_\iota}} \frac{\partial}{\partial z}$, the cyclic word \mathcal{W}_X consists of exactly $2(\nu_\iota + 1)$ hyperbolic sectors H , see Figure 1:

$$(107) \quad ((\mathbb{C}_z, p_\iota), \Re(X)) \longmapsto \mathcal{W}_X = \underbrace{HH \cdots HH}_{2(\nu_\iota + 1)}.$$

The Poincaré–Hopf index is $PH(X, p_\iota) = -\nu_\iota$.

Example 12.2 (A cyclic word at ∞ , from a zero of X). Recall the rational vector field $X(z) = \frac{1}{(z-p_1)^{\nu_1}(z-p_1)^{\nu_2}} \frac{\partial}{\partial z}$ in Example 8.2, in our language the description of the singularity at infinity is

$$(108) \quad ((\widehat{\mathbb{C}}_z, \infty), \Re(X)) \longmapsto \mathcal{W}_X = \underbrace{EE \cdots EE}_{\nu_1 + \nu_2 + 2}.$$

The Poincaré–Hopf index is $PH(X, \infty) = \nu_1 + \nu_2 + 2$, also see Figure 1.

Example 12.3 (The cyclic word at ∞ of the exponential vector field has two entire sectors). Recall the exponential vector field $X(z) = e^z \frac{\partial}{\partial z}$ in Example 8.3 and Figure 11, we have

$$(109) \quad ((\widehat{\mathbb{C}}_z, \infty), \Re(X)) \mapsto \mathcal{W}_X = E\mathcal{E}H\mathcal{E} \sim \mathcal{E}\mathcal{E}.$$

The Poincaré–Hopf index of X at ∞ is 2.

Example 12.4 (The error function). The vector field

$$X(z) = \mu \frac{\sqrt{\pi}}{4} e^{z^2} \frac{\partial}{\partial z}, \quad \mu \in \mathbb{C}^*,$$

has associated the error function

$$\Psi(z) = \mu^{-1} \frac{2}{\sqrt{\pi}} \int_0^z e^{-\zeta^2} d\zeta.$$

Case $\mu = 1$, the logarithmic branch points are

$$\{(\infty_1, -1, -\infty), (\infty_2, 1, -\infty), (\infty_3, \infty, -\infty), (\infty_4, \infty, -\infty)\},$$

using the notation in equations (31), and the $\Re(X)$ -invariant decomposition is

$$(\widehat{\mathbb{C}}_z, X) = \bigcup_{\sigma=1}^{\infty} (\overline{\mathbb{H}}_{\sigma}^2, \frac{\partial}{\partial z}).$$

The cyclic word is

$$((\widehat{\mathbb{C}}_z, \infty), \Re(X)) \mapsto \mathcal{W}_X = E\mathcal{E}HH\mathcal{E}E\mathcal{E}HH\mathcal{E}.$$

See Figure 22.

Case $\mu = i$, the logarithmic branch points are

$$\{(\infty_1, -i, -\infty), (\infty_2, i, -\infty), (\infty_3, \infty, -\infty), (\infty_4, \infty, -\infty)\},$$

and the $\Re(X)$ -invariant decomposition is

$$(\widehat{\mathbb{C}}_z, X) = \left(\bigcup_{\sigma=1}^{\infty} (\overline{\mathbb{H}}_{\sigma}^2, \frac{\partial}{\partial z}) \right) \cup \{ -1 \leq \Im(z) \leq 1 \}, \frac{\partial}{\partial z}.$$

The cyclic word is

$$((\widehat{\mathbb{C}}_z, \infty), \Re(X)) \mapsto \mathcal{W}_X = E\mathcal{E}HH\mathcal{E}P_{2i}E\mathcal{E}HH\mathcal{E}P_{-2i},$$

note that the appearance of two opposite parabolic sectors having displacements $\pm 2i$ is due the horizontal strip in the decomposition. See Figure 22.

In both cases the Poincaré–Hopf index of X at ∞ is 2.

Remark 12.2. *The singularity at infinity does not determine the analytic class of X .* 1. For $X \in \mathcal{E}(3, 0)$ having simple zeros, all the germs $((\widehat{\mathbb{C}}_z, \infty), X)$ are analytically equivalent. Thus the singularity at infinity does not determine the analytic class of X in $\mathcal{E}(3, 0)/\text{Aut}(\mathbb{C})$.

2. We further note that the vector field

$$\tilde{X}(p_3, z) = \mu \frac{2p_3 - 1}{12z(z-1)(z-p_3)} e^{z^4} \frac{\partial}{\partial z} \in \mathcal{E}(3, 4),$$

has the same behaviour in $\{z \in \mathbb{C} \mid |z| < R\} \subset \mathbb{C}_z$, for adequate choices of $\mu \in \mathbb{C}^*$ and $R > 0$, as $X(p_3, z)$ given by (51), hence the singularity at infinity does not determine the analytic class of X in $\mathcal{E}(3, 4)/\text{Aut}(\mathbb{C})$, see [2] §9 and §10.

Thus, for vector fields in $\mathcal{E}(r, d)$, $r + d \geq 3$, the $\text{Aut}(\mathbb{C})$ -equivalence notion from (53) is very rigid.

We now have that for the essential singularity:

Theorem 12.3.

1) Let be $X \in \mathcal{E}(r, d)$, the cyclic word \mathcal{W}_X at ∞ is recognized as

$$(110) \quad ((\widehat{\mathbb{C}}_z, \infty), \Re(X)) \mapsto \mathcal{W}_X = W_1 W_2 \cdots W_k, \quad W_i \in \{H, E, P, \mathcal{E}\},$$

with exactly $\varepsilon = 2d$ letters $W_i = \mathcal{E}$.

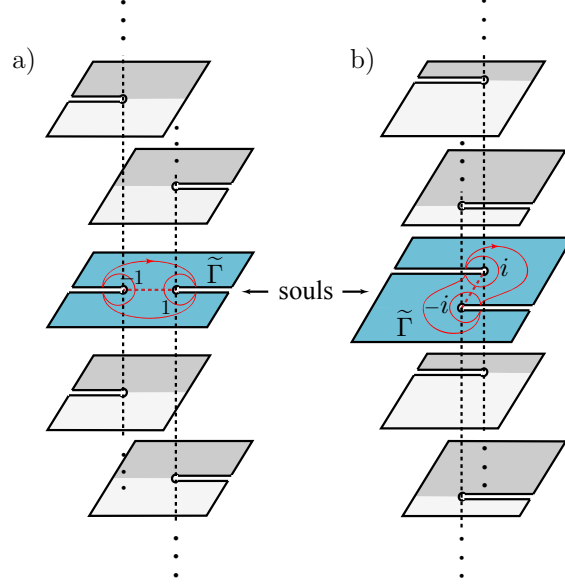


FIGURE 22. The Riemann surfaces of X and $e^{i\pi/2}X$ for $X \in \mathcal{E}(0, 2)$. In (a) is the one associated to the error function $\Psi_{X_1}(z) = \frac{2}{\sqrt{\pi}} \int_0^z e^{-\zeta^2} d\zeta$, having a diagonal Δ_{12} which determines a homoclinic trajectory of $\Re(X)$. In (b) is the one corresponding to $\Psi_{X_2}(z) = \frac{2i}{\sqrt{\pi}} \int_0^z e^{-\zeta^2} d\zeta$. The red curves represent taut $\tilde{\Gamma}$'s that allow the recognition of the words. The global topologies of the corresponding $\Re(X)$, $X \in \mathcal{E}(0, 2)$, are described in the third row of Table 2, and the germ of singularities at ∞ in Example 12.4.

Moreover, $h - e = 2(d - r - 1)$.

- 2) The word W_X is a local topological invariant of the germ $((\hat{\mathbb{C}}_z, \infty), \Re(X))$.
- 3) Conversely, a germ of a singular complex analytic vector field $((\mathbb{C}, 0), Y)$ is the restriction of an $X \in \mathcal{E}(r, d)$ at ∞ if and only if the point 0 is an isolated essential singularity of Y and satisfies that
 - i) the residue of the word $\text{Res}(\omega_Y) = 0$,
 - ii) the Poincaré–Hopf index of the word $PH(Y, 0) = 2 + r$,
 - iii) W_Y is an admissible cyclic word having exactly $2d$ entire sectors \mathcal{E} .

Proof. The proof of statement (1) follows the arguments in §5, §9 and §10 of [2].

Step 1: Take a simple path $\gamma \subset (\hat{\mathbb{C}}_z, \infty)$ enclosing only ∞ (γ does not enclose any poles of X).

Step 2: Lift γ to Γ in $\mathcal{R}_X \subset \hat{\mathbb{C}}_z \times \hat{\mathbb{C}}_t$. Note that a priori, Γ does not lie completely in the soul of \mathcal{R}_X , recall Definition 9.7.

Step 3: The singularity at ∞ of X has a certain self-similarity (as the examples in §8 shown), hence in order to recognize a simple word describing it, a suitable deformation of Γ is required. That is, we deform Γ to a taut deformation $\tilde{\Gamma}$ in the soul of \mathcal{R}_X . For examples of a taut deformation $\tilde{\Gamma}$ see Figures 22 and 25. For the

appropriate technical definitions and another example see pp. 211–212 of [2], in particular figure 17.

The taut deformation $\tilde{\Gamma}$ recognizes letters W_i at ∞ as follows:

- letters P when $\tilde{\Gamma}$ crosses finite height strip flows,
- letters H when $\tilde{\Gamma}$ makes a half circle around a branch point of \mathcal{R}_X ,
- letters E when $\tilde{\Gamma}$ makes a half circle around (the branch point at) ∞ on a sheet of \mathcal{R}_X ,
- letters \mathcal{E} when $\tilde{\Gamma}$ touches a component of the boundary of the soul; see Figures 21 and 22.

As for the difference $h - e$ between the number of sectors H and E appearing in the cyclic word \mathcal{W}_X at ∞ , we shall use the Poincaré–Hopf index theory extended to these kinds of singularities (Theorem A in §6 of [2] with $M = \widehat{\mathbb{C}}_z$).

From the fact that $X \in \mathcal{E}(r, d)$ has exactly r poles (counted with order) in \mathbb{C}_z and since $PH(X, p_i) = -\nu_i$ for a pole p_i of order $-\nu_i$, then equation (6.6) of [2] gives us

$$(111) \quad 2 = \chi(\widehat{\mathbb{C}}) = PH(X, \infty) + \sum_{p_i \in \mathcal{P}} PH(X, p_i) = PH(X, \infty) - r.$$

On the other hand from equation (6.5) of [2]

$$PH(X, \infty) = 1 + \frac{e - h + 2d}{2},$$

the result follows.

Assertion (2) follows by simple inspection.

For assertion (3), use a slight modification of corollary 10.1 of [2]. The only change arises from the fact that $X \in \mathcal{E}(r, d)$ has exactly r poles (counted with order) in \mathbb{C}_z . Once again, by (111) the result follows. \square

Example 12.5 (Cyclic words at ∞). 1. Recall the vector field in Example 8.6

$$X(z) = \frac{e^z}{(z - 9i\frac{\pi}{2})(z + i\frac{\pi}{2})} \frac{\partial}{\partial z}$$

Figure 14 shows the $(2, 1)$ -skeleton of Λ_X together with the soul of Λ_X . Here we also show a *taut* curve $\tilde{\Gamma}_1 \cup \dots \cup \tilde{\Gamma}_{10} = \tilde{\Gamma}(\tau) = (\gamma(\tau), (\Psi_X \circ \gamma)(\tau)) \subset \mathcal{R}_X$ where $\gamma(\tau)$ is a simple closed curve enclosing $\infty \in \widehat{\mathbb{C}}_z$ with $p_1 = 9i\frac{\pi}{2}$ and $p_2 = -i\frac{\pi}{2}$ lying in its exterior. As shown in [2] §9.1, we can read the admissible cyclic word

$$(112) \quad \mathcal{W}_X = \underbrace{EE}_{\tilde{\Gamma}_1} \underbrace{P}_{\tilde{\Gamma}_2} \underbrace{EE}_{\tilde{\Gamma}_3} \underbrace{EE}_{\tilde{\Gamma}_4} \underbrace{P}_{\tilde{\Gamma}_5} \underbrace{EE}_{\tilde{\Gamma}_6} \underbrace{EPE\mathcal{E}HH}_{\tilde{\Gamma}_7} \underbrace{HH}_{\tilde{\Gamma}_8} \underbrace{HH}_{\tilde{\Gamma}_9} \underbrace{HH\mathcal{E}EPE}_{\tilde{\Gamma}_{10}},$$

so that the number of elliptic, hyperbolic and entire sectors are $e = 12$, $h = 8$ and $\varepsilon = 2$ respectively. Thus we may calculate the Poincaré–Hopf index at ∞ , which in this case turns out to be

$$\begin{aligned} PH(X, \infty) &= 1 + \frac{e - h + \varepsilon}{2} \\ &= 1 + 3 = 4. \end{aligned}$$

2. Recall the vector field $X(z) = \frac{-e^{z^3}}{3z^2} \frac{\partial}{\partial z}$ in Example 8.7,

$$(113) \quad \left((\widehat{\mathbb{C}}_z, \infty), \Re(X) \right) \mapsto \mathcal{W}_X = \mathcal{E}\mathcal{E}\mathcal{E}\mathcal{E}\mathcal{E}\mathcal{E}$$

The Poincaré–Hopf index of X at ∞ is 4.

3. Recall the vector field $X(z) = \frac{e^{z^3}}{3z^3-1} \frac{\partial}{\partial z}$ in Example 8.8,

$$(114) \quad ((\hat{\mathbb{C}}_z, \infty), \Re(X)) \mapsto \mathcal{W}_X = \mathcal{E}EE\mathcal{E}\mathcal{E}\mathcal{E}\mathcal{E}\mathcal{E}.$$

The Poincaré–Hopf index of X at ∞ is 5.

In the next example we show that it is possible to calculate, among other things, the Poincaré–Hopf index.

Example 12.6. [Example 8.10 revisited.] Considering Example 8.10 once again, Figure 23 shows the $(r, 4)$ -skeleton of Λ_X together with the soul of Λ_X . Here we also show a *taut* curve $\tilde{\Gamma}(\tau) = (\gamma(\tau), (\Psi_X \circ \gamma)(\tau)) \subset \mathcal{R}_X$ where $\gamma(\tau)$ is a simple closed curve enclosing $\infty \in \hat{\mathbb{C}}_z$ with p_1 and p_2 lying in its exterior. As shown in [2] §9.1 and §6, we can read the admissible cyclic word

$$(115) \quad \mathcal{W}_X = \underbrace{EE}_{\tilde{\Gamma}_1} \underbrace{P\mathcal{E}HH\mathcal{E}EPE}_{\tilde{\Gamma}_2} \underbrace{EE}_{\substack{\tilde{\Gamma}_3 \\ (\nu_1-2) \\ \text{copies}}} \underbrace{P}_{\tilde{\Gamma}_4} \underbrace{EE}_{\substack{\tilde{\Gamma}_5 \\ -K(2,3)-1 \\ \text{copies}}} \underbrace{P\mathcal{E}HH\mathcal{E}EPE}_{\tilde{\Gamma}_6} \\ \underbrace{EE}_{\substack{\tilde{\Gamma}_7 \\ -K(2,4)+K(2,3)-1 \\ \text{copies}}} \underbrace{P}_{\tilde{\Gamma}_8} \underbrace{EE}_{\substack{\tilde{\Gamma}_9 \\ \nu_2 \\ \text{copies}}} \underbrace{EPE}_{\tilde{\Gamma}_{10}} \underbrace{EE}_{\substack{\tilde{\Gamma}_{11} \\ -K(2,6)+K(2,4)-1 \\ \text{copies}}} \underbrace{P\mathcal{E}HH\mathcal{E}EPE\mathcal{E}HH}_{\tilde{\Gamma}_{12}} \\ \underbrace{HH}_{\substack{\tilde{\Gamma}_{13} \\ -K(2,6)+K(2,4)-1 \\ \text{copies}}} \underbrace{HH}_{\tilde{\Gamma}_{14}} \underbrace{HH}_{\substack{\tilde{\Gamma}_{15} \\ -K(2,4)+K(2,3)-1 \\ \text{copies}}} \underbrace{HH}_{\tilde{\Gamma}_{16}} \underbrace{HH}_{\substack{\tilde{\Gamma}_{17} \\ -K(2,3)-1 \\ \text{copies}}} \underbrace{HH\mathcal{E}EPE}_{\tilde{\Gamma}_{18}},$$

and thus calculate the Poincaré–Hopf index at ∞ , which in this particular case turns out to be

$$\begin{aligned} PH(X, \infty) &= 1 + \frac{1}{2} (2(\nu_1 + \nu_2 - K(2, 6) + 1) - 2(-K(2, 6) + 4) + 8) \\ &= 2 + \nu_1 + \nu_2. \end{aligned}$$

13. RELATIONS WITH OTHER WORKS

13.1. The case that all critical and asymptotic values are real. Recall the following result.

Theorem 13.1 (Eremenko et al., [22], [23]). If all critical points of a rational function $\frac{Q}{P}(z)$ are real, then it is equivalent to a real rational function.

This immediately implies that for such a rational function all the critical values are also real.

Motivated by the above, we have.

Corollary 13.2 (Real critical and asymptotic values).

- 1) If all critical and asymptotic values of Ψ_X for $X \in \mathcal{E}(r, d)$ are in \mathbb{R} , then the following assertions hold.
 - a) \mathcal{R}_X , as in (103), is the union of half planes.
 - b) $\Psi_X : U \subset \hat{\mathbb{C}} \rightarrow \mathbb{H}^2$ is a Schwartz–Christoffel map, for each half plane U .
 - c) X is unstable in $\mathcal{E}(r, d)$, thus a bifurcation for $\Re(X)$ occurs.
- 2) The critical and asymptotic values are in \mathbb{R} if and only if the family of rotated vector fields $\{\Re(e^{i\theta} X) \mid \theta \in \mathbb{R}/2\pi n\}$ bifurcates exactly at $\theta = n\pi$ for $n \in \mathbb{Z}$.

□

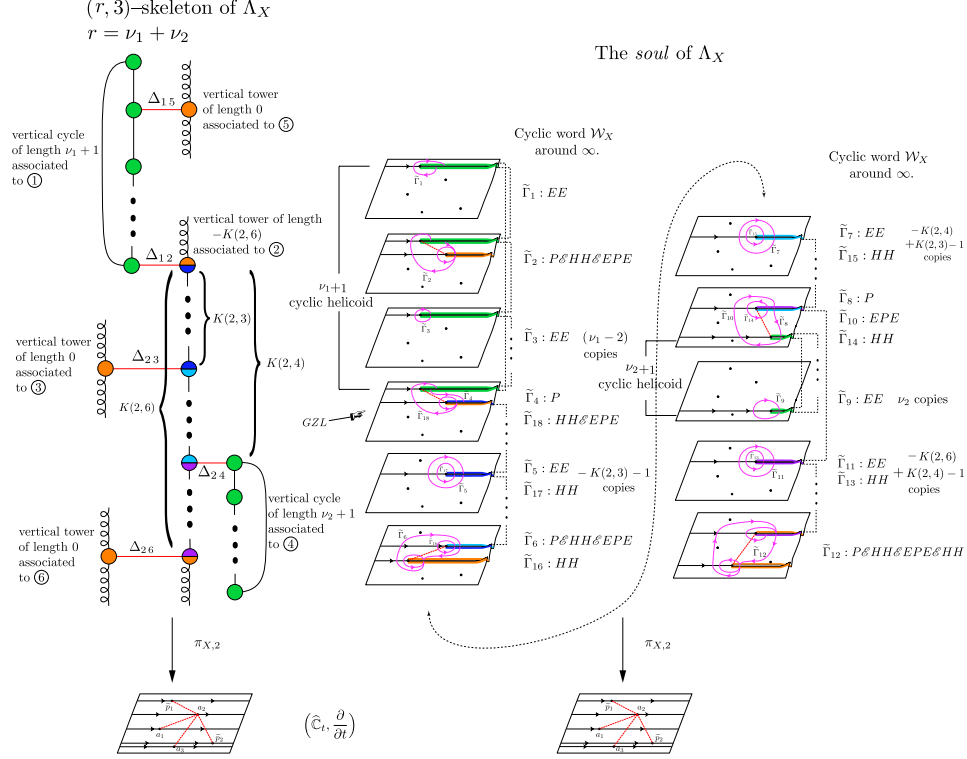


FIGURE 23. **The soul of Λ_X and the cyclic word \mathcal{W}_X .** The left hand side shows the $(r, 4)$ -skeleton of Λ_X of Example 8.10, in the middle the corresponding soul together with the curve $\tilde{\Gamma}$ decomposed into the corresponding $\tilde{\Gamma}_i$ on each sheet of the soul. On the right hand side are the corresponding syllables of the cyclic word \mathcal{W}_X around $\infty \in \hat{\mathbb{C}}_z$. See Example 12.6.

13.2. Relations with Belyi's functions. A rational function $\frac{Q}{P}(z)$ is Belyi if it has only three critical values $\{0, 1, \infty\}$, the original source is [7], see [31] Ch. 2 for current developments. Recently Ch. J. Bishop [12] develops analogous combinatorial and analytic ideas for entire functions.

By Lemma 4.1, we have that for $X \in \mathcal{E}(r, d)$, the distinguished parameter Ψ_X has an even number $2d$ of asymptotic values (counted with multiplicity). Hence, the construction of a certain $\Psi_X(z)$ having three asymptotic values, say at $\{0, 1, \infty\}$ set theoretically, as in Belyi's theory, is possible.

Example 13.1. Let $X(z) = \frac{\sqrt{\pi}}{4} e^{z^2} \frac{\partial}{\partial z}$ be as in Example 12.4, having associated the error function $\Psi(z) = \frac{2}{\sqrt{\pi}} \int_0^z e^{-\zeta^2} d\zeta$ with logarithmic branch points,

$$\{(\infty_1, -1, -\infty), (\infty_2, 1, -\infty), (\infty_3, \infty, -\infty), (\infty_4, \infty, -\infty)\},$$

using the notation in Equations (31) and Definition 5.1. In set theoretically language, its asymptotic values are $\{-1, 1, \infty\}$, hence it is a Belyi function.

Example 13.2. A transcendental Belyi function that does not belong to the family Ψ_X , for $X \in \mathcal{E}(r, d)$. With the present techniques, we can describe the following

vector field arising from a transcendental Belyĭ function due to R. Nevanlinna [40] p. 292. Let \mathcal{R} be the Riemann surface that consists of half a Riemann sphere (cut along the extended real line $\mathbb{R} \cup \{\infty\} \subset \widehat{\mathbb{C}}$) glued to three semi-infinite towers of copies of $\widehat{\mathbb{C}} \setminus (a, b]$ where $(a, b] \in \{(-\infty, 0], (0, 1], (1, \infty]\}$, as in Figure 25. The general version of the dictionary ([2] Lemma 2.6) shows that a transcendental function $\Upsilon(z) : \mathbb{C}_z \longrightarrow \widehat{\mathbb{C}}_t$ and a vector field $X(z) = \frac{1}{\Upsilon'(z)} \frac{\partial}{\partial z}$ are associated to \mathcal{R} .

The (logarithmic) branch points of $\Upsilon(z)$ are

$$\{(\infty_1, 0), (\infty_2, 1), (\infty_3, \infty)\}.$$

Of course there is only one such possible Riemann surface (up to Möbius transformation). Compare also with the line complex description as in p. 292 of [40].

The cyclic word is

$$\left((\widehat{\mathbb{C}}_z, \infty), \Re(X) \right) \mapsto \mathcal{W}_X = H\mathcal{E}E\mathcal{E}H\mathcal{T}.$$

Note the appearance of a new angular sector \mathcal{T} having an accumulation point of double zeros of X : the phase portrait of $\Re(X)$ is obtained by considering the pullback of $\Re\left(\frac{\partial}{\partial t}\right)$ via Υ , see Figure 24.c. The 1-order of X is finite and at least 1.

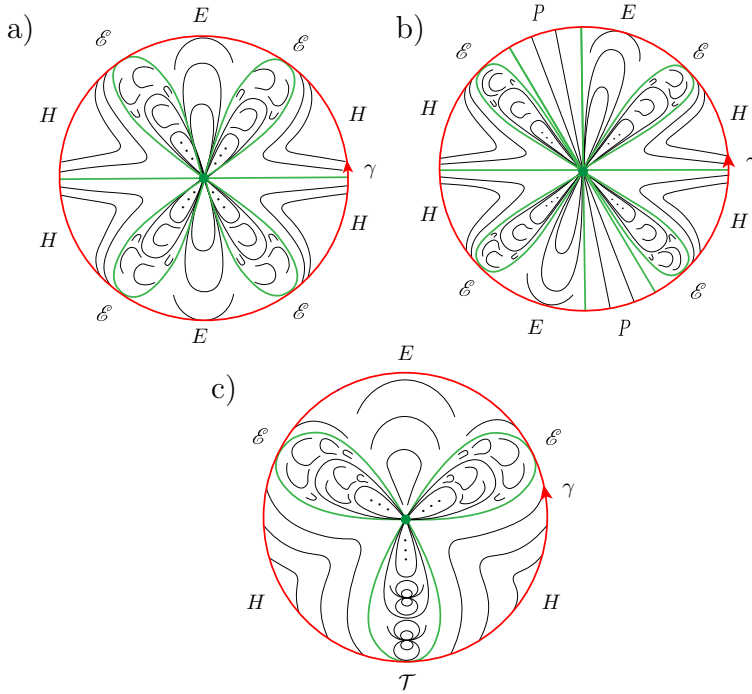


FIGURE 24. The cyclic words (a)–(b) appearing in Examples 12.4 and (c) in 13.2. Numerical models for (a)–(b) appeared as figures 15 and 16 in [2].

13.3. Relation with complex correspondence principle in mechanics. C. Bender *et al.* studies the relation between classical and quantum mechanics using a \mathbb{C} complex framework, see [8], [9] and [10]. Motivated by the correspondence

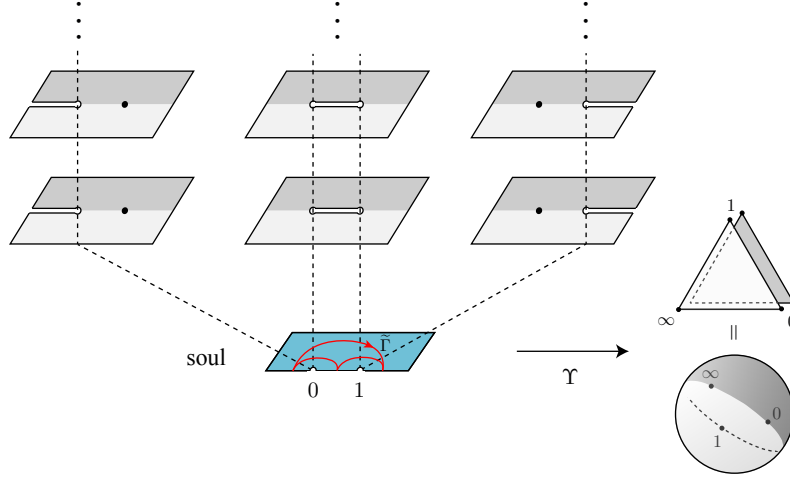


FIGURE 25. Riemann surface corresponding to a transcendental Belyi function Υ . The path $\tilde{\Gamma}$ is a taut deformation of $\Gamma = (\Psi_X \circ \gamma)$ originated by a γ bounding the singularity $((\hat{\mathbb{C}}, \infty), X_\Upsilon)$. Note that topologically this is the only possible surface with exactly three logarithmic branch points. Compare with Lemma 4.1 and note that the singularities in the central column are topologically different from semi-infinite helicoids in Figure 4.

principle, asserting that quantum mechanics resembles classical mechanics in the high-quantum-number limit. These works introduce the concept of a local quantum probability density $\rho(z)$ in the complex plane. C. Bender proposes the novel approach of constructing a complex contour C on which $\rho(z)dz$ is an infinitesimal probability measure. Thus, C must satisfy

$$\begin{aligned} \text{condition I:} & \quad \Im(\rho(z)dz) = 0, \\ \text{condition II:} & \quad \Re(\rho(z)dz) > 0, \\ \text{condition III:} & \quad \int_C \rho(z)dz = 1, \end{aligned}$$

see [8]. In our language, we consider $\rho(z)dz$ as entire 1-form on \mathbb{C} . By using the singular complex analytic Dictionary Proposition 2.5 and conditions I–II, we have that C can be interpreted as a trajectory of

$$\Re\left(\frac{1}{\rho(z)}\frac{\partial}{\partial z}\right), \text{ where } \frac{1}{\rho(z)}\frac{\partial}{\partial z} \in \mathcal{E}(r, 2),$$

condition III is a certain normalization. The works of C. Bender *et al.* illustrate the application of the corresponding trajectory structures.

13.4. Future work.

13.4.1. *Relations with Dessin's d'enfants.* In the combinatorial framework, dessin's d'enfants are well known plane bipartite trees associated to Belyi functions; in their modern form were promoted and named by A. Grothendieck. Among other things, they have been used to study the action of the absolute Galois group of \mathbb{Q} , see [25].

By the singular complex analytic Dictionary Proposition 2.5, we may consider a polynomial Belyi function Ψ_X as the distinguished parameter of the associated vector field $X \in \mathcal{E}(r, 0)$, $r \geq 2$. That is, up to action of $\text{Aut}(\mathbb{C})$ on the target, we

assume that the critical values of Ψ_X are $\{0, 1, \infty\}$. By assigning the color black to the vertices associated to the critical value 0 and the color white to the vertices associated to the critical value 1, we see that Λ_X is a bipartite graph, as in the usual theory.

The extension of the theory for Ψ_X , $X \in \mathcal{E}(r, d)$ with $r \geq 1$ is possible and is an interesting subject. In fact, *(r, d) -configuration trees Λ_X that lie over exactly three critical or asymptotic values are a natural extension of dessins d'enfant of the structurally finite Belyi functions Ψ_X .*

13.4.2. Topological classification of $\Re(X)$ for $X \in \mathcal{E}(r, d)$. As suggested by the results of §11; a careful study of the (r, d) -skeleton of Λ_X allows for a global topological classification of $\Re(X)$ for $X \in \mathcal{E}(r, d)$, in terms of the placement of the critical and asymptotic values. This study is in progress, however the technical language needed to provide a clear exposition would require too much space, thus it has been left for a future work. A particularly interesting case is the bound for the number of topological classes $\{\Re(X) \mid \mathcal{E}(r, 0)\}$, $r \geq 3$.

13.4.3. Dynamical coordinates for other families of vector fields. As Example 13.2 suggests, there are other families of vector fields where the construction of the dynamical coordinates Λ_X is certainly possible.

For instance, when considering the family

$$\mathcal{E}(s, r, d) = \left\{ X(z) = \frac{Q(z)}{P(z)} e^{E(z)} \frac{\partial}{\partial z} \mid \begin{array}{l} Q, P, E \in \mathbb{C}[z], \\ \deg Q = s, \deg P = r, \deg E = d \end{array} \right\},$$

as in [3], we are presented with two intrinsically different cases:

- 1) If Ψ_X is single valued (this is equivalent to requiring that the associated 1-form ω_X have all its residues zero), then vertices of the form (q_i, ∞, ν_i) , corresponding to the zeros $\mathcal{Z} = \{q_i\}_{i=1}^s$ of X , need to be added to the description of Λ_X .
- 2) If Ψ_X is multivalued (there appear at least two non zero residues for ω_X) then extra structure will be required, because of the appearance of logarithmic singularities over those $q_i \in \mathbb{C}_z$ where the associated 1-form has non-zero residue.

13.4.4. On cyclic words.

Cyclic words as topological or analytical invariants for germs. The word \mathcal{W}_X (as in Theorem 12.3), is a local topological invariant of a germ $((\widehat{\mathbb{C}}_z, \infty), \Re(X))$, $X \in \mathcal{E}(r, d)$.

Moreover, the word \mathcal{W}_X in general, is not a global topological invariant of $X \in \mathcal{E}(r, d)$. For example all the vector fields $X \in \mathcal{E}(r, 0)$, $r \geq 3$, with all critical and asymptotic values in \mathbb{R} , have the same word $\mathcal{W}_X = \underbrace{EE \cdots EE}_{2r+2}$ at ∞ .

However, it is possible to modify the definitions of angular sectors P_ν , E and \mathcal{E} so that in fact the corresponding \mathcal{W}_X is a *global analytic invariant* of X modulo $\text{Aut}(\mathbb{C})$. This is left for a future project.

Other angular sectors as letters for cyclic words. As shown in Example 13.2 and in examples 5.9, 5.12 and figures 2, 5 of [2]; there are certainly other possible angular sectors that can be used as letters for cyclic words. In this context and considering the above examples, it is clear that there are an infinite number of topologically different angular sectors (letters) that can appear in a cyclic word associated to an essential singularity for a vector field X .

However, it is not immediately clear *how many topologically different letters there are when we specify the p -order of X* , that is the coarse analytic invariant of functions and vector fields. For instance, by once again considering Example 13.2, $X(z) = \Upsilon^*(\frac{\partial}{\partial t})(z) = \frac{1}{\Upsilon'(z)} \frac{\partial}{\partial z}$; we may also consider $Y(z) = \Upsilon^*(\mu t \frac{\partial}{\partial t})(z) = \mu \frac{\Upsilon(z)}{\Upsilon'(z)} \frac{\partial}{\partial z}$ which provides a (very) different vector field.

14. EPILOGUE

The second part of the proof of the Main Theorem provides a proof of the following result of independent interest. Recalling Equations (25), (28), (39) and (40) we have.

Corollary 14.1. *Given $r + d$ values*

$$\tilde{p}_1, \dots, \tilde{p}_r, a_1, \dots, a_d \in \mathbb{C}_t,$$

possibly repeated, with the exception that if $d \geq 1$ there are at least two non-repeated values. Then there exists a (non unique) vector field $X \in \mathcal{E}(r, d)$ having these $r + d$ ramification values, i.e. a collection of $n + d$ realizable vertices, see (45),

$$\{(p_\iota, \tilde{p}_\iota, -\nu_\iota)\}_{\iota=1}^n \cup \{(\infty_\sigma, a_\sigma, -\infty)\}_{\sigma=1}^d$$

for the corresponding Ψ_X .

Remark 14.2. In our case, the complete collection of ramification values are $\{\tilde{p}_1, \dots, \tilde{p}_n, a_1, \dots, a_d, \infty\} \subset \widehat{\mathbb{C}}_t$. Moreover, the use of ramification values t_a provides information of the moduli space of Ψ_X . Recalling the classical Riemann's idea that for ramified cover maps over $\widehat{\mathbb{C}}_t$ with $n \geq 4$ ramification values, we can specify three of them, and the other $n - 3$ determine holomorphic deformations of the cover maps $\pi_{X,2}$.

Because of the singular complex analytic Dictionary Proposition 2.5, the works of R. Thom [47] and J. Mycielski [39], describes the situation for polynomials Ψ_X , i.e. the case $d = 0$. However the answer is not unique, that is given a set of preassigned critical values $\{\tilde{p}_1, \dots, \tilde{p}_n\}$ there are a finite number of polynomials Ψ_X with the above set as critical values, namely

Theorem (Mycielski–Thom). Given r points $\tilde{p}_1, \dots, \tilde{p}_r \in \mathbb{C}_t$, there exist r points $p_1, \dots, p_r \in \mathbb{C}_z$ such that the (monic) polynomial of degree $r + 1$

$$\Psi(z) = (r + 1) \int^z \prod_{\iota=1}^r (\zeta - p_\iota) d\zeta$$

satisfies

- 1) $\Psi(p_\iota) = \tilde{p}_\iota$ and $\Psi'(p_\iota) = 0$, for $\iota = 1, \dots, r$.
- 2) If β occurs k times in the collection p_1, \dots, p_r then $(z - \beta)^{k+1}$ divides $\Psi(z) - \Psi(\beta)$. \square

Proof of Corollary 14.1. Recalling Equation (45), we want to show that there exists:

- a) r points $p_1, \dots, p_r \in \mathbb{C}_z$, determining a (monic) polynomial $P(z) = \prod_{\iota=1}^r (z - p_\iota)$,
- b) a polynomial $E(z)$ of degree d ,
- c) d asymptotic paths $\alpha_\sigma(\tau)$,

such that the distinguished parameter $\Psi_X(z) = \int^z P(\zeta) e^{-E(\zeta)} d\zeta$ satisfies

- i) $\Psi_X(p_\iota) = \tilde{p}_\iota$ and $\Psi_X^{(\ell)}(p_\iota) = 0$, for $1 \leq \ell \leq \nu_\iota - 1$,
- ii) $\lim_{\tau \rightarrow \infty} \Psi_X(\alpha_\sigma(\tau)) = a_\sigma$, for $\sigma = 1, \dots, d$.

Furthermore, the polynomials $P(z)$ and $E(z)$ are non-unique.

Note that the *geometrical* construction carried out in §9.2 (the second part of the proof of the Main Theorem) can be carried out *by only specifying the critical and asymptotic values and the corresponding $K(\mathfrak{a}, \mathfrak{r})$* of the (r, d) -configuration tree, this uses Lemma 5.3 actively.

That is we can construct a Riemann surface \mathcal{R} by glueing sheets \mathbb{C}_t with branch cuts starting at $\{\tilde{p}_1, \dots, \tilde{p}_r, a_1, \dots, a_d\}$. As before, \mathcal{R} is recognized as a simply connected Riemann surface \mathcal{R}_X corresponding to some $X \in \mathcal{E}(r, d)$; thus showing that for every possible choice of $(\tilde{p}_1, \dots, \tilde{p}_r, a_1, \dots, a_d) \in \mathbb{C}^{r+d}$ there are polynomials $P(z)$ and $E(z)$ of degrees r and d respectively such that Ψ_X has precisely $\{\tilde{p}_1, \dots, \tilde{p}_r, a_1, \dots, a_d\}$ as critical and asymptotic values.

For the non-uniqueness of the polynomials $P(z)$ and $E(z)$ note that: when $d = 0$ generically, by Bezout's Theorem, there are $(r+1)^r$ solutions of the system (45). For the case $r = 3, d = 0$ see Equation (52) and for $r = 0, d = 3$, recall Example 8.5 where there are an infinite number of solutions for each vertex of finite asymptotic values $a_1, a_2, a_3 \in \mathbb{C}_t$: each parameter $K(1, 3) \in \mathbb{Z}$ provides a different $X \in \mathcal{E}(0, 3)$. The general case now follows easily from the above examples. \square

Remark 14.3. 1. Corollary 14.1 gives rise to a complex analytic set in $\overline{\mathbb{C}}_z^{r+d} \times \mathbb{C}_t^{r+d}$ consisting of the sets of branch points that determine \mathcal{R}_X with $X \in \mathcal{E}(r, d)$.
2. Corollary 14.1 can be interpreted as saying that the map from $\mathbb{C}[z]_{=r} \times \mathbb{C}[z]_{=d}$ to \mathbb{C}^{r+d} given by the Equation (45) is surjective.

Recalling (6) and (7), there are two obvious ways of parametrizing $\mathcal{E}(r, d)$:

- 1) Specifying the coefficients of $P(z)$ and $E(z)$.
- 2) Specifying the roots of $P(z)$ and $E(z)$ together with the non zero coefficient μ .

Noting that the roots of $P(z)$ correspond to the poles of X , equivalently to the critical points of Ψ_X . In the particular case of $d = 0$, the usual geometrical/dynamical interpretation of (2) arises. However, we are not aware of a geometrical/dynamical interpretation of the roots of $E(z)$; compare with [3] where a study of the discrete symmetries of X is provided.

- 3) A third kind of “parametrization” is given by Corollary 14.1: given a set of critical and asymptotic values $\{\tilde{p}_1, \dots, \tilde{p}_n, a_1, \dots, a_d\}$, there are non-unique $X \in \mathcal{E}(r, d)$ such that the above set are precisely the critical and asymptotic values of Ψ_X . Note that the non-uniqueness arises from the solution of the system of transcendental equations (45).

Recalling Diagram 12, parametrizations (2) case $d = 0$ and (3) can be represented in Diagram 116 by specifying the left hand side or the bottom part, respectively:

$$(116) \quad \begin{array}{ccc} \mathbb{C}_z \supset \{p_1, \dots, p_n, \infty_1, \dots, \infty_d\} & \xleftarrow{\pi_{X,1}} & \{(p_\iota, \tilde{p}_\iota, -\nu_\iota)\}_{\iota=1}^n \cup \{(\infty_\sigma, a_\sigma, -\infty)\}_{\sigma=1}^d \subset \mathcal{R}_X \\ & \searrow \Psi_X & \downarrow \pi_{X,2} \\ & & \{\tilde{p}_1, \dots, \tilde{p}_r, a_1, \dots, a_d\} \subset \mathbb{C}_t. \end{array}$$

Is there another way of parametrizing $X \in \mathcal{E}(r, d)$?

Striving for a unique geometrical/dynamical solution in the general case $r, d \geq 1$, (r, d) -configuration trees provide a “mixed approach”. Further study of the above question and effective parameters from Diagram 116 is the goal of a future project.

REFERENCES

- [1] M. Abramowitz, I. A. Stegun (Eds.). *Hypergeometric Functions*, Ch. 15 in Handbook of Mathematical Functions with Formulas, Graphs, and Mathematical Tables, 9th printing. New York: Dover, (1972) 555–566.
- [2] A. Alvarez-Parrilla, J. Muciño-Raymundo, *Dynamics of singular complex analytic vector fields with essential singularities I*, Conform. Geom. Dyn., 21 (2017), 126–224. <http://dx.doi.org/10.1090/ecgd/306>
- [3] A. Alvarez-Parrilla, J. Muciño-Raymundo, *Symmetries of complex analytic vector fields with an essential singularity on the Riemann sphere*, Advances in Geom. to appear, (2019), 25 pages. <http://arxiv.org/abs/1904.11667>
- [4] A. Alvarez-Parrilla, J. Muciño-Raymundo, S. Solorza and C. Yee-Romero, *On the geometry, flows and visualization of singular complex analytic vector fields on Riemann surfaces*, Proceedings of the 2018 Workshop in Holomorphic Dynamics, C. Cabrera *et al.* Eds., Instituto de Matemáticas, UNAM, México, *Serie Papirhos*, Actas 1 (2019), 21–109. <https://arxiv.org/abs/1811.04157>
- [5] A. A. Andronov, E. A. Levitch, I. I. Gordon, A. G. Maier, *Qualitative Theory of Second-Order Dynamic Systems*, J. Wiley & Sons, New-York, Toronto, 1973.
- [6] V. I. Arnold, Y. Ilyashenko, *Ordinary Differential Equations*, in Dynamical Systems I, D. V. Anosov, V. I. Arnold Eds., Springer-Verlag, Berlin, 1994.
- [7] G. V. Belyi, *On Galois extensions of a maximal cyclotomic field*, Math. USSR Izvestija, 193, (1980), no 14, 247–256. <https://doi.org/10.1070/IM1980v014n02ABEH001096>
- [8] C. M. Bender, D. W. Hook, P. N. Meisinger, Q.-H. Wang, *Complex correspondence principle*, Physical Review Letters PRL 104, 12 February (2010) 061601–0616014. <https://doi.org/10.1103/PhysRevLett.104.061601>
- [9] C. M. Bender, D. W. Hook, P. N. Meisinger, Q.-H. Wang, *Probability density in the complex plane*, Annals of Physics 325 (2010) 2332–2362. <https://doi.org/10.1016/j.aop.2010.02.011>
- [10] C. M. Bender, *PT symmetry in quantum and classical physics*, With contributions from P. E. Dorey, C. Dunning, A. Fring, D. W. Hook, H. F. Jones, S. Kuzhel, G. Lévai, R. Tateo, World Sci., Hackensack, NJ (2019).
- [11] W. Bergweiler, A. Eremenko, *On the singularities of the inverse to a meromorphic function of finite order*, Revista Matemática Iberoamericana, 11, 2, (1995) 355–373. <http://dx.doi.org/10.4171/RMI/176>
- [12] Ch. J. Bishop, *Constructing entire functions by quasiconformal folding*, Acta Math., 214 (2015) 1–60. <https://doi-org.pbidi.unam.mx:2443/10.1007/s11511-015-0122-0>
- [13] K. Biswas, R. Pérez-Marco, *Log-Riemann surfaces, Caratheodory convergence and Euler's formula*, Contemporary Math., 639 (2015) 197–203. <http://de.doi.org/10.1090/com/639/12826>
- [14] K. Biswas, R. Pérez-Marco, *Uniformization of simply connected finite type Log-Riemann surfaces*, Contemporary Math., 639 (2015) 205–216. <http://de.doi.org/10.1090/com/639/12827>
- [15] K. Biswas, R. Pérez-Marco, *The ramificant determinant*, SIGMA 15 (2019), 086, 28 pages. <https://www.emis.de/journals/SIGMA/2019/086/sigma19-086.pdf>
- [16] W. M. Boothby, *The topology of regular curve families with multiple saddle points*, Amer. J. Math., Vol. 73, No. 2 (Apr., 1951), 405–438. <https://www.jstor.org/stable/2372185>
- [17] W. M. Boothby, *The topology of the level curves of harmonic functions with critical points*, Amer. J. Math., Vol. 73, No. 3 (Jul., 1951), 512–538. <https://www.jstor.org/stable/2372305>
- [18] B. Branner, K. Dias, *Classification of complex polynomial vector fields in one complex variable*, J. Difference Equ. Appl., 16, 5–6, (2010), 463–517. <https://doi.org/10.1080/10236190903251746>
- [19] J. Cheeger, D. Gromoll, *The structure of complete manifolds of nonnegative curvature*, Bull. Amer. Math. Soc., 74 (1968), 1147–1150. <https://doi-org.pbidi.unam.mx:2443/10.1090/S0002-9904-1968-12088-9>
- [20] K. Dias, L. Tan, *On parameter space of complex polynomial vector fields in \mathbb{C}* , J. Differential Equations, 260, 1 (2016), 628–652. <http://dx.doi.org/10.1016/j.jde.2015.09.001>
- [21] G. Elfving, *Über eine Klasse von Riemannschen Flächen und ihre Uniformisierung*, Acta Soc. Sci. Fennicae, N.S. 2, Nr. 3 (1934), 1–60.

- [22] A. Eremenko, A. Gabrielov, *Rational functions with real critical points and the B. and M. Shapiro conjecture in real enumerative geometry*, Ann. of Math. (2) 155 (2002), no. 1, 105–129. <http://dx.doi.org/10.2307/3062151>
- [23] A. Eremenko, A. Gabrielov, *An elementary proof of the B. and M. Shapiro conjecture for rational functions*, In Notions of positivity and the geometry of polynomials, 167–178, Trends Math., Birkhäuser/Springer Basel AG, Basel, 2011. http://dx.doi.org/10.1007/978-3-0348-0142-3_10
- [24] M. E. Frías-Armenta, J. Muciño-Raymundo, *Topological and analytic classification of vector fields with only isochronous centers*, J. Eqs. Appl., 19, 10, (2013), 1694–1728. <https://doi.org/10.1080/10236198.2013.772598>
- [25] A. Grothendieck, *Equisse d'un programme*, In Geometric Galois actions 1, L. Schneps *et al.* Ed., vol. 242 London Math. Soc. Lecture Note Ser., (1997) 7–48. <https://doi.org/10.1017/CB09780511758874.003>
- [26] K. Hockett, S. Ramamurti, *Dynamics near the essential singularity of a class of entire vector fields*, Transactions of the AMS, vol. 345, 2 (1994), 693–703. <https://doi.org/10.1090/S0002-9947-1994-1270665-5>
- [27] X.-H. Hua, Ch.-Ch. Yang, *Dynamics of Transcendental Functions*, Gordon and Breach (1998).
- [28] M. Klimeš, Ch. Rousseau, *Generic 2-parameter perturbations of parabolic singular points of vector fields in \mathbb{C}* , Conform. Geom. Dyn., 22 (2018) 141–184. <https://doi.org/10.1090/ecgd/325>
- [29] F. Klein, *On Riemann's Theory of Algebraic Functions and Their Integrals*, Dover Publications Inc., New York, (1963). <http://www.gutenberg.org/ebooks/36959>
- [30] J. Jenkins, *Univalent Functions and Conformal Mapping*, Ergebnisse Der Mathematik Und Iher Grenzgebiete, Springer-Verlag, Berlin, 1958. <https://doi.org/10.1007/978-3-642-88563-1>
- [31] S. K. Lando, A. K. Zvonkin, *Graphs on Surfaces and Their Applications*, EMS 141, Springer-Verlag (2004). <https://doi.org/10.1007/978-3-540-38361-1>
- [32] J. K. Langley, *Trajectories escaping to infinity in finite time*, Procc. Amer. Math. Soc. Vol. 145, Num. 5, May (2017), 2107–2117. <https://dx.doi.org/10.1090/proc/13377>
- [33] J. L. López, J. Muciño-Raymundo, *On the problem of deciding whether a holomorphic vector field is complete*, in Operator Theory: Advances and Applications 114, (2000), 171–195. https://doi.org/10.1007/978-3-0348-8698-7_13
- [34] J. C. Magaña-Cacères, *Classification of 1-forms on the Riemann sphere up to $PSL(2, \mathbb{C})$* , Bull. Mexican Math. Soc., (3), 25, 3 (2019), 597–617. <https://doi.org/10.1007/s40590-018-0217-7>
- [35] D. Masoero, *Painlevé I, coverings of the sphere and Belyi functions*, Constr. Approx., 39, 1 (2014), 43–74. <https://doi.org/10.1007/s00365-013-9185-3>
- [36] H. Masur, S. Tabachnikov, *Rational billiards and flat structures*, in Handbook of Dynamical Systems, Vol. 1A, B. Hasselblatt *et al.* Ed., North-Holland, Amsterdam, 2002, 1015–1089. [https://doi.org/10.1016/S1874-575X\(02\)80015-7](https://doi.org/10.1016/S1874-575X(02)80015-7)
- [37] J. Muciño-Raymundo, *Complex structures adapted to smooth vector fields*, Math. Ann., 322, (2002), 229–265. <https://doi.org/10.1007/s002080100206>
- [38] J. Muciño-Raymundo, C. Valero-Valdéz, *Bifurcations of meromorphic vector fields on the Riemann sphere*, Ergod. Th. & Dynam. Sys., 15, (1995), 1211–1222. <https://doi.org/10.1017/S0143385700009883>
- [39] J. Mycielski, *Polynomials with preassigned values at their branching points*, Amer. Math. Montly 77:8, 853–855, <https://doi.org/10.1080/00029890.1970.11992599>
- [40] R. Nevanlinna, *Analytic Functions*, Springer-Verlag, (1970). <https://doi.org/10.1007/978-3-642-85590-0>
- [41] R. Nevanlinna, *Über Riemannsche Flächen mit endlich vielen Windungspunkten*, Acta Math., 58(1), 295–373, (1932). <https://doi.org/10.1007/BF02547780>
- [42] H. A. Schwarz, *Ueber diejenigen Fälle, in welchen die Gaussische hypergeometrische Reihe eine algebraische Function ihres vierten Elementes darstellt*, J. Reine Angew. Math., 75, (1873), 292–335. <https://doi.org/10.1515/crll.1873.75.292>
- [43] A. Speiser, *Über Riemannsche Flächen*, Comment. Math. Helv., 2 (1930), 284–293.
- [44] K. Strebel, *Quadratic Differentials*, Springer-Verlag (1984). <https://doi.org/10.1007/978-3-662-02414-0>

- [45] M. Taniguchi, *Explicit representations of structurally finite entire functions*, Proc. Japan Acad. Ser. A Math. Sci., Vol. 77, (2001), 68–70. <https://projecteuclid.org/euclid.pja/1148393085>
- [46] M. Taniguchi, *Synthetic deformation space of an entire function*, Cont. Math., Vol. 303, (2002), 107–136. <http://dx.doi.org/10.1090/conm/303/05238>
- [47] R. Thom, *L'équivalence de une fonction différentiable et d'un polynome*, Topology, 3, 2 (1965) 297–307. [https://doi.org/10.1016/0040-9383\(65\)90079-0](https://doi.org/10.1016/0040-9383(65)90079-0)
- [48] W. P. Thurston, *Three-Dimensional Geometry and Topology. Vol. 1.*, Princeton University Press, USA (1997).

Email address: alvaro.uabc@gmail.com

Email address: muciray@matmor.unam.mx